universite PARIS-SACLAY

CNRS

École Doctorale PHENIICS Doctoral School

Measurements of the Higgs boson produced in association with a vector boson and decaying to a pair of *b*-quarks with the ATLAS detector

Konie Al Khoury

Supervisor: Nicolas Morange

Thesis defense - 23/09/2020

ATLAS EXPERIMENT

IJCLab Irène Joliot-Curie

Outline

I- The Standard Model of particles and the ATLAS experiment

II- Characterisation of the liquid argon calorimeter pre-amplifiers for the Phase-II upgrade

III- Measurements of the Higgs boson produced in association with a vector boson and decaying to a pair of b-quarks using 139fb^{-1} data

I- The Standard Model of particles and the ATLAS experiment

The Standard Model of particle physics

- Describes the elementary particles and 3 fundamental interactions
- Two different types of particles:
  - **Fermions:** make up matter, leptons and quarks, three generations
  - **Bosons**: carriers of interactions
- Brout-Englert-Higgs (BEH) mechanism implies spontaneous electroweak symmetry breaking to explain the origin of mass of these particles
  - Predicts the existence of the Higgs boson particle
- The measurements allow to test the Standard Model with precision and look for physics beyond it

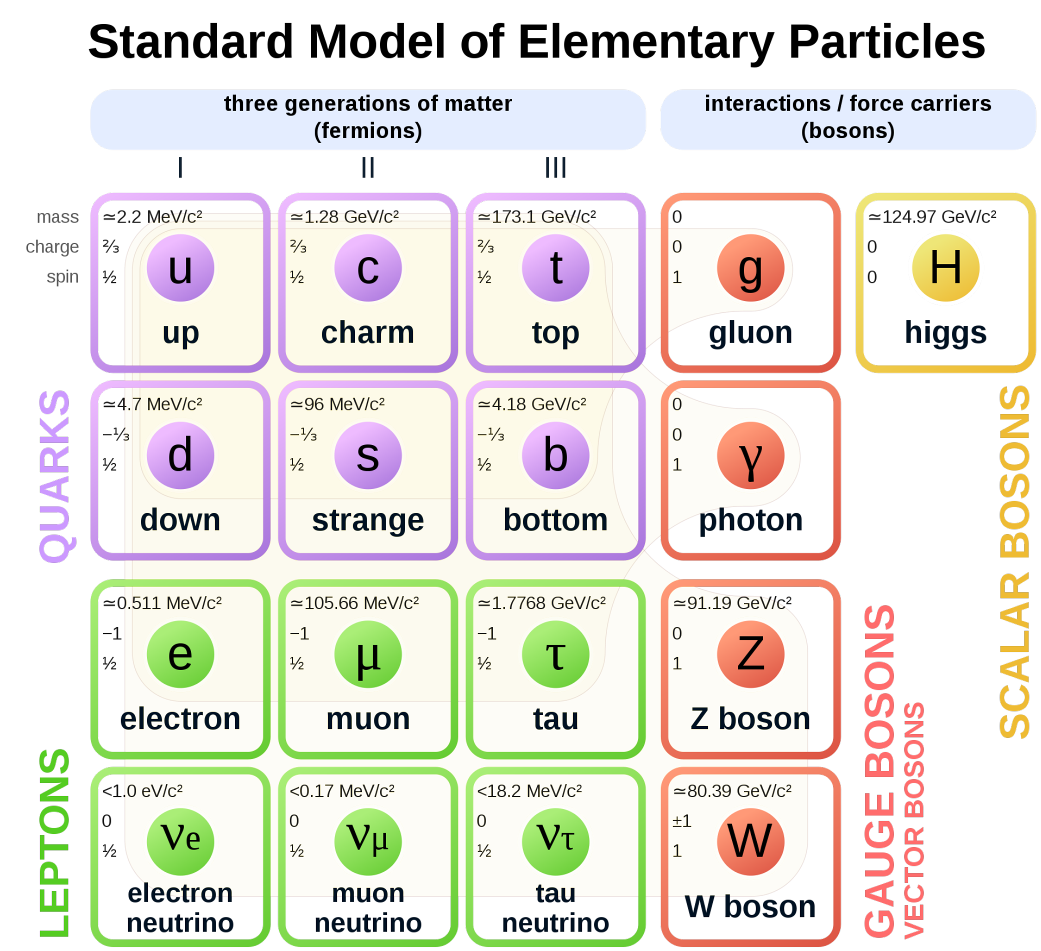

$$
\begin{aligned}
\mathcal{L} = & -\frac{1}{4} F_{\mu\nu} F^{\mu\nu} \\
& + i \bar{\psi} \not{D} \psi + h.c. \\
& + \psi_i y_{ij} \psi_j \phi + h.c. \\
& + |D_\mu \phi|^2 - V(\phi)
\end{aligned}
$$

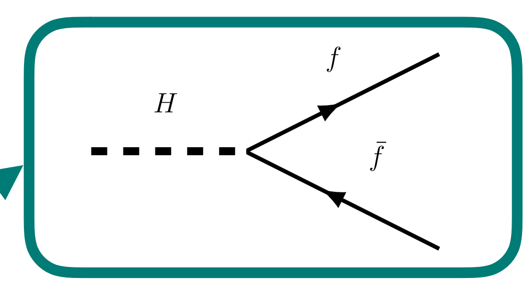

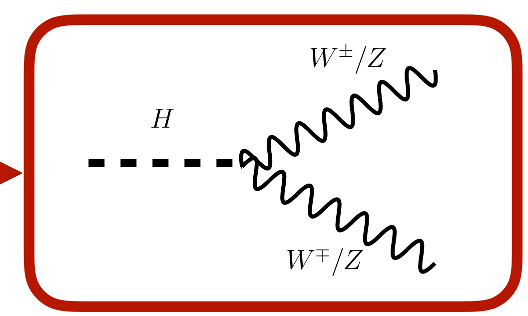

The Higgs boson properties

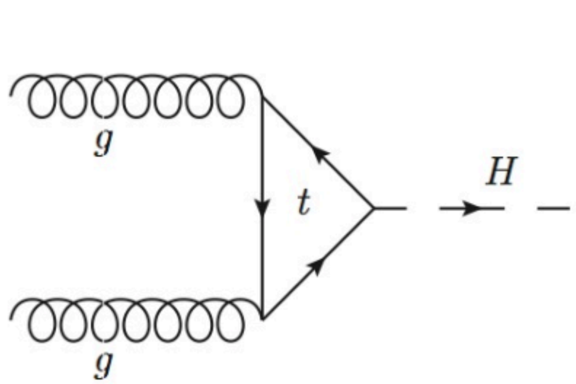

Gluon fusion (ggH): 88%

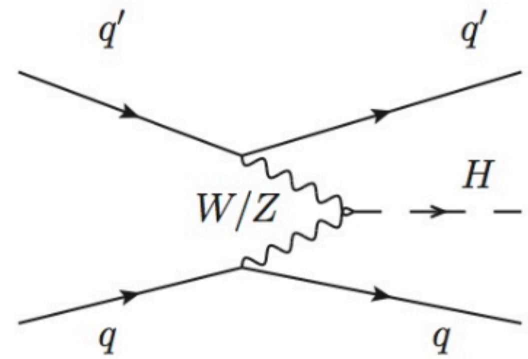

Vector boson fusion (VBF): 7%

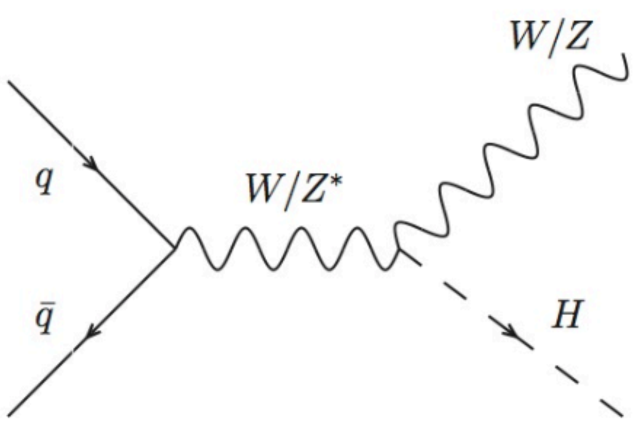

Higgs-strahlung (*VH*): 3%

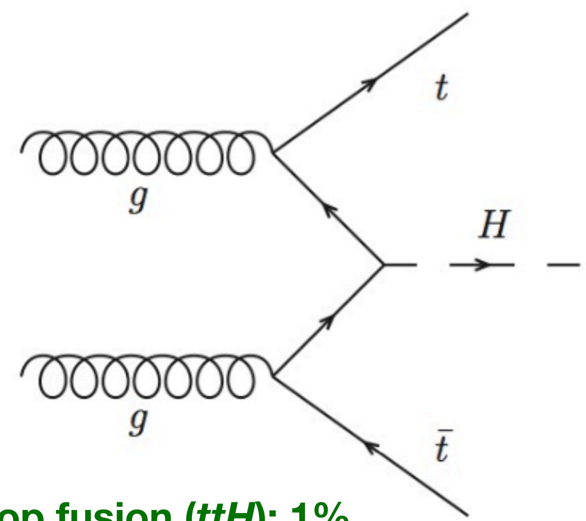

Top fusion (*ttH*): 1%

- 4 main production modes at the LHC
- Many decay modes accessible at the LHC
- First observed in 2012 independently by ATLAS and CMS to confirm the theory
  - Mostly in the γγ and ZZ decay modes: highest sensitivity and mass resolution
  - Became an active field to measure the properties of this particle

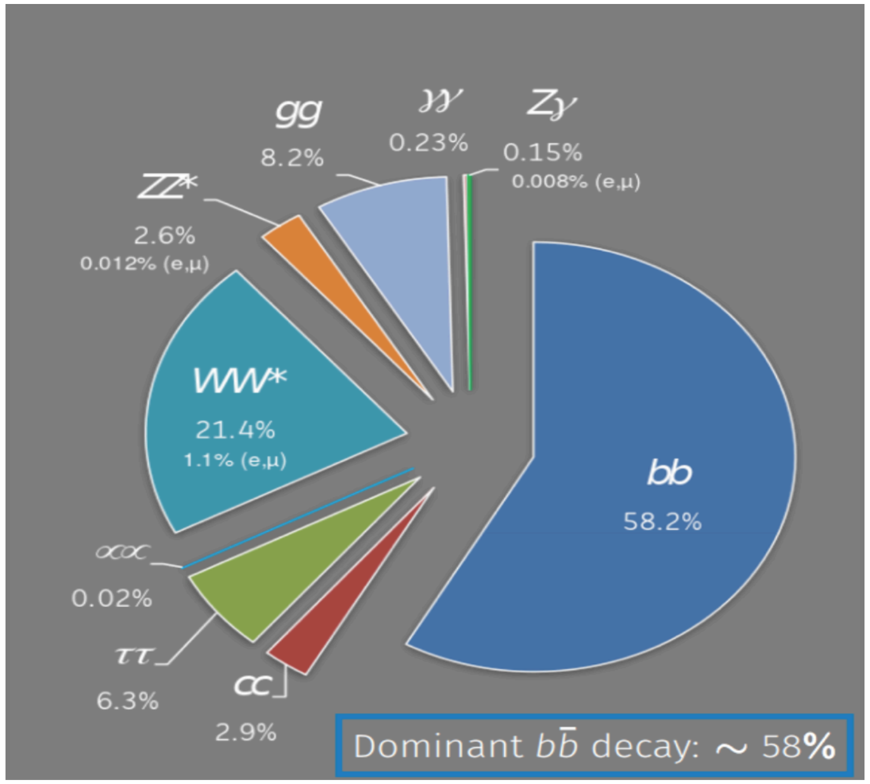

- The direct coupling of the Higgs boson to other particles allows:
  - To assess the compatibility with the Standard Model (or beyond)
  - To bring additional constraints when measured in different channels

The Large Hadron Collider

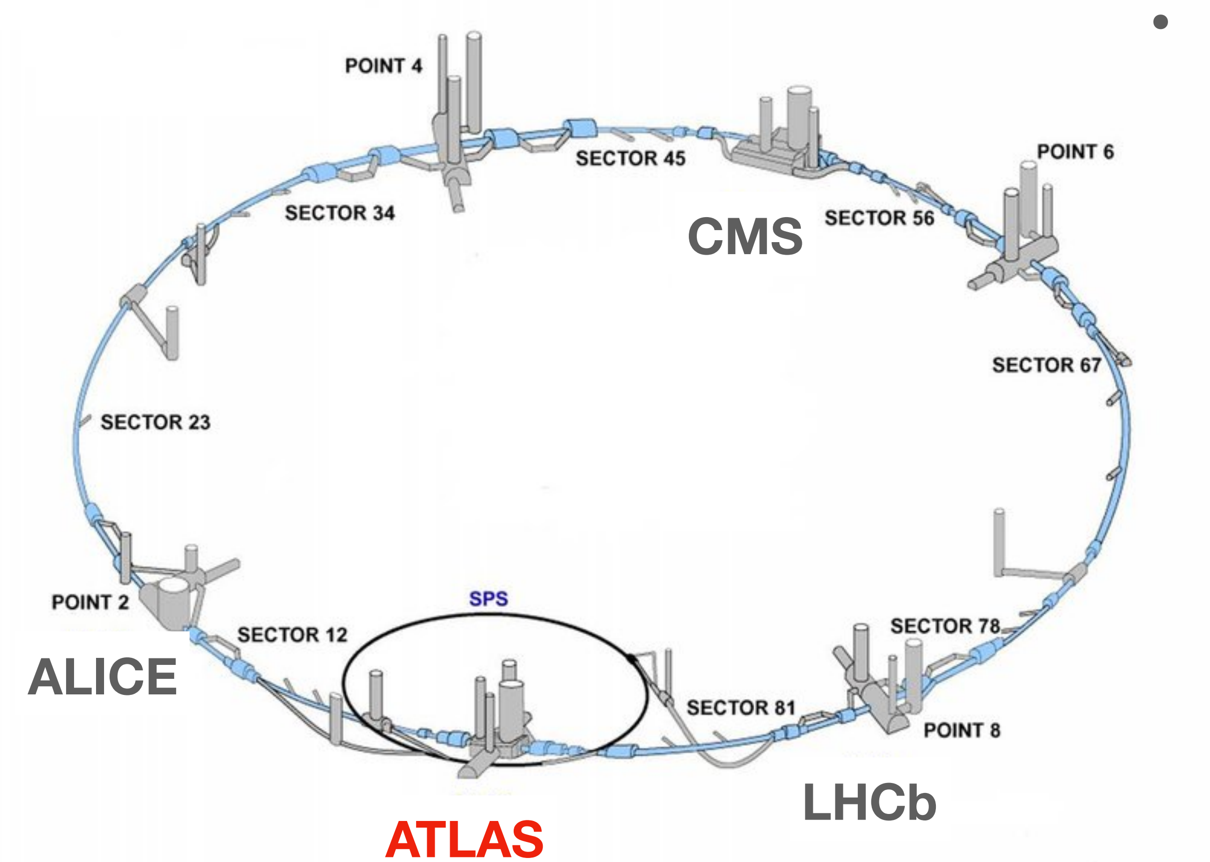

- The most powerful and largest particle accelerator, with a ring of 27km
  - Proton beams circulate in two different beam pipes under vacuum, in opposite directions
  - Particles arranged in up to 2808 bunches separated by 25ns
  - 8.3T superconducting magnets to guide the proton bunches
  - Protons accelerated up to an energy of 6.5TeV using radio frequency (RF) cavities

- 4 experiments are placed alongside the LHC ring:
  - **ATLAS:** studies a wide range of physics
  - **CMS**: CMS and ATLAS have a similar physics program
  - **ALICE**: uses heavy ion collisions to study quark-gluon plasma
  - **LHCb**: dedicated for heavy flavour physics

The ATLAS detector

- One of the two multi-purpose detectors at the LHC
- Made of sub-detector wrapped with an onion-layer configuration
  - Inner detector (ID)
  - Calorimeters
  - Muon spectrometer (MS)
- Run-2: 139fb^{-1} of data collected and large pile-up
- The ATLAS physics program:
  - Precision measurements of the Standard Model
  - Search for physics beyond the Standard Model
  - Measurement of the Higgs boson properties

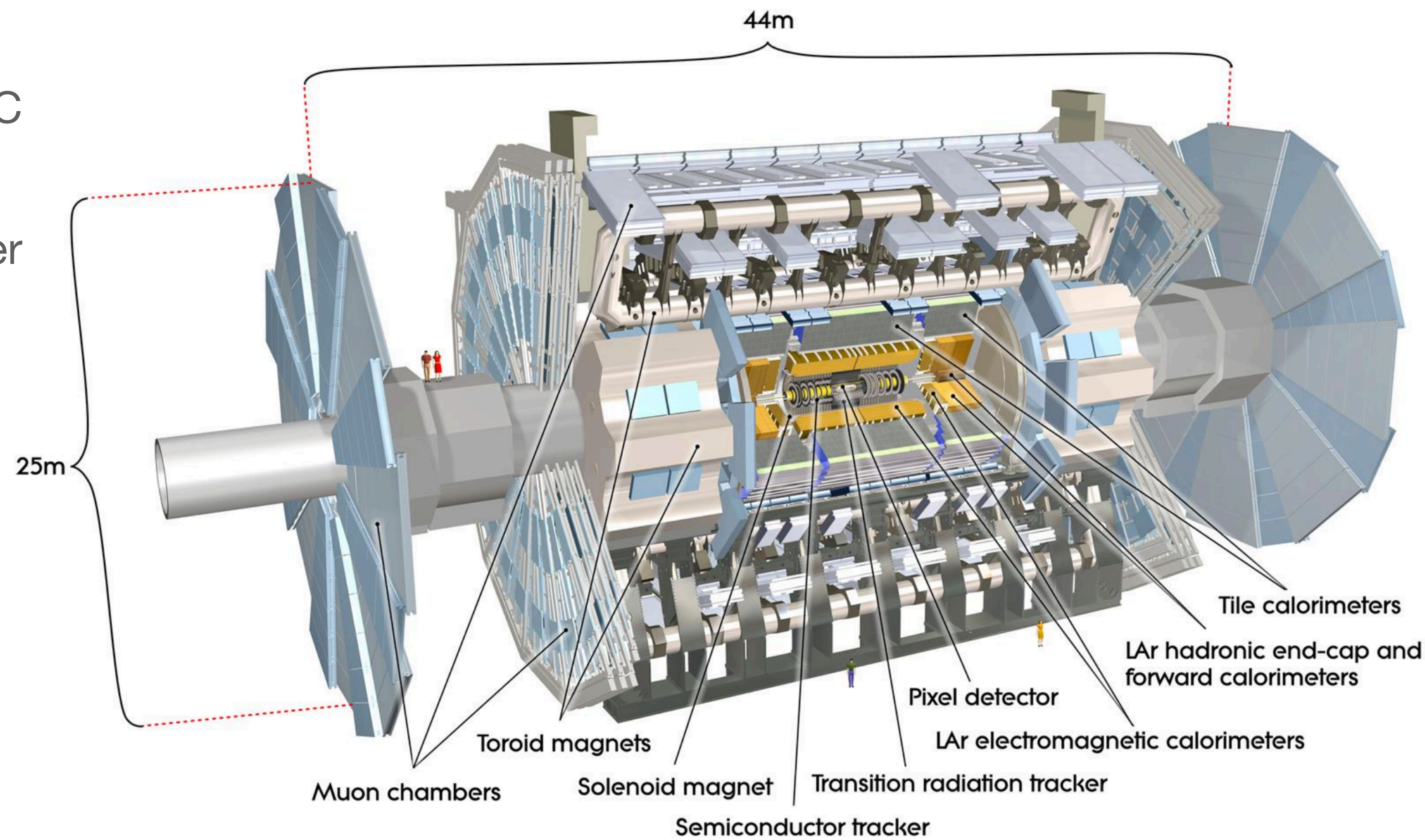

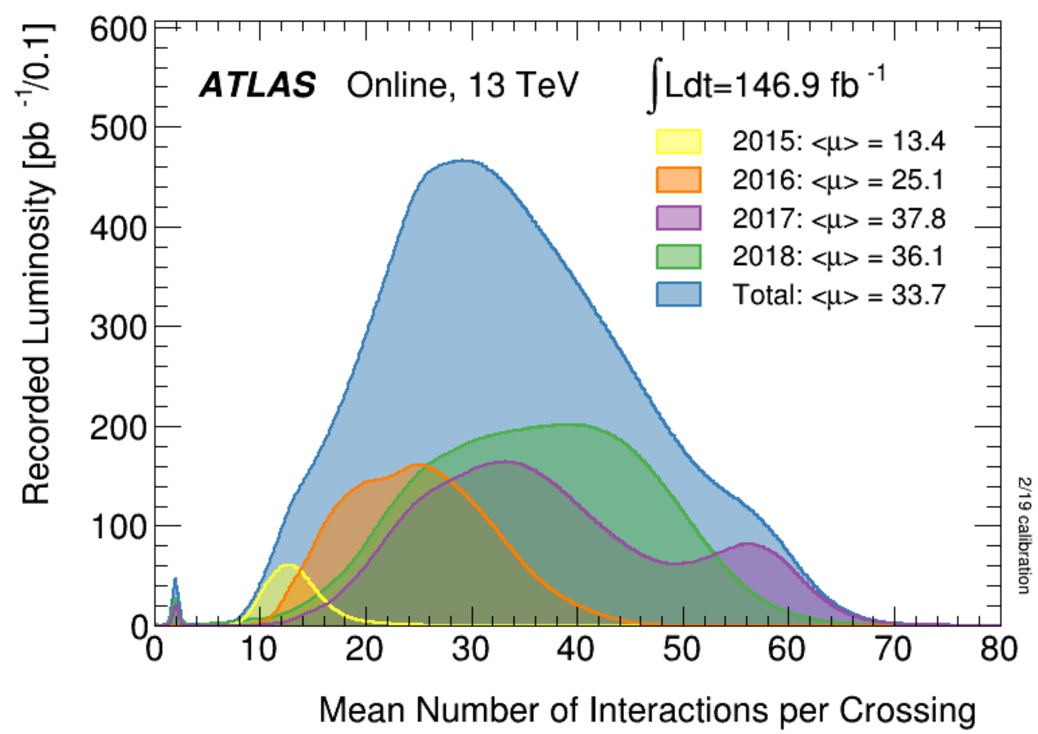

II- Characterisation of the liquid argon calorimeter pre-amplifiers for the Phase-II upgrade

- LAr calorimetry and the readout electronics
- Physics requirements for the LAr readout Phase-II Upgrades
- Results of the test performed on the proposed designs

Liquid argon (LAr) calorimetry

- The LAr technology is used in the EM calorimeter: EMB, EMEC and FCal
    - Accordion shaped lead/LAr sampling with copper-kapton electrodes
- Up to 4 layers with different cells granularity: pre-sampler, front, middle and back layers
- Incident particles create shower inside the calorimeter and ionise the LAr to create signal current which is collected by the electrodes

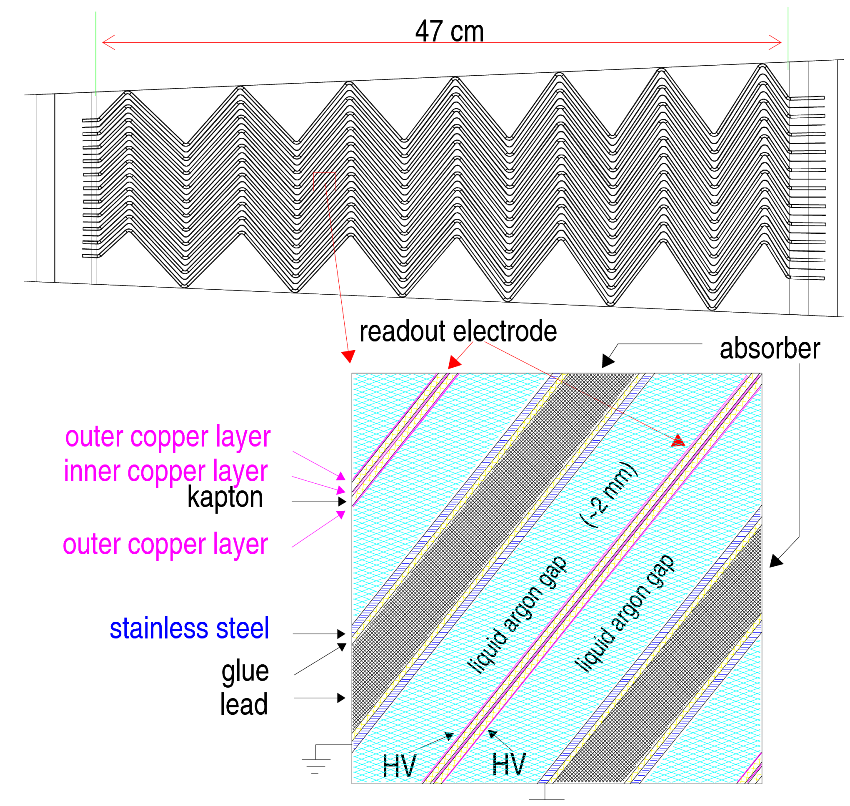

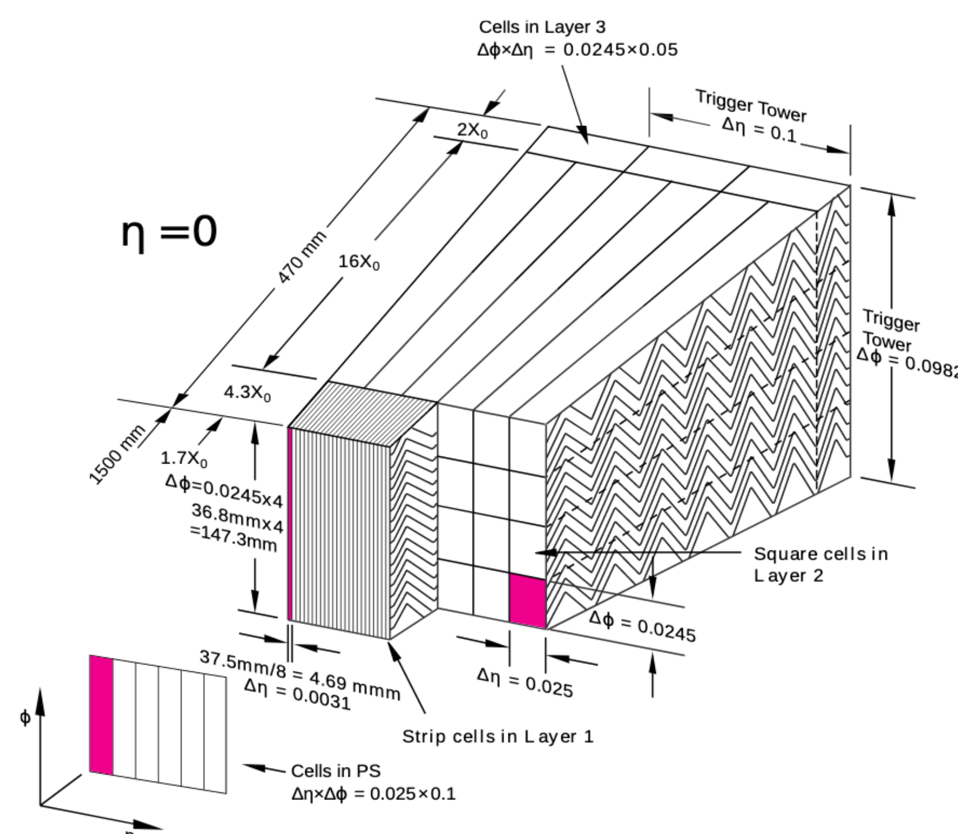

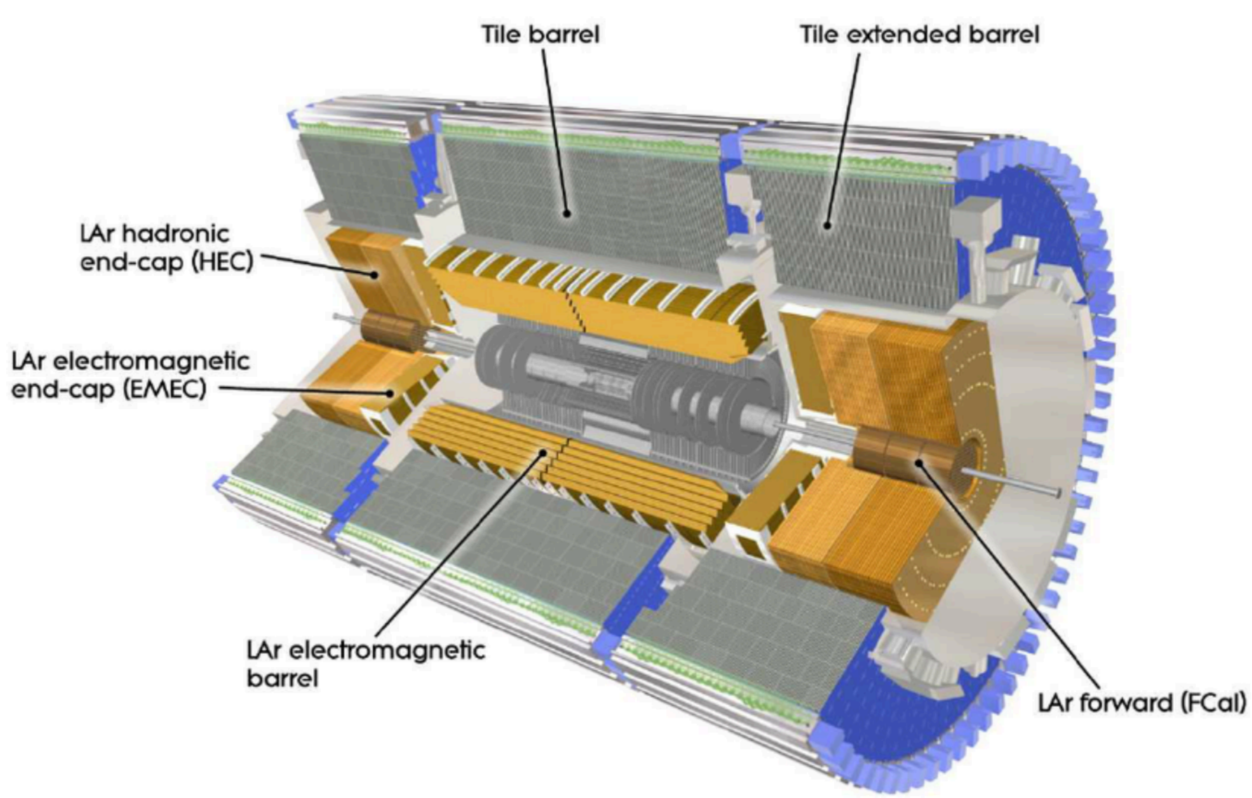

LAr current readout electronics

- The current coming from the detector is collected as a triangular pulse and then processed by the on- and off-detector electronics
- On-detector electronics, the **Front-End Boards (FEBs)** are the main elements
  - Amplify the signal pulse above the electronic noise
  - Shape into a bipolar signal using CR-(RC)^2 shaper
  - Sample at 40MHz and digitise
  - System of 3 output gains (low, middle and high)
- Sent to the off-detector for energy and time computation

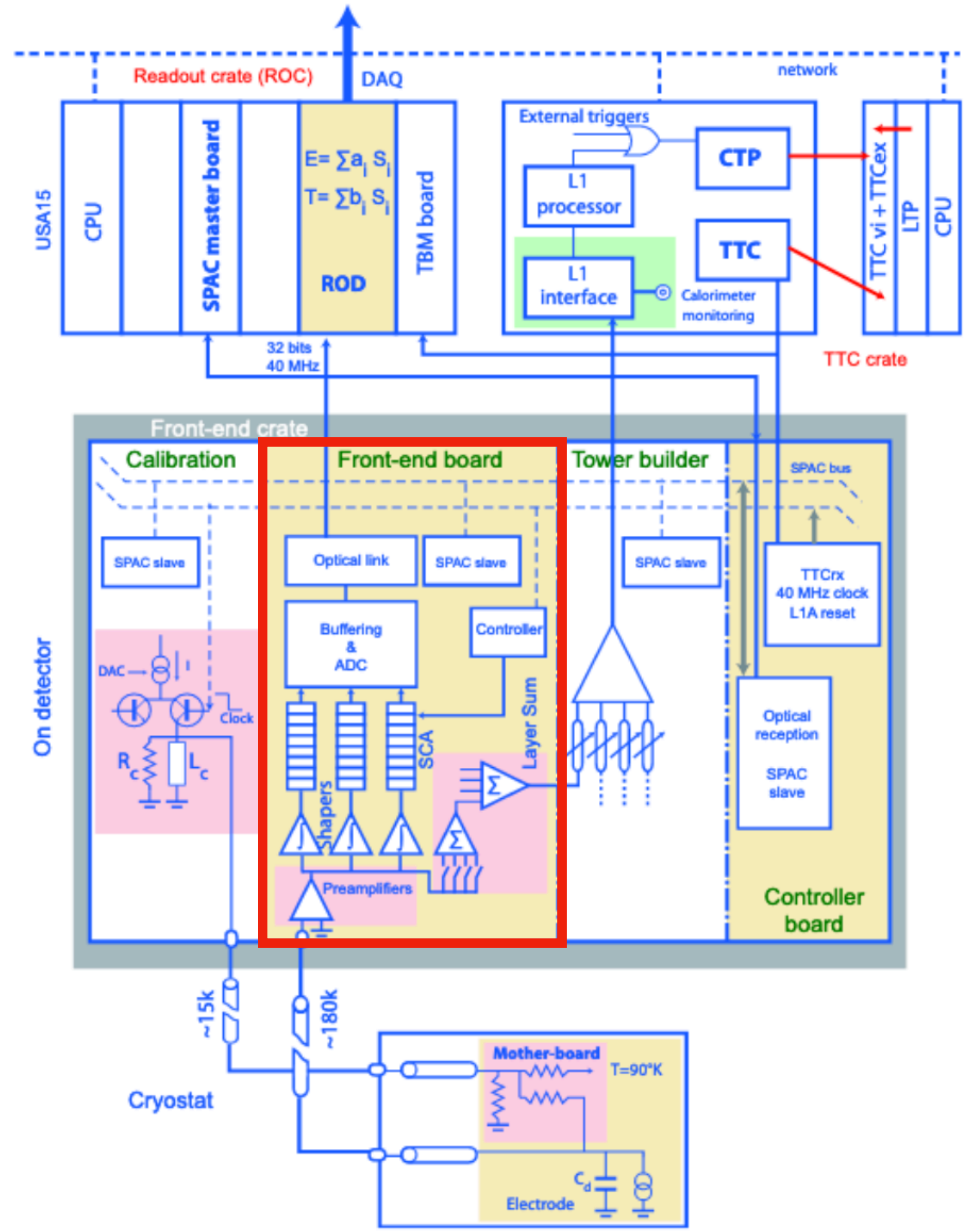

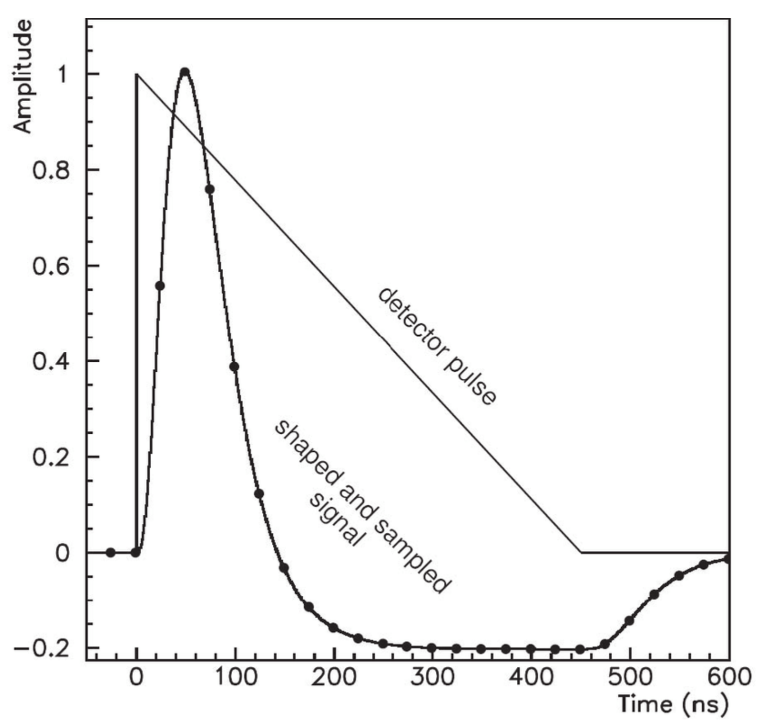

Requirements for Phase-II upgrade

- The HL-LHC project will take place after Run-3
  - Aiming to the energy up to 14TeV and deliver an integrated luminosity of $3000 fb^{-1}$
  - The LAr readout electronics will be replaced during LS3 (in 2024-2026)
- The following requirements are needed for the electronics to operate under the HL-HLC condition
  - Large dynamic range to reach up to 3 TeV
  - Linearity at the per-mill level
  - Low electronic noise: lower than the muon MIP and ideally similar to the existing electronics
  - A two gain system replacing the current three gain system

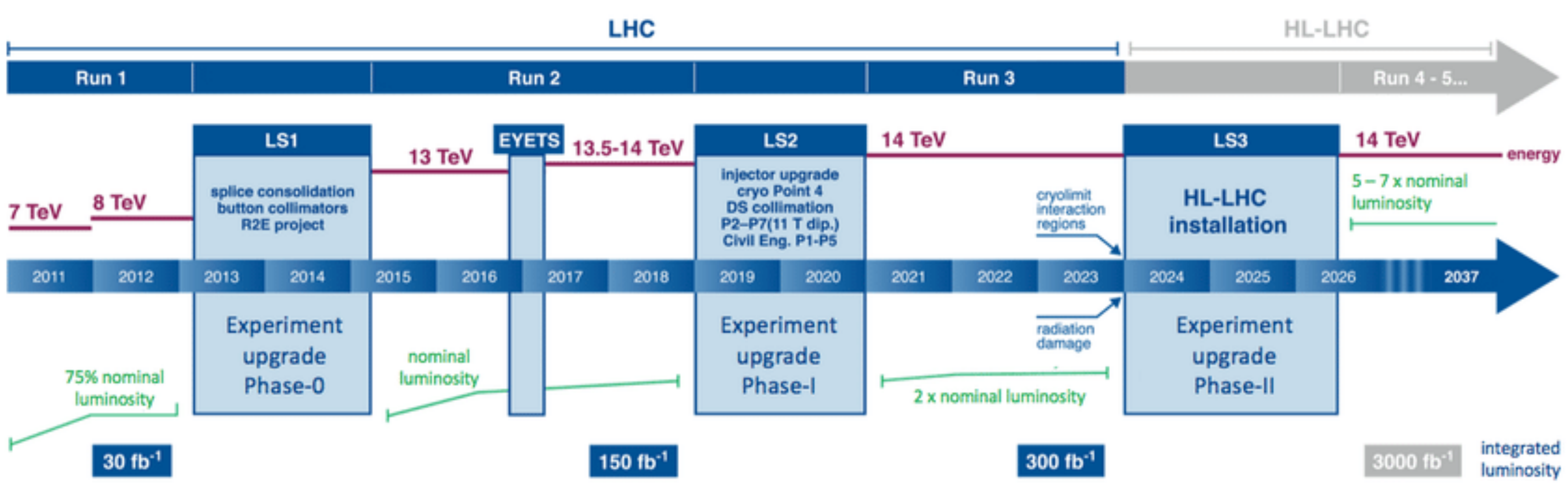

LAUROC0 and HLC1 pre-amplifier designs

- Two different types of line-adapted pre-amplifiers (PA)
  - 25Ω and 50Ω used in the middle/back and PS/front part of the detector
  - Amplify the signal into two output gains: low and high gain (LG and HG)
- Two PA/shaper ASIC designs: LAUROC0 and HLC1
- **LAUROC0:**
  - Designed at OMEGA/IJCLab using 130nm CMOS technology and received in October 2016
  - 8 different line adapted PA: 25Ω, 50Ω and 25_50Ω channels
  - HG is made on the same PA as LG
- **HLC1:**
  - Designed at BNL using 65nm CMOS technology and received in July 2017
  - 8 identical fully differential 25_50Ω channels
  - PA delivers a LG then makes an amplified copy to give the HG

LAUROC0

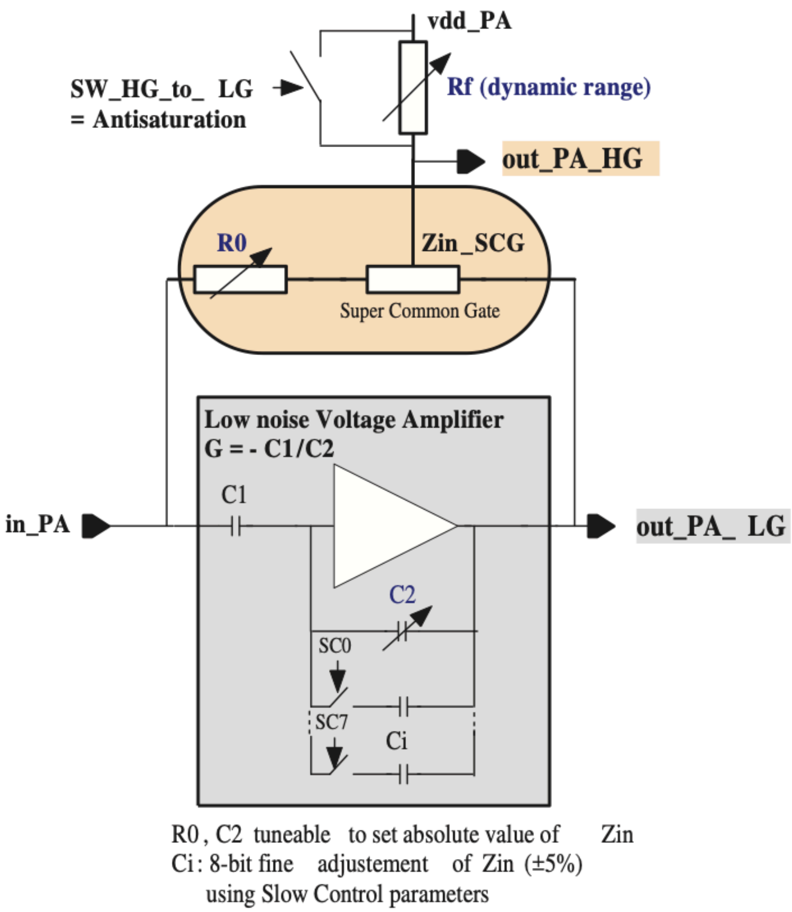

HLC1

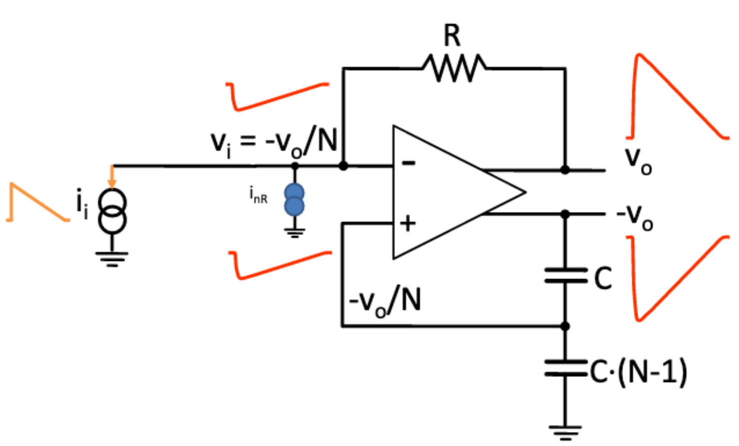

Noise measurement

- The pre-amplifier noise is measured in ENI (equivalent noise current)
- Requirements: an ENI lower than 300nA (120nA) in the 25Ω (50Ω) channel
- The existing electronic noises :150nA (45nA) in 25Ω (50Ω) channel
- Test performed using the same test bench for both designs
- The measured ENI was found to be twice larger than the expected level from simulation

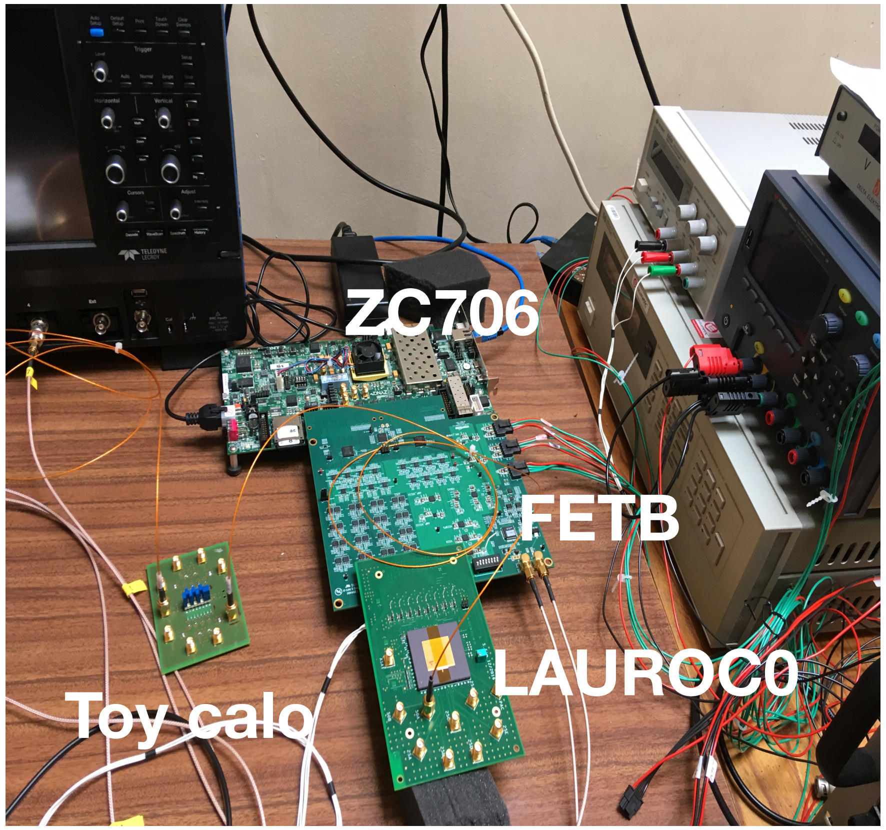

Channel	Peaking time (ns)	ENI (nA)	MIP (nA)	ENI currently (nA)
LAUROC0 25Ω A	45	326	300	150
LAUROC0 50Ω B	40	73	120	45
LAUROC0 25_50 [25Ω]	45	295	300	150
LAUROC0 25_50 [50Ω]	40	83	120	45
HLC1 25Ω	67	293	300	150
HLC1 50Ω	60	97	120	45

- The noise was **lowered** in the next iterations: 250nA for the 25Ω in LAUROC1 and 150nA for the 25Ω in ALFE

Linearity measurements

- The measured amplitudes are for each current value are fitted up to the end of the expected dynamic range to compute the non-linearity integral (INL)
- Requirements:
  - INL < 0.2% on 80% of dynamic range
  - INL< 2% at the end of the dynamic range
- A dynamic range up to 10 (2) mA in 25Ω (50Ω) channels

LAUROC0

- 25Ω LG linearity at the per mille level up to 10mA
- 50Ω LG linearity at the per mille level **only** up to 1 mA
- 25Ω and 50Ω HG: good linearity

HLC1

- All okay within requirements

- Mostly **linearity within specifications** in all channels
- The range of the 50Ω channel in LAUROC0 was **fixed** in the next iteration

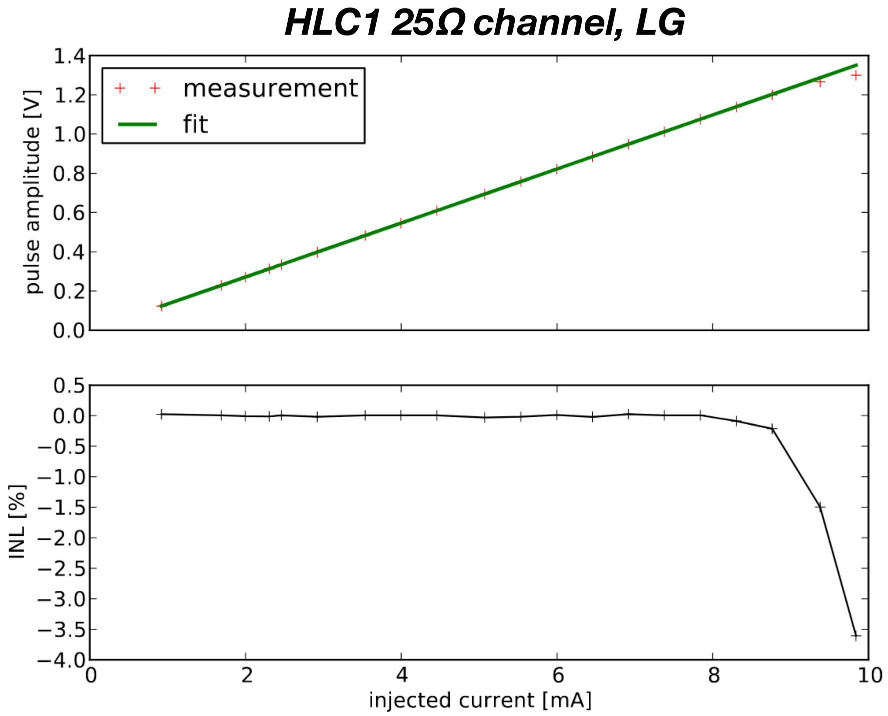

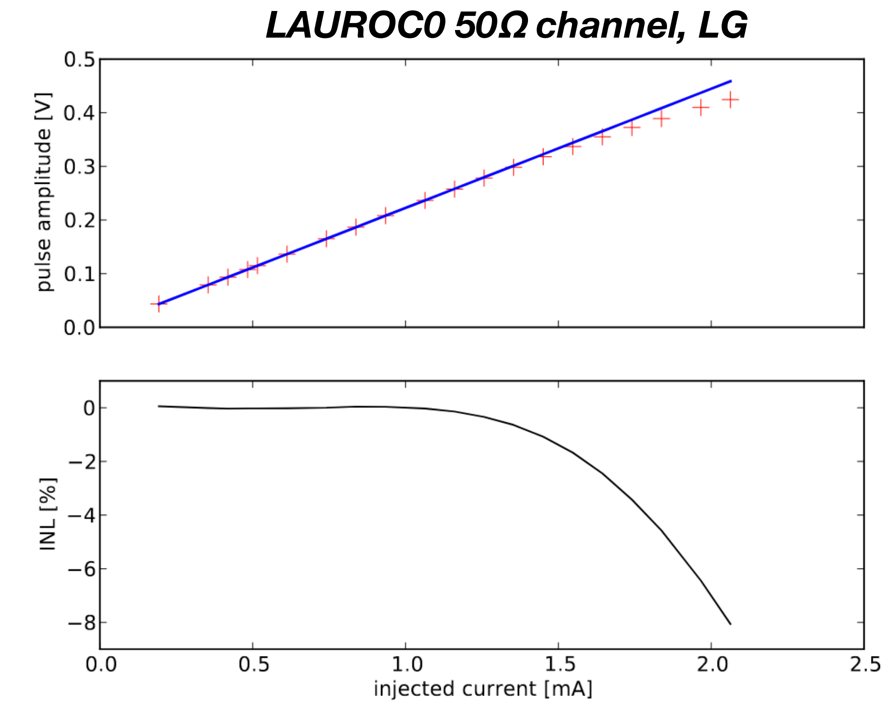

The gain scheme: Requirements

- Last step of the on-detector processing is the digitisation
- Simulation study to test the proposed two gain scheme replacing the **existing three gain system**
- Conflicting requirements to be fulfilled:
    - Digitise the whole dynamic range
    - Lowest energy: quantisation noise < electronic noise
    - Gain switching energy: quantisation noise << LAr resolution (to not degrade the total resolution)
    - All photons from $H \rightarrow \gamma\gamma$ should be in High Gain cells (necessary to reduce the intercalibration uncertainties in Higgs mass measurement)
- Assume two 14-bits ADCs to cover the 16-bits wide physics range
- Typical gain ratio : 23

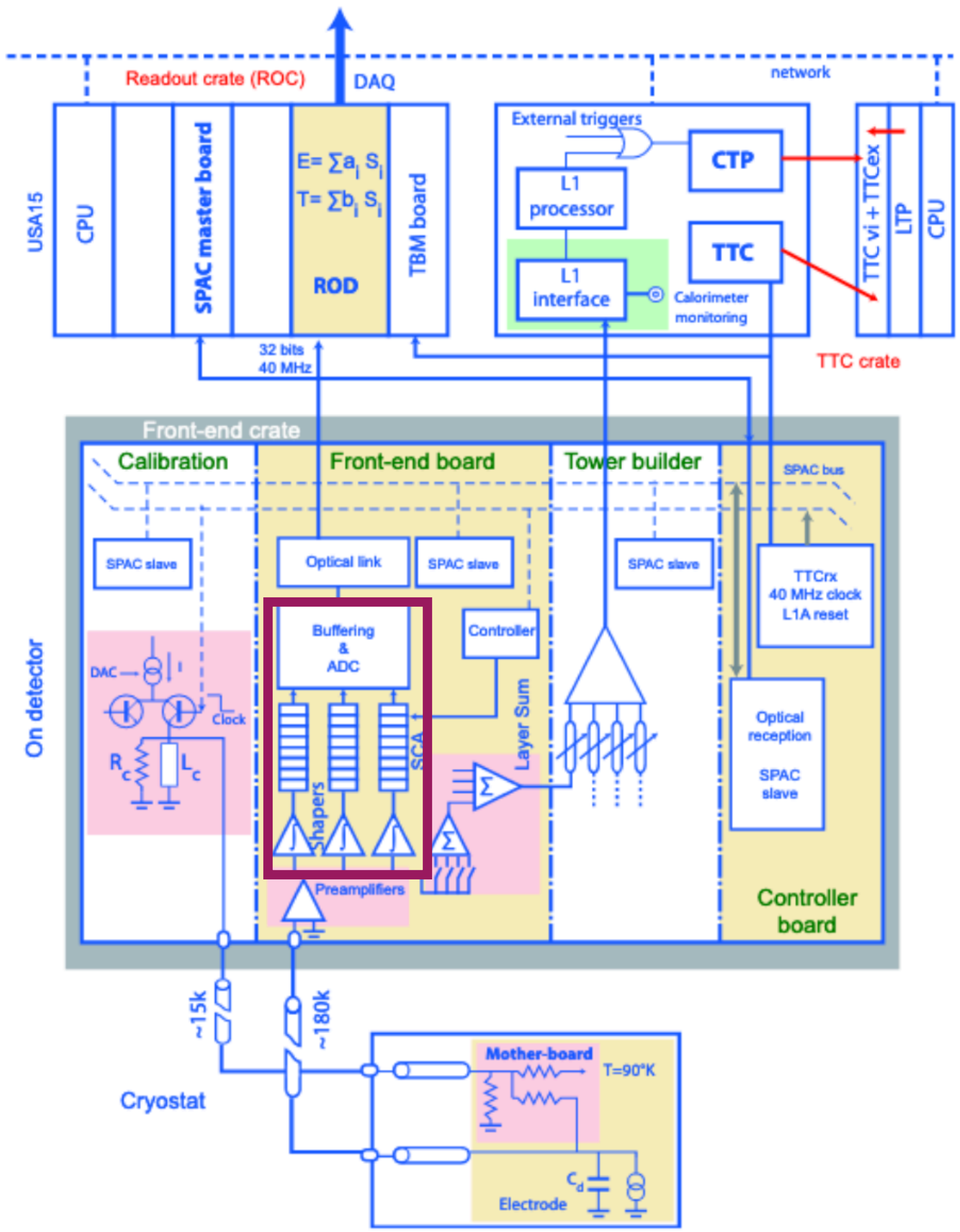

Gain ratio specification

- At gain switching energy: quantisation noise is an order of magnitude lower than the intrinsic LAr resolution: 10%/√E [GeV] ⊕ 0.2%

- Calo cells energies from H→γγ showers should be within the HG dynamic range to avoid the gain intercalibration uncertainties

  - The proposed scheme **meets the specifications:** 1.8% of the photons be in the LG front layer and 1.1% in the LG middle layer

  - Other ratios were tested and the final specification is a gain ratio of 23 ± 5

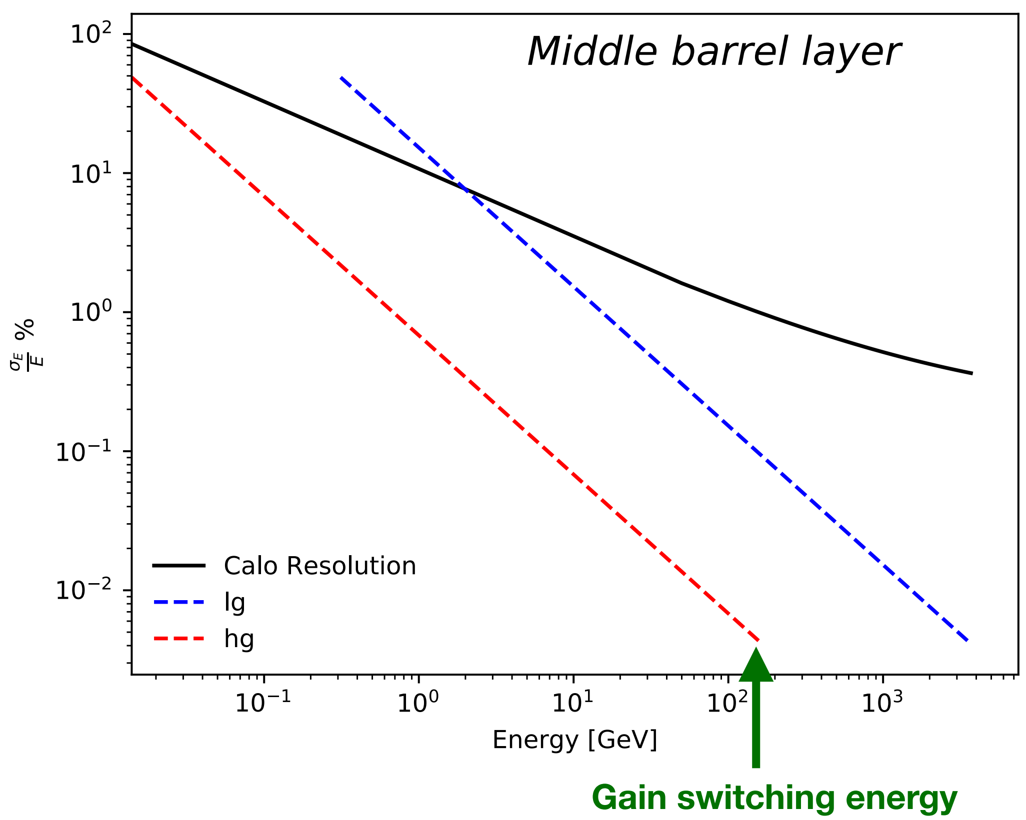

Fraction of photons with cells in the Low Gain

Gain ratio	Front layer	Middle layer
Proposed design	1.8 %	1.1%
15	0.7%	0.2%
20	2.1%	0.7%
25	4.2%	1.6%
30	6.5%	3%

III- Measurements of the Higgs boson produced in association with a vector boson and decaying to a pair of b-quarks using 139fb^{-1} data

- Overview of the *VH* ($H \rightarrow b\bar{b}$) analysis: objects and event selection, background composition and signal topology
- Events categorisation into signal and control regions
- Multi-jet background estimation
- Background modelling uncertainties using multi-dimensional reweighting method
- Results of the signal measurements

VH, H→bb motivations

- *H→ bb* is the dominant decay mode (BR~58%)
  - allows to measure the Higgs boson coupling to *b*-quarks
  - Cannot be measured inclusively: measured in the *VH* production channel
- *VH* (*WH*/*ZH*) production with leptonic V decays is of interest
  - For efficient trigger and multi-jet background suppression
  - The most sensitive channel to measure *H→ bb* decay
  - Interesting to measure the Higgs boson coupling to vector boson at high energies
- This analysis is very challenging since the signal is overwhelmed by backgrounds by many orders of magnitude

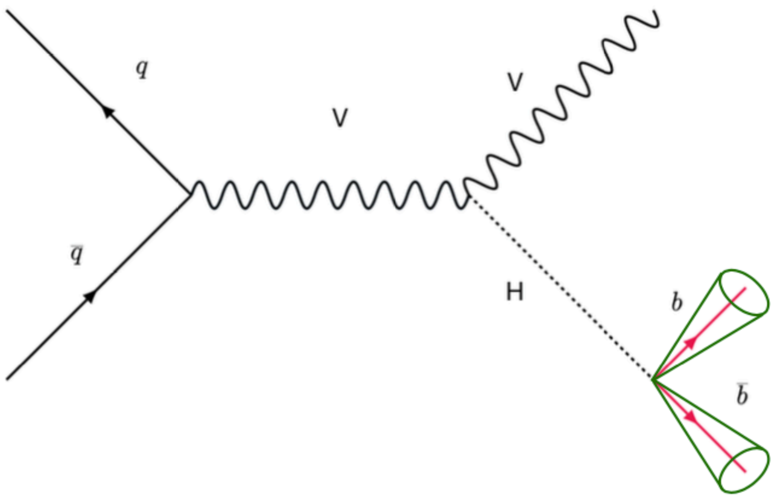

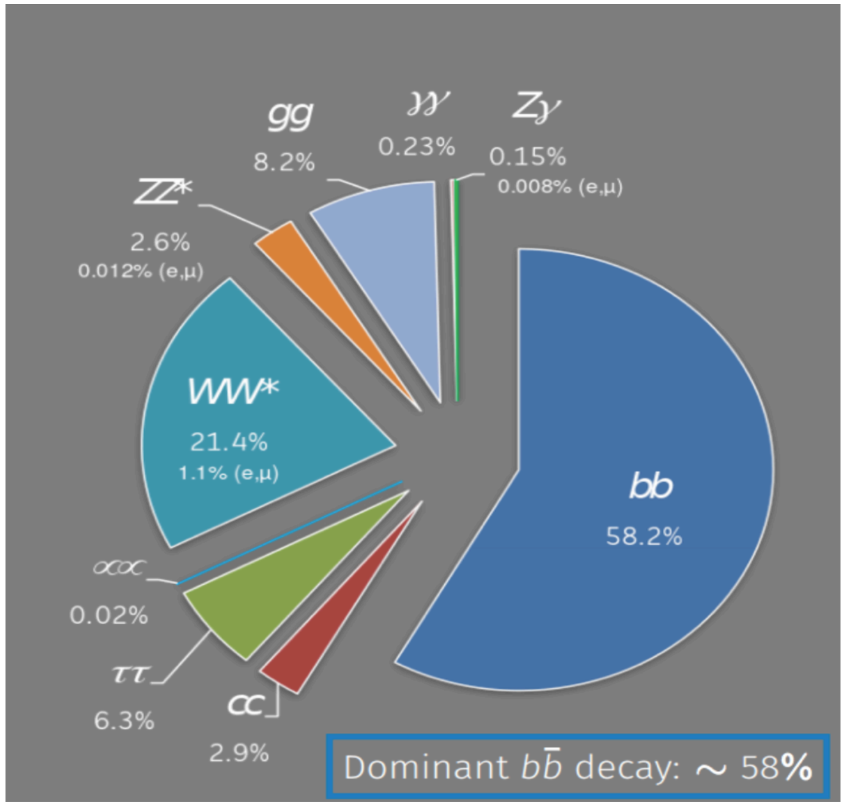

The analysis strategy

- 3 channels depending on the number of charged lepton (e or μ) in the final state
  - Targeting the following decays: *Z(➔νν)H(➔bb)*, W(➔lν)H(➔bb) and *Z(➔ll)H(➔bb)*
- Event selection to reject background events
- Event categorisation into signal and control regions
- Multivariate analysis to increase sensitivity
  - constructing a BDT with input kinematic variables
- Two cross-check analyses to validate the results: di-jet mass and diboson analyses
- A binned likelihood fit performed to measure the signal

0-lepton

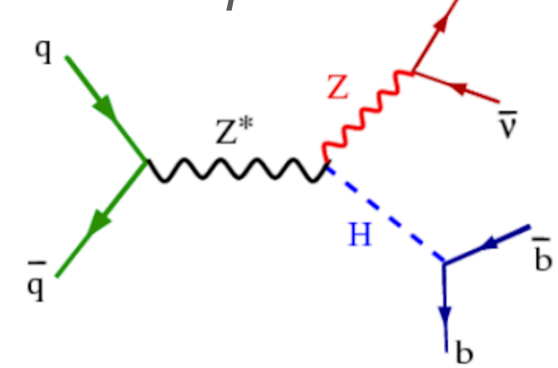

1-lepton

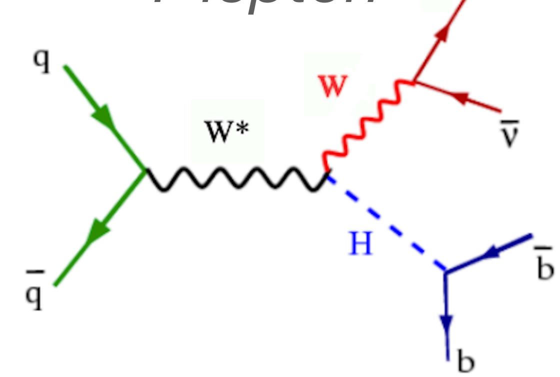

2-lepton

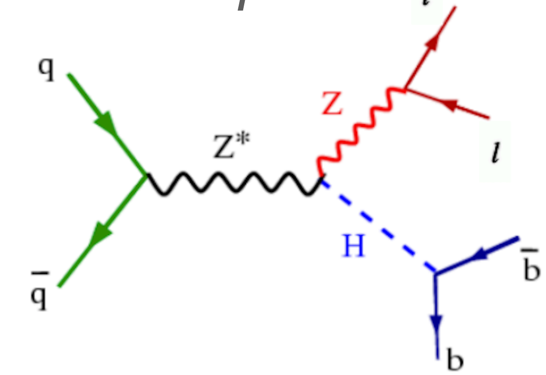

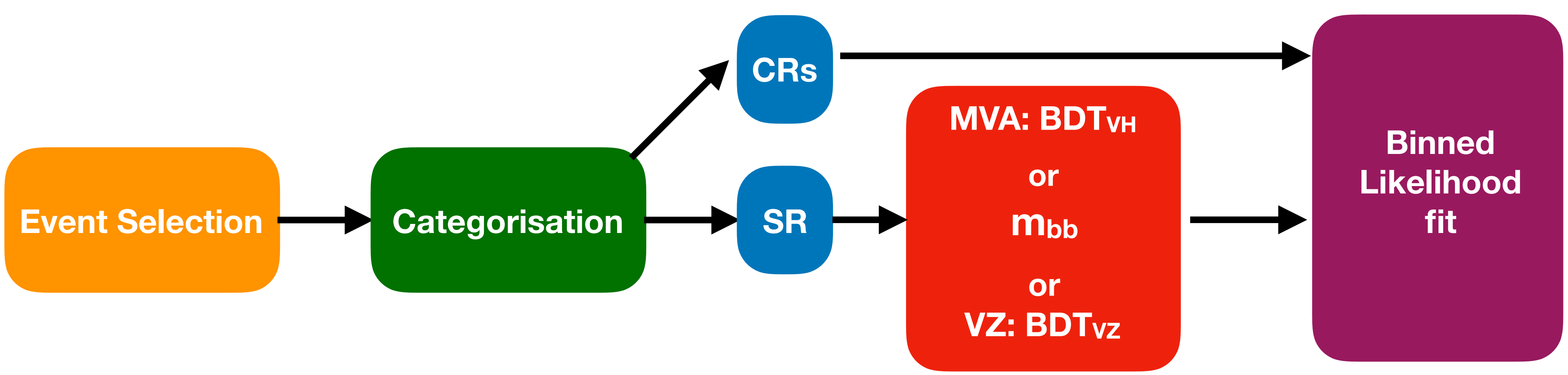

Events selection

- Events are split depending on the kinematic of the events
  - Into 2 jets or 3 jets (>= 3jets in the 2-lepton channel only) categories
- Selection cuts optimised in the three channels:

0-lepton	*1-lepton*	*2-lepton*
Common cuts		
• Leading (sub-leading) jet p_T>45 (20) GeV • Selection of events with exactly 2 *b*-jets using *b*-tagging		
Cuts on the reconstructed vector boson		
• MET trigger • 0 isolated lepton	• Single lepton or MET trigger • 1 isolated lepton	• Single lepton trigger • 2 isolated lepton • 81 GeV<m_{ll}< 101 GeV • Leptons of opposite charges for *Z(➔μμ)H* sub-channel
Cuts to reduce QCD multi-jet background		
• Anti-QCD angular cuts	• MET > 30GeV in W*(➔eν)H* sub-channel to reduce multi-jet background	

Background composition

- Use state-of-the-art Monte Carlo generators to model dominant backgrounds
  - **W+jets (Sherpa 2.2.1):** dominant in the 0- and 1-lepton channels
  - **Z+jets (Sherpa 2.2.1):** dominant in the 0- and 2-lepton channels
  - ttbar and **single-top (PowhegPythia8):** dominant in the 0- and 1-lepton channels
    - Data-driven method used to estimate the top background in the 2-lepton channel
  - **Diboson (Sherpa 2.2.1):** present in the 3 channels at lower m_{bb}
- **Multijet:** Small contribution in the 1-lepton channel

0-lepton

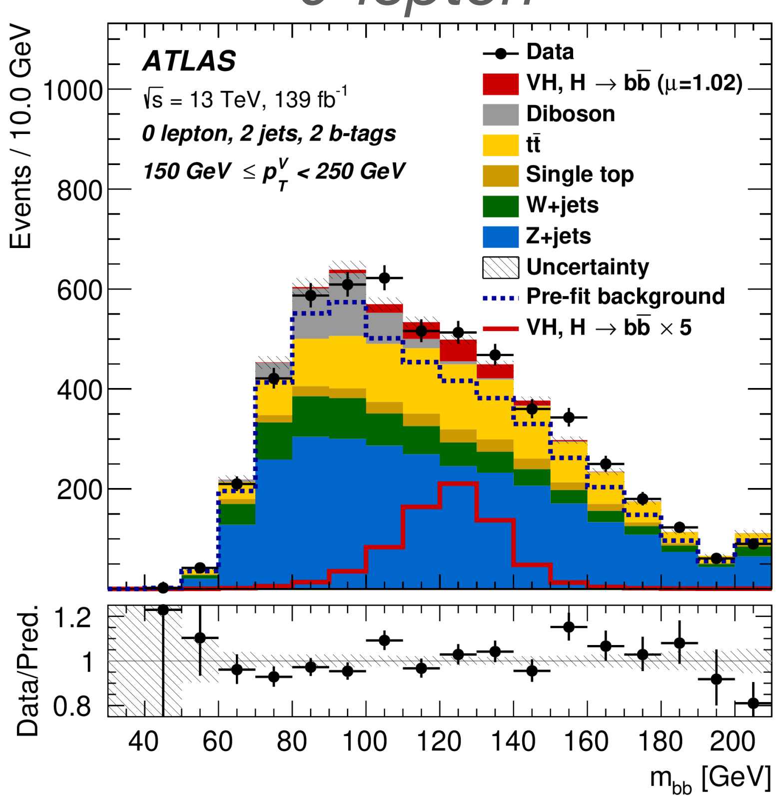

1-lepton

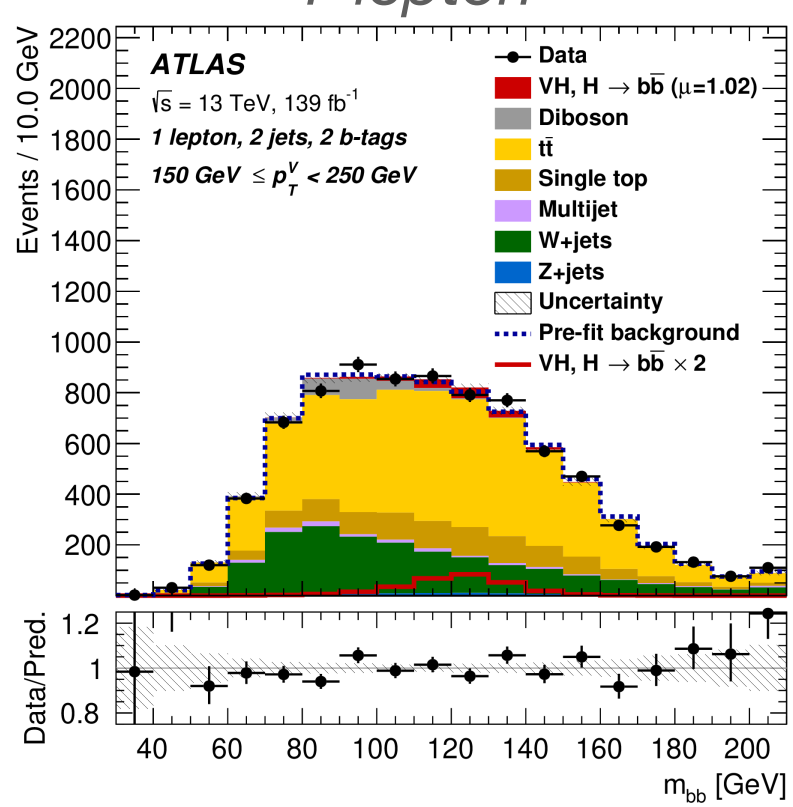

2-lepton

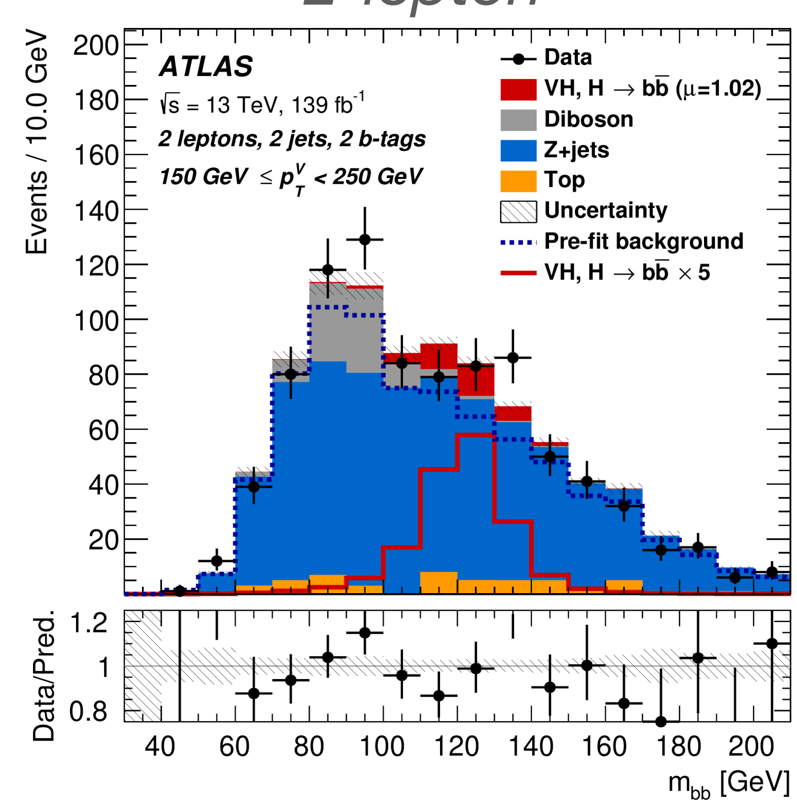

Topology of the signal

- Signal has a harder p_T^V spectrum than backgrounds
  - Improved sensitivity at high p_T^V
  - Motivation to split the spectrum into bins of p_T^V:
    - 75GeV < p_T^V < 150GeV in the 2-lepton channel
    - 150GeV < p_T^V < 250GeV and p_T^V > 250GeV in all three lepton channels
- Jets are more collimated at high p_T^V : $\Delta R_{bb} \sim 2m_{bb} / p_T^V$
- p_T^V is a very important variable in the analysis: used in the BDT training and for the event categorisation

p_T^V →
- 0-lepton: E_T^{miss}
- 1-lepton: $p_T (l + \nu)$
- 2-lepton: $p_T (l^+ + l^-)$

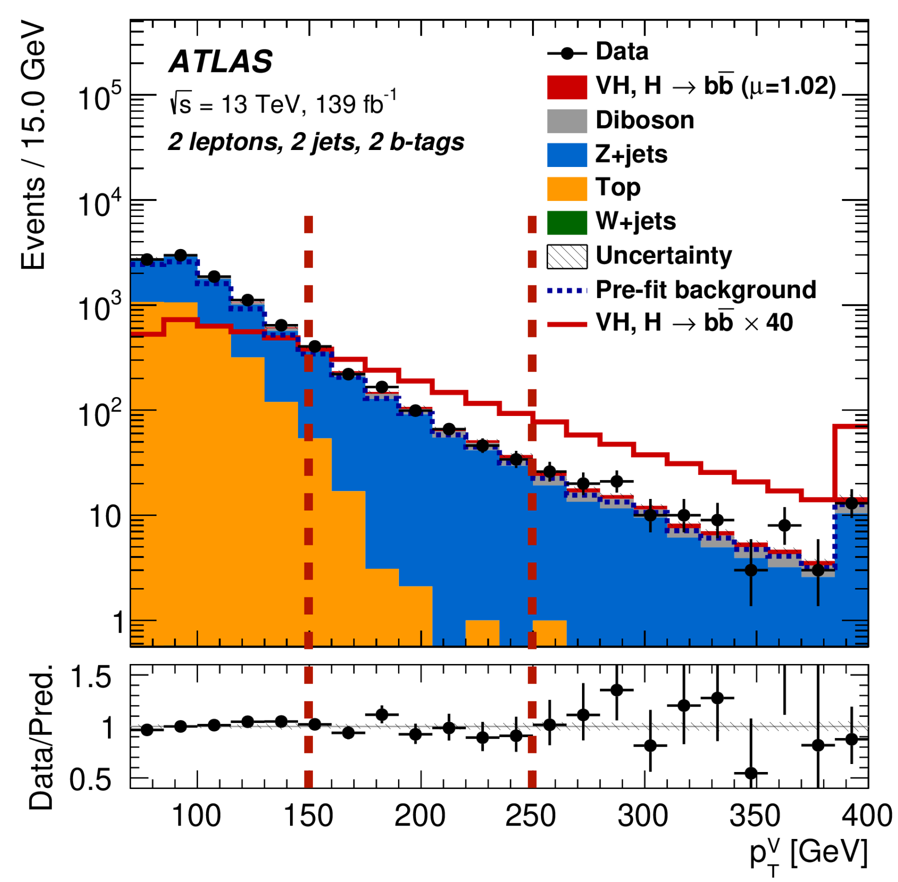

Events categorisation: Motivations

- Event selection leads to low signal purity ➔ classify events into signal and control regions
- Signal regions designed to improve the sensitivity especially in the di-jet mass analysis
- Dedicated CRs are designed to control top and W+jets background in the 1-lepton channel
  - ΔR_{bb} is a good discriminant between **W+jets** and **top**
- SR and CR studied in 1-lepton channel, but common for the three channels and the three analyses

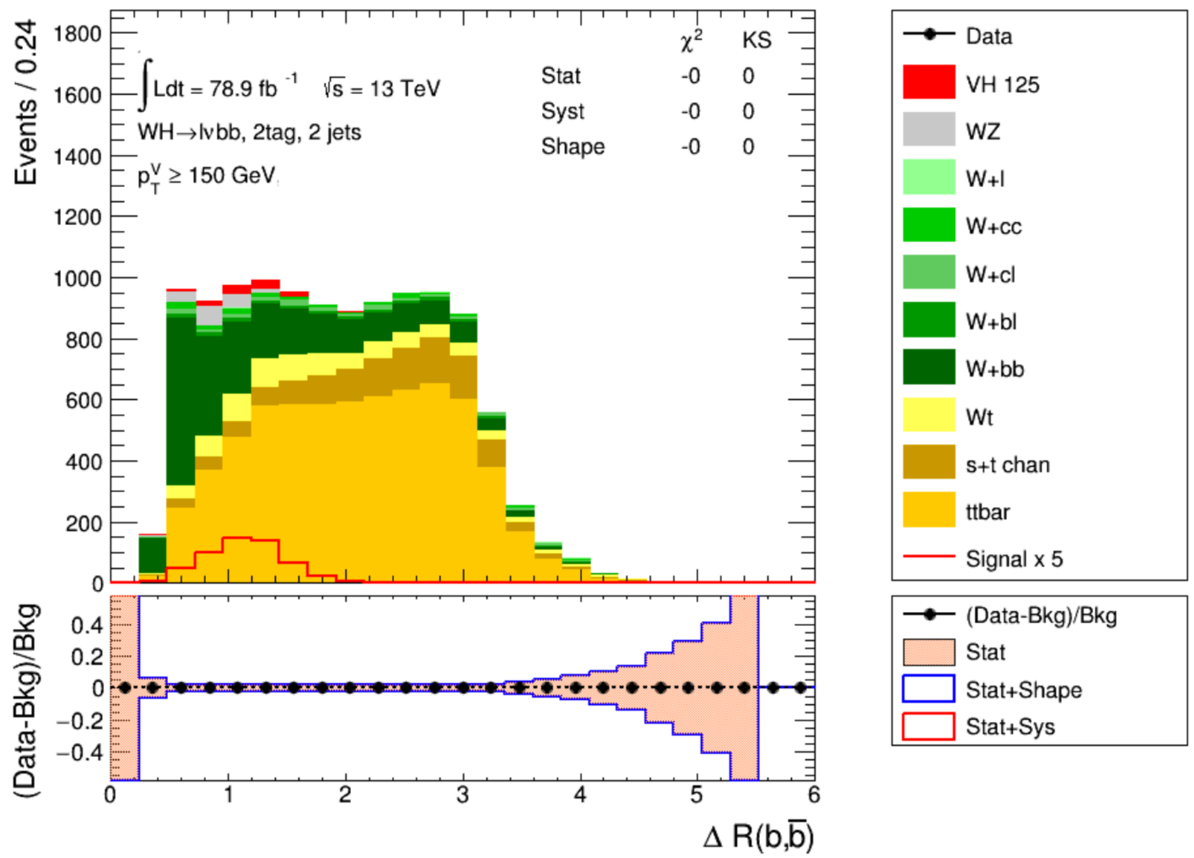

Events categorisation: Define SR/CR

- Defined using **two** continuous cuts on the signal distribution in the ΔR_{bb}-p_T^V plane
  - Cuts optimisation: low ΔR_{bb} control region highly pure in W+jets events and high ΔR_{bb} control region in ttbar events
  - Small fraction of signal (~5-15%) goes into the CRs
  - Negligible loss of sensitivity
- 0-lepton channel: high and low ΔR_{bb} control regions are rich in top and W+jets events
- 2-lepton channel: both CRs are rich in Z+jets events

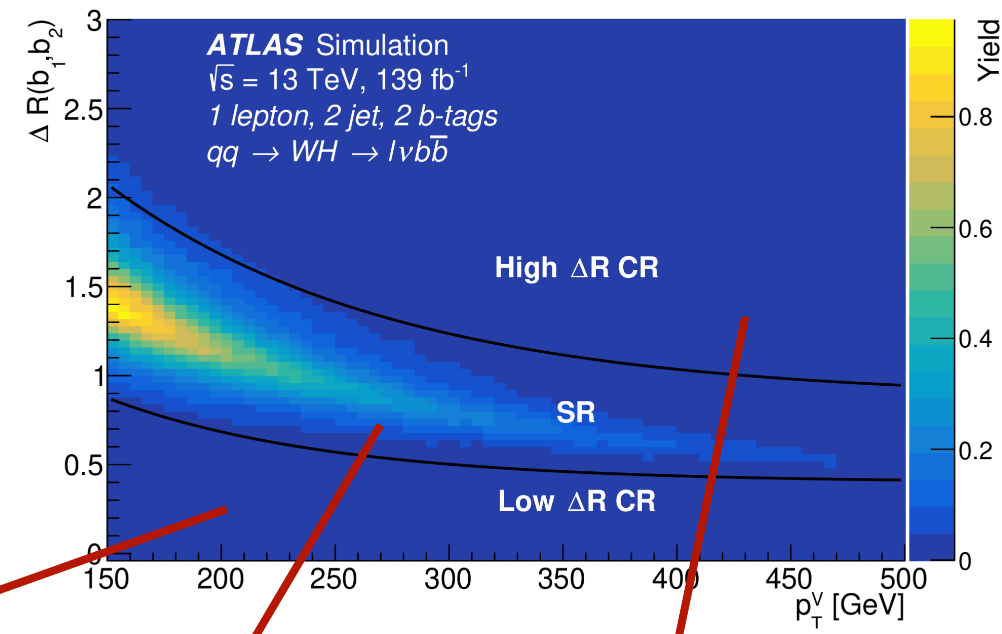

~40-~50% of W+jets

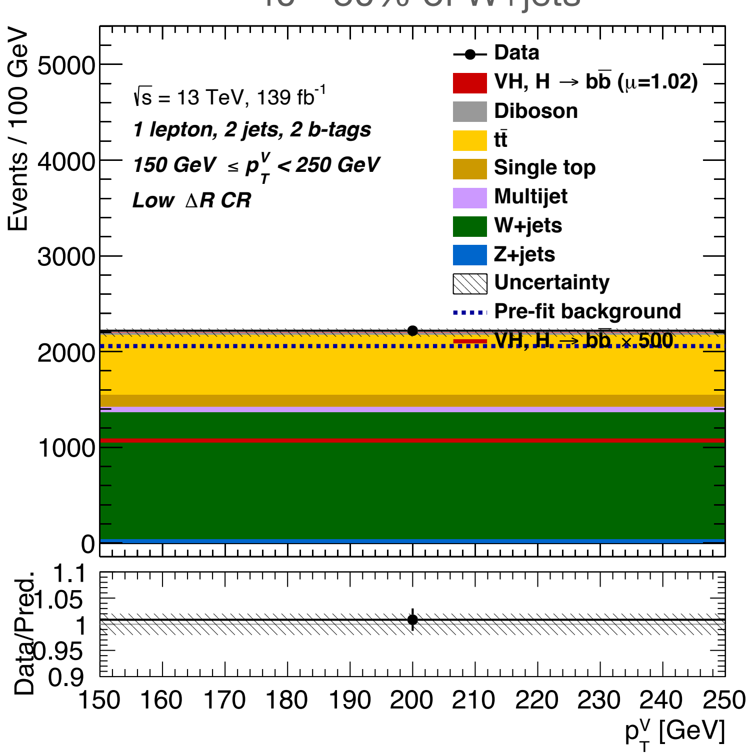

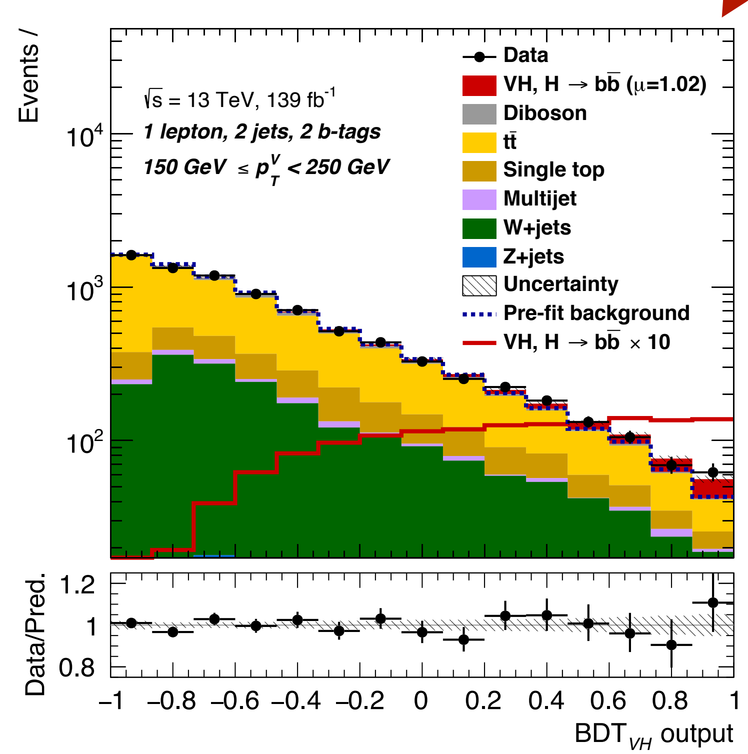

~60-~80% of top

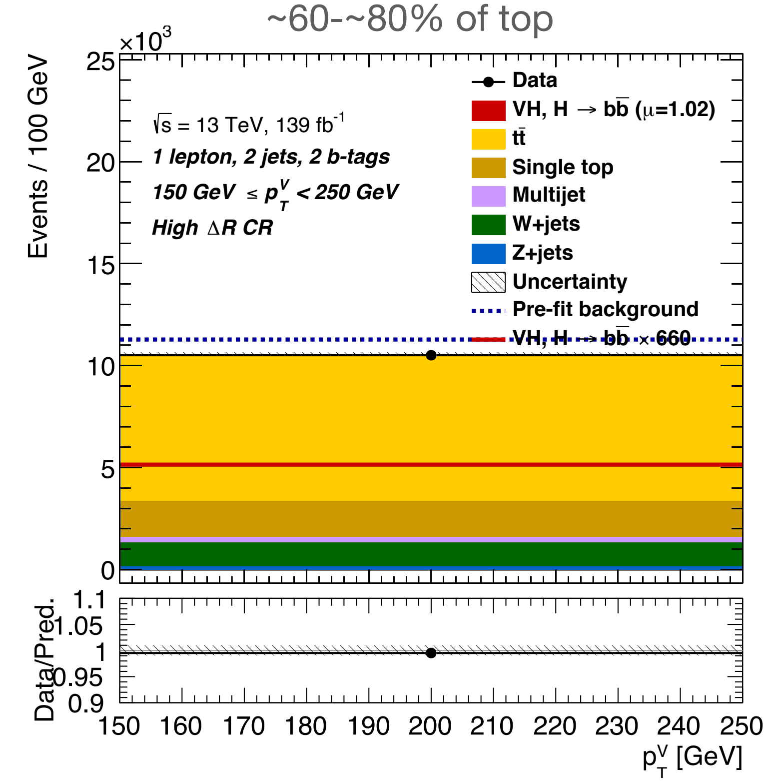

The analysis regions

- Having CRs allows to better constrain the ttbar and W+jets modelling systematics
  - Constraints were studied to make sure they are legitimate
- The analysis includes 14 signal regions and 28 control regions
  - The BDT_{VH}, m_{bb} or the BDT_{VZ} shapes are used in the SR
  - The yields are used in the CRs
- The background constraints are propagated across the three channels

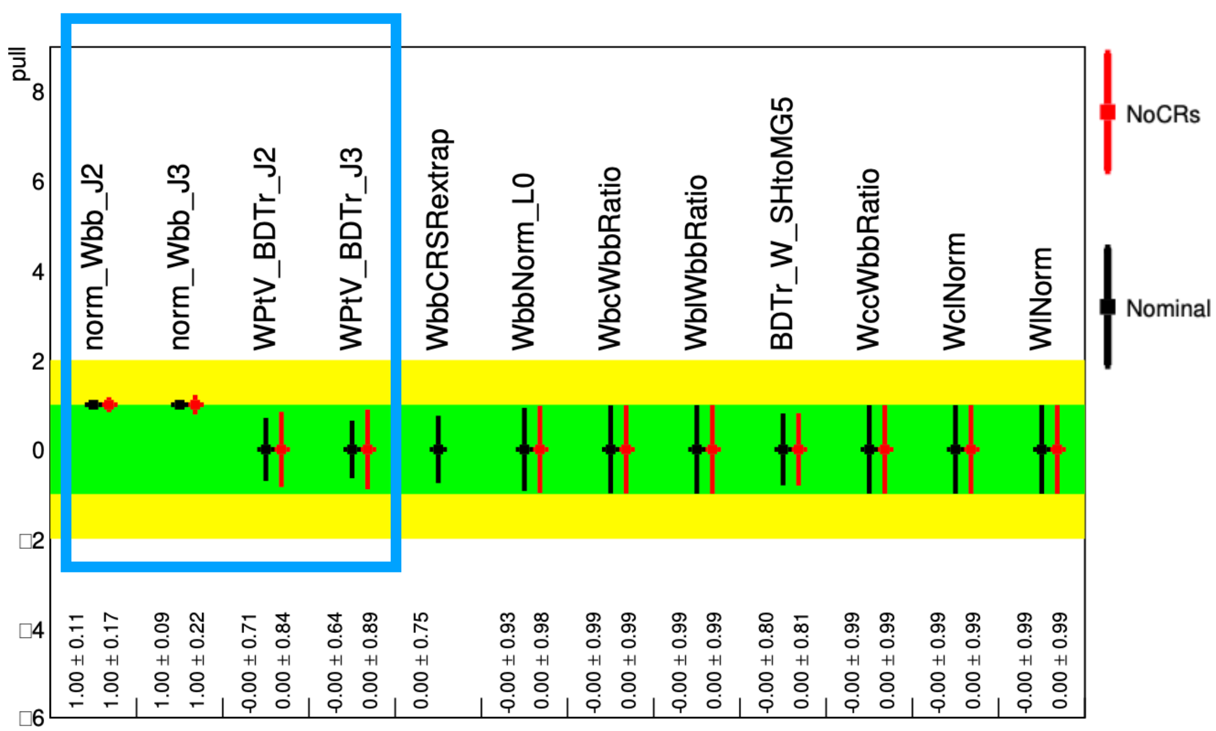

Multi-jet in the 1-lepton channel

- The multi-jet (MJ) contamination is negligible in the 0-lepton and in the 2-lepton due to event selection
- Small multi-jet contamination is expected in the 1-lepton channel
  - **Isolation selection** reduces the contamination of this background
  - Coming from non-prompt objects: semi-leptonic decays of hadrons inside the detector, converted photons and mis-identified jets
  - Different MJ sources coming from electrons and muons
  - Important to correctly estimate this background
- Monte Carlo generators cannot be used for the modelling
  - Difficulties to reproduce accurately fake leptons and lack of statistics
- A data-driven method have been developed for the MJ modelling

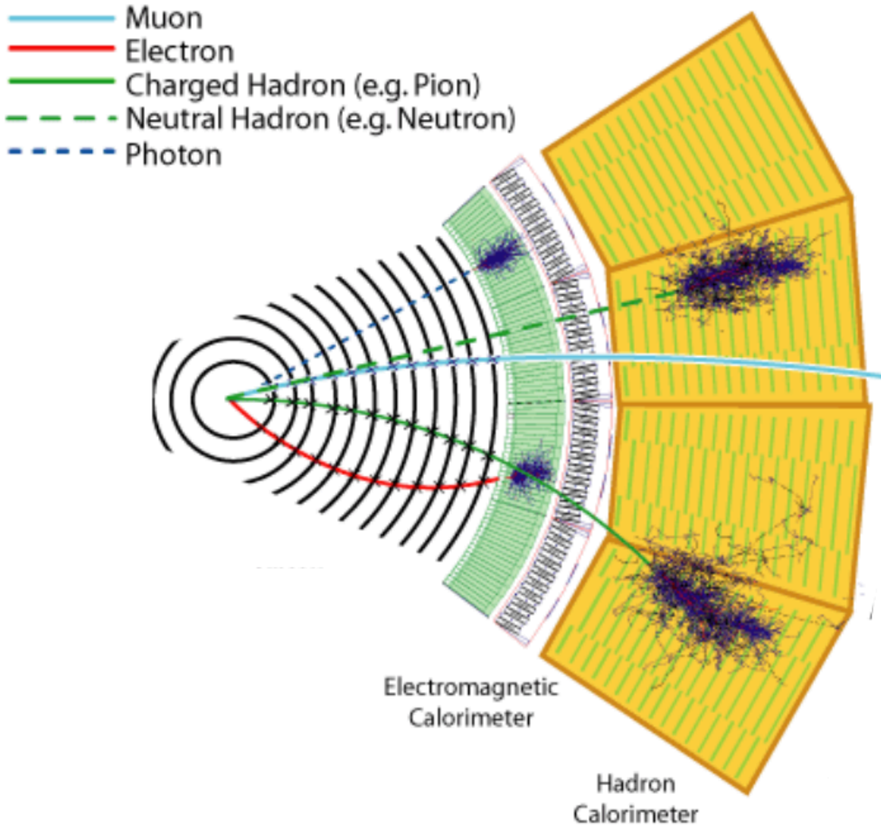

Multi-jet estimation

- MJ estimation using template fit method
  - template obtained in the **1 *b*-tag region with inverted lepton isolation**
  - from subtracting EW bkg from data
- Template fit performed in the **2 *b*-tag region with isolated lepton**
  - On the m_T^W distribution (best discriminant) to fix the **Top**, **W+jets** and **MJ** normalisations
- MJ fractions of less than 1% but up to ~4% in the muon 2-jet channel

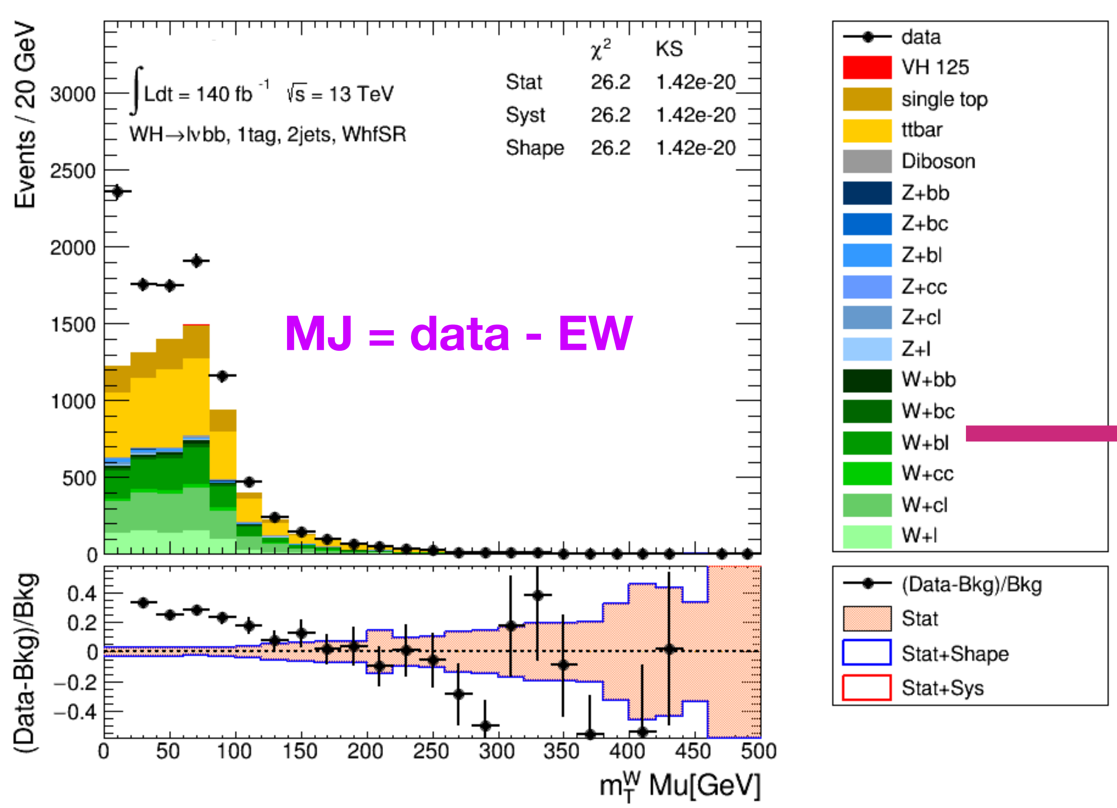

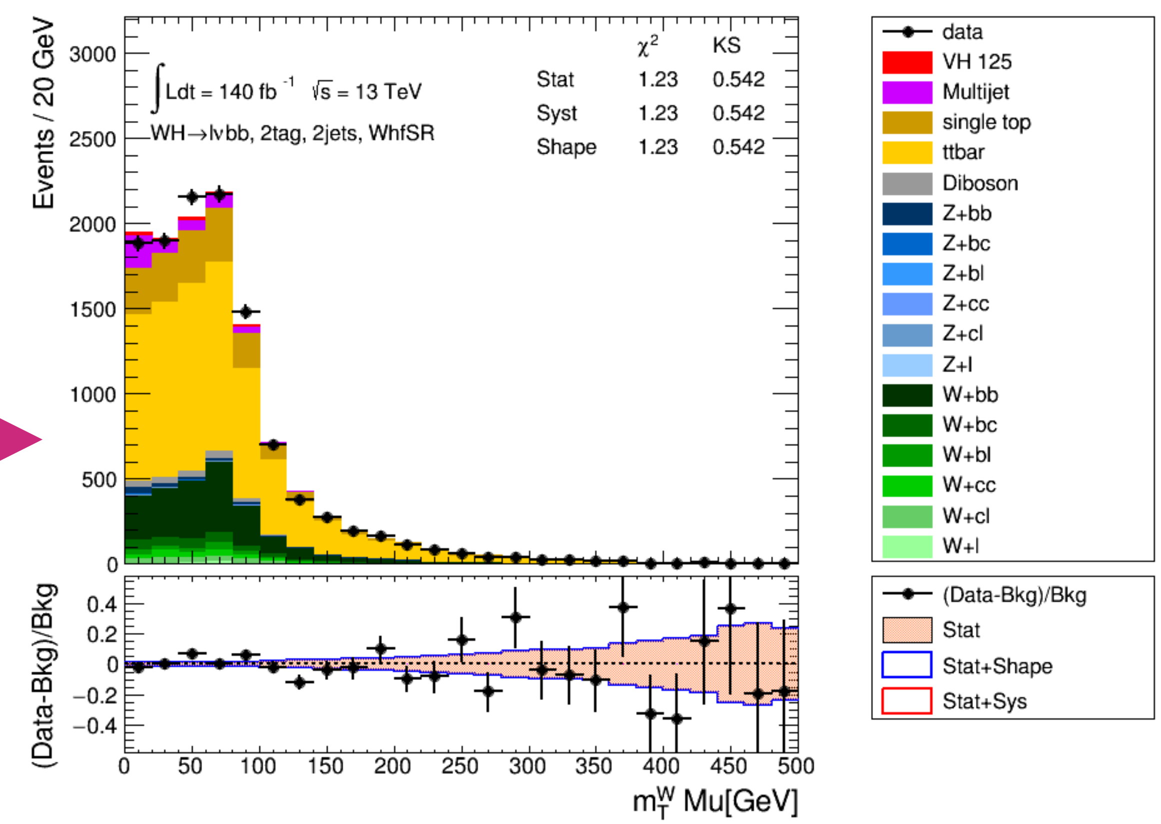

Multi-jet systematic uncertainties

- Many sources of uncertainties were assessed to the estimation
- They cover the multi-jet **shape** uncertainties by changing the multi-jet BDT distribution entering the final likelihood fit
  - Vary the definition of the MJ isolation selection
  - Vary the normalisation of the Top and W+jet backgrounds
- They cover the multi-jet **normalisation** uncertainties by changing the multi-jet m_T^W distribution in the template fit
  - Using the $\Delta\Phi$(MET,lep) discriminant instead of m_T^W
  - Remove the cuts intended to reduce the multi-jet contamination

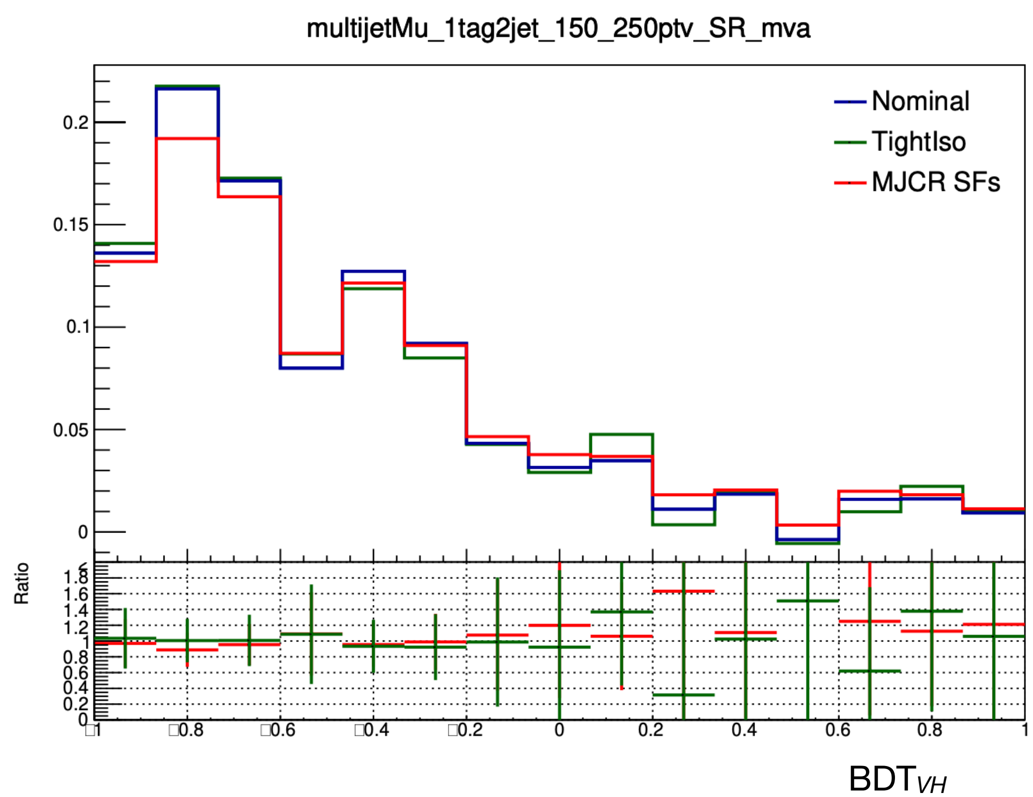

Region	MJ Fractions (%)
$p_T^V > 150\,GeV$ region	
2-tag, 2-jet, e	$0.7^{+1.4}_{-0.7}$
2-tag, 2-jet, μ	$3.8^{+1.8}_{-1.1}$
2-tag, 3-jet, e	$0.13^{+0.13}_{-0.13}$
2-tag, 3-jet, μ	$0.06^{+0.06}_{-0.06}$

Background modelling

- Normalisations of the main backgrounds floated within the global likelihood fit (**ttbar**, **W+jets**, **Z+jets**)
    - Small uncertainties because of the dedicated control regions

Process and Category	Normalisation factor
$t\bar{t}$ 2-jet	0.98 ± 0.09
$t\bar{t}$ 3-jet	0.93 ± 0.06
$W+$ heavy flavors 2-jet	1.06 ± 0.11
$W+$ heavy flavors 3-jet	1.15 ± 0.09
$Z+$ heavy flavors 2-jet, $75 < p_T^V < 150\,\text{GeV}$	1.28 ± 0.08
$Z+$ heavy flavors 3-jet, $75 < p_T^V < 150\,\text{GeV}$	1.17 ± 0.05
$Z+$ heavy flavors 2-jet, $p_T^V > 150\,\text{GeV}$	1.16 ± 0.07
$Z+$ heavy flavors 3-jet, $p_T^V > 150\,\text{GeV}$	1.09 ± 0.04

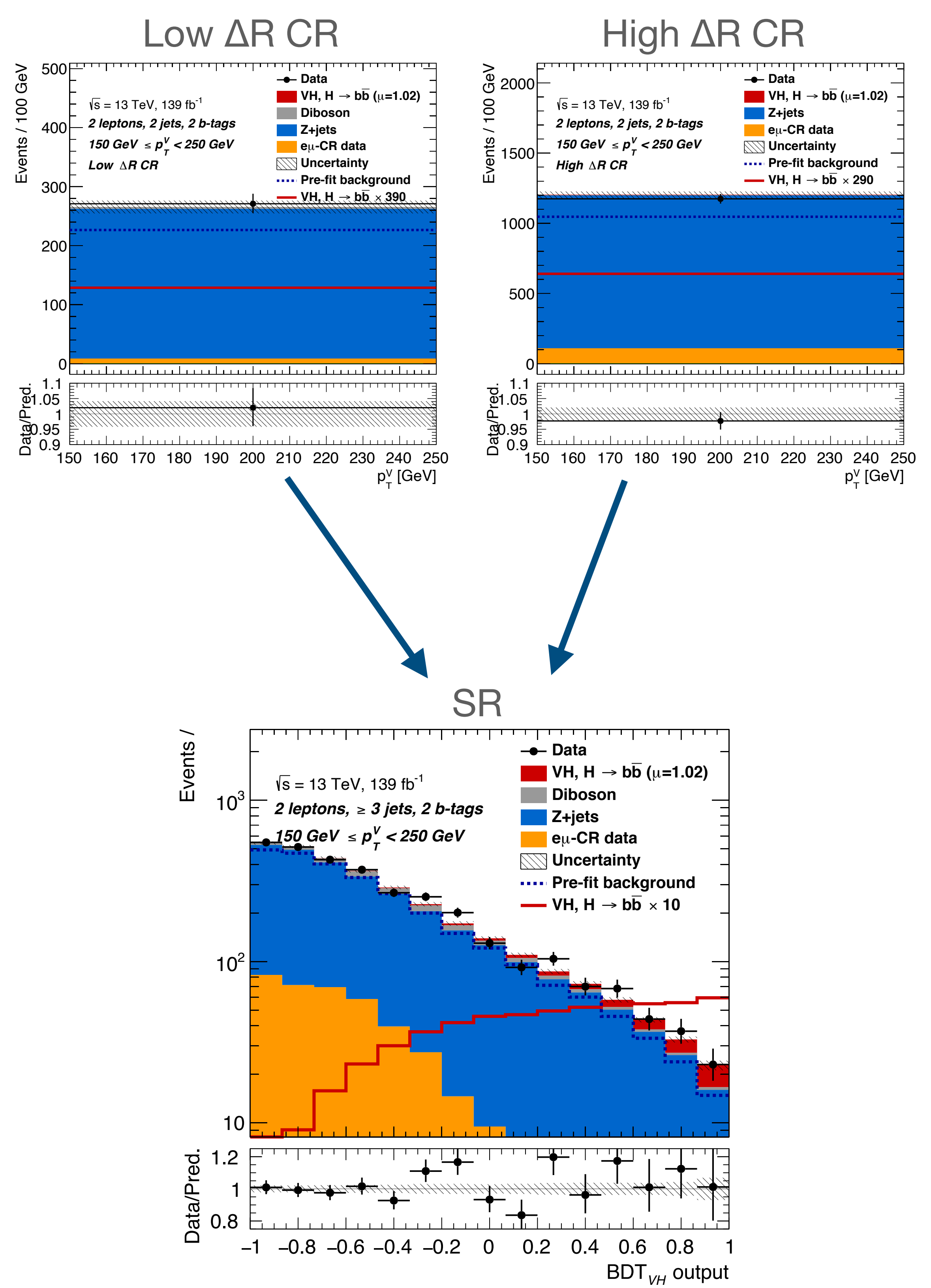

- Systematic uncertainties are assigned to Monte Carlo background predictions
- Acceptance uncertainties are assigned to the bkg predictions:
    - To account for extrapolation between regions/categories and flavour composition
- Shape uncertainties also implemented
    - To quantify the effect of the change in the Monte Carlo template prediction

Background shape uncertainties

- The usual method is to compare bin-by-bin to all possible variations on the final discriminant of the analysis
  - Cannot be done due to lack of MC statistics in the alternative generators
- Therefore re-weight the nominal distribution to morph it into the variation
- Parametrised from MC generator variations
  - From the p_T^V and the m_{bb} distributions (most important variables of the analysis)
- A new N-dimensional reweighting method have been developed using BDTs
  - To probe different corners of the phase space
  - Allows to cover the shape variation on all the kinematic variables

ttbar, 1-lepton, 3-jet

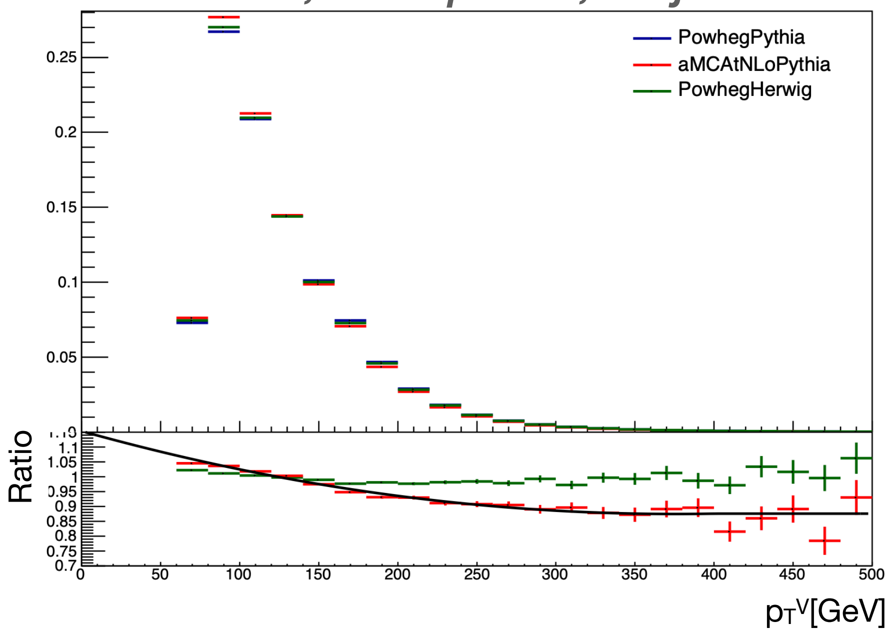

ttbar, 0-lepton, 3-jet

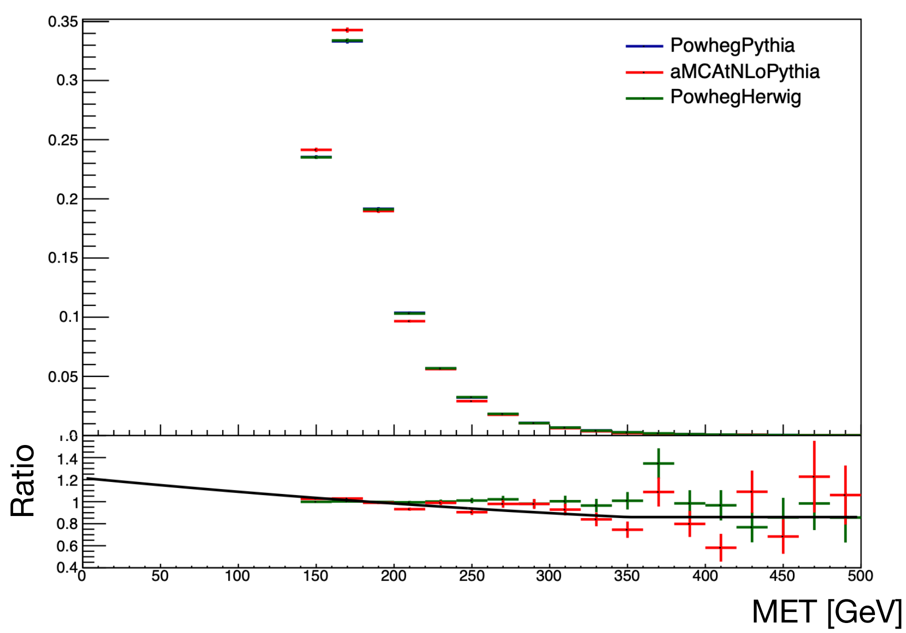

BDT-based systematics: Methodology

- N-dimensional reweighting, or BDT reweighting (BDTr), does not focus only on m_{bb} and p_T^V but takes into account the correlations between all variables
  - By using a BDT to separate the nominal and the alternative generator
- Method studied and developed in the 1-lepton channel for ttbar background
  - Systematics derived from the matrix element and parton shower variations separately
- Method adopted for ttbar and W+jets modelling in the 0- and 1-lepton channels

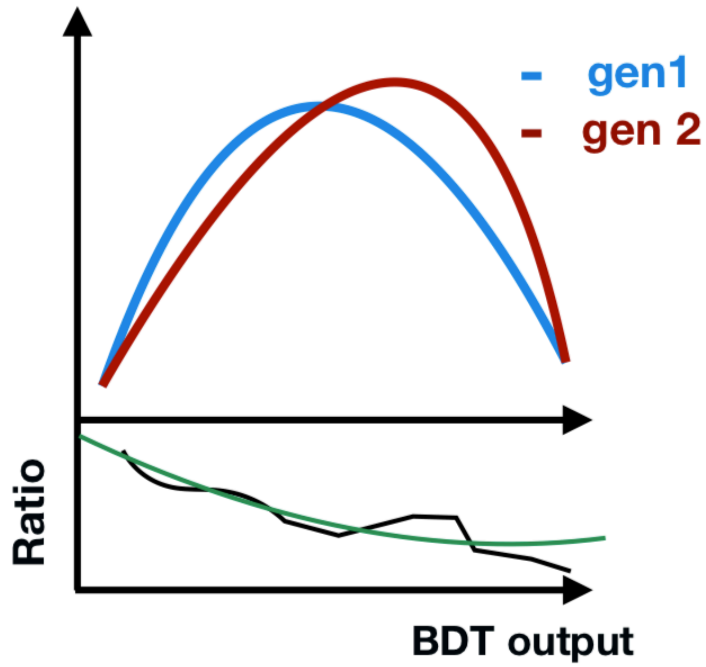

BDT-based systematics: Application

- Two different BDTs are trained to separate between the nominal PowhegPythia8 generator and either aMCAtNLoPythia8 (ME) or PowhegHerwig7 (PS) alternative generators

- The BDT outputs ratio is used to re-weight the distributions entering the fit

- The BDT-based reweighting method allowed to transform the nominal into the alternative generator with good closure

    - Sometimes not perfect in the tails, but was shown to have negligible effect

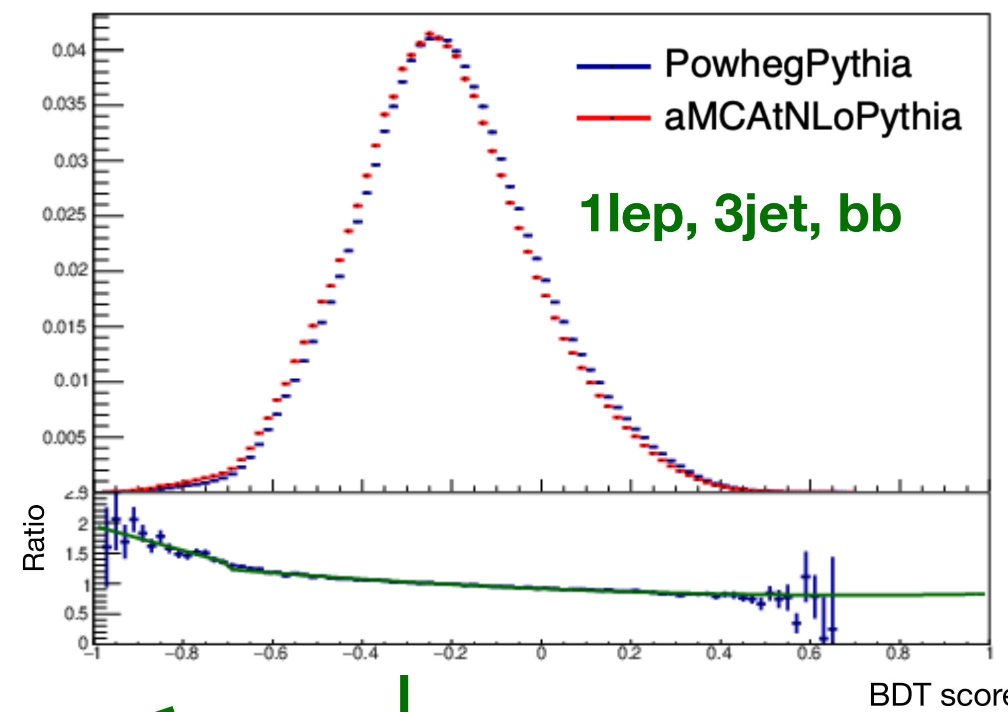

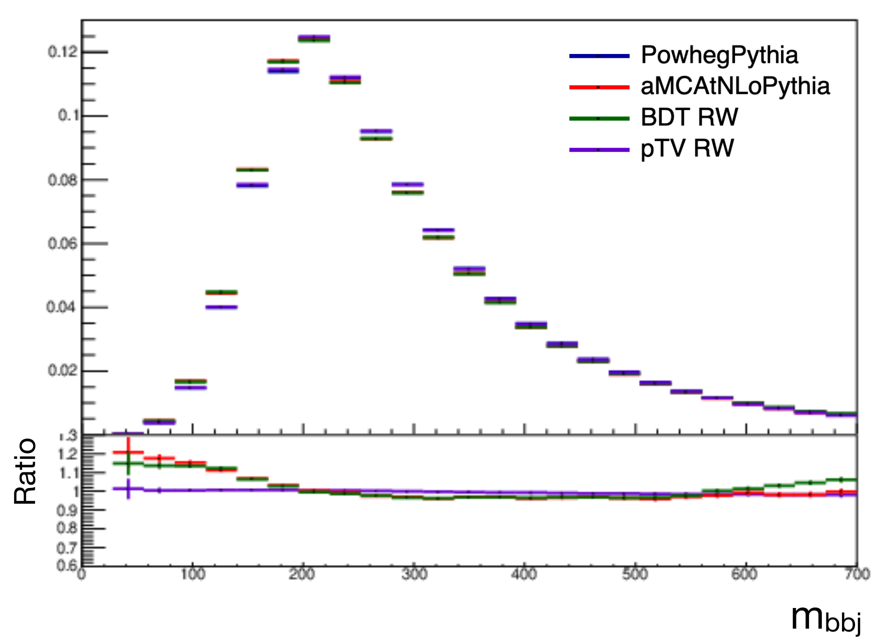

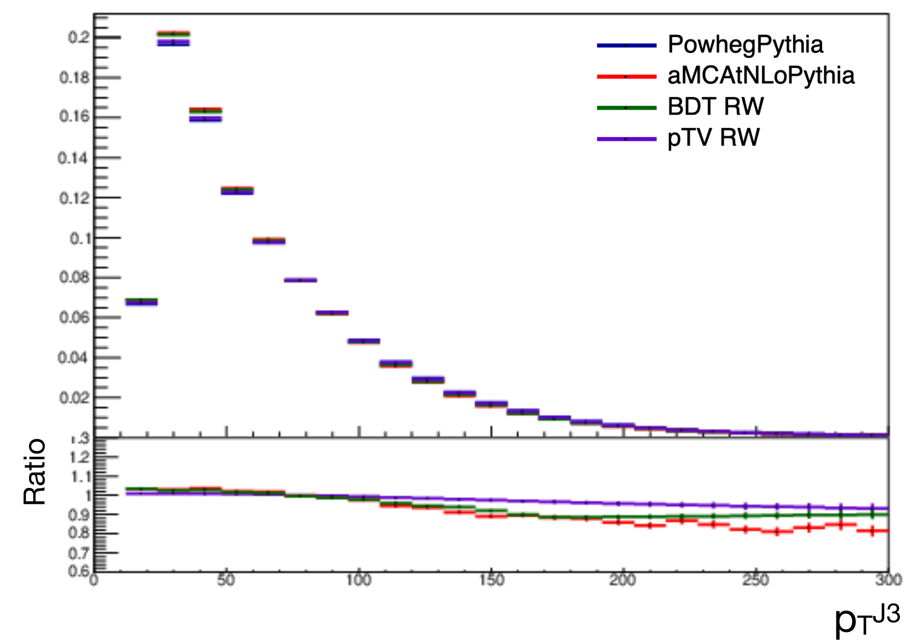

Validation analysis

- The diboson analysis is a robust validation of the background model since the process is very similar to *VH*
  - The *VZ* signal is measured to validate the method before looking at the *VH* analysis
  - The results were shown to be in good agreement with the Standard Model prediction
- Once the results are validated, the *VH* signal can be unblinded and measured

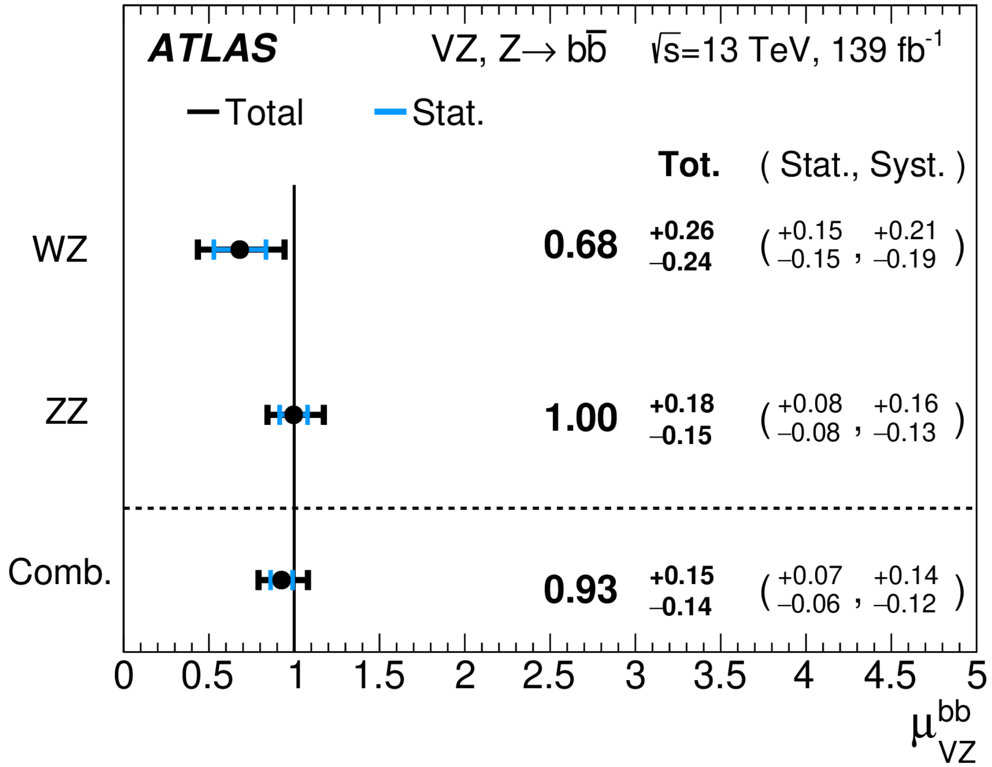

Results of the *VH* MVA

$$\mu = \frac{\sigma \times BR}{\sigma_{\rm SM} \times BR_{\rm SM}}$$

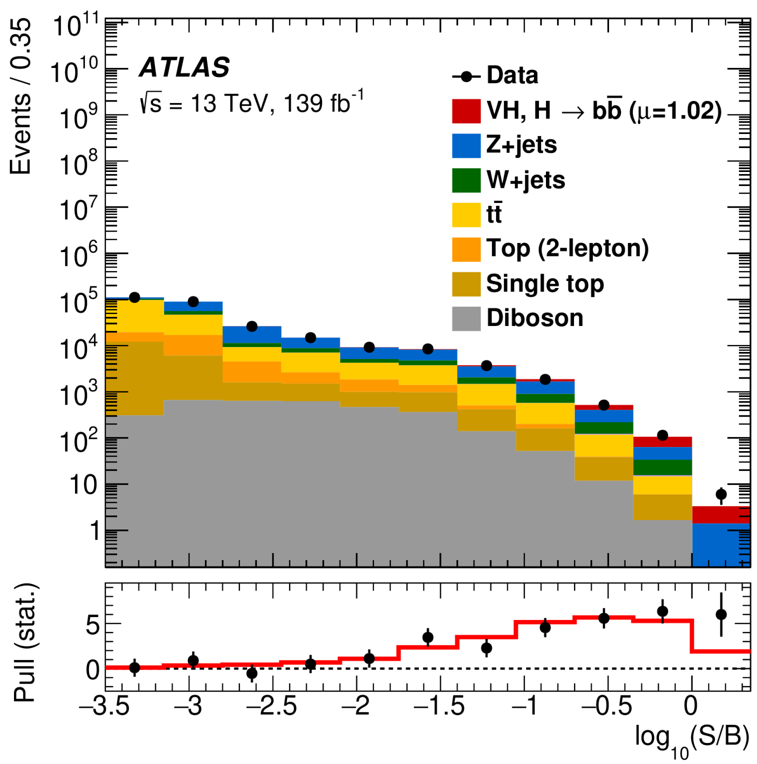

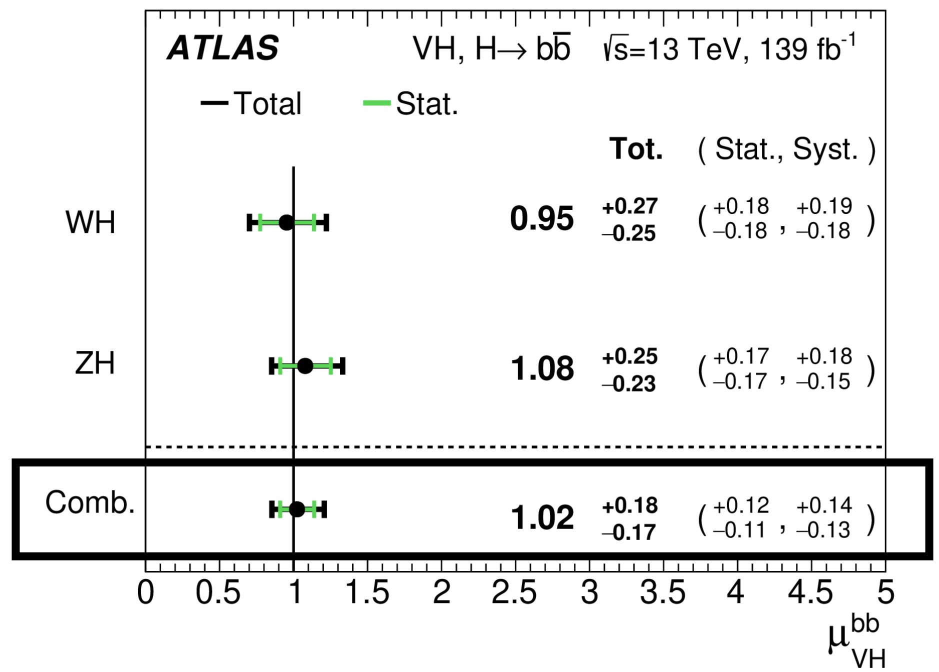

Source of uncertainty		σ_μ VH	WH	ZH
Total		0.177	0.260	0.240
Statistical		0.115	0.182	0.171
Systematic		0.134	0.186	0.168
Statistical uncertainties				
Data statistical		0.108	0.171	0.157
$t\bar{t}$ $e\mu$ control region		0.014	0.003	0.026
Floating normalisations		0.034	0.061	0.045
Experimental uncertainties				
Jets		0.043	0.050	0.057
$E_{\rm T}^{\rm miss}$		0.015	0.045	0.013
Leptons		0.004	0.015	0.005
b-tagging	b-jets	0.045	0.025	0.064
	c-jets	0.035	0.068	0.010
	light-flavour jets	0.009	0.004	0.014
Pile-up		0.003	0.002	0.007
Luminosity		0.016	0.016	0.016
Theoretical and modelling uncertainties				
Signal		0.052	0.048	0.072
Z + jets		0.032	0.013	0.059
W + jets		0.040	0.079	0.009
$t\bar{t}$		0.021	0.046	0.029
Single top quark		0.019	0.048	0.015
Diboson		0.033	0.033	0.039
Multi-jet		0.005	0.017	0.005
MC statistical		0.031	0.055	0.038

- Observation of the *VH* signal with 6.7σ (expected 6.7)
- Observation of the *ZH* signal with 5.3σ (5.2σ expected)
- Strong evidence of the *WH* signal with 4.0σ (4.1σ expected)
- Signal strengths in good agreement with the Standard Model
- The measurement is dominated by systematic uncertainties: **signal** and **background** modelling, **MC stat**, ***b*-tagging**

Differential cross-section measurements

- Differential cross-section (STXS) measurements were performed
- The analysis categories match the STXS bins definition
  - STXS measurement in 5 p_T^V bins
- Measured σ*BR in each of the bins in agreement with the SM within uncertainties

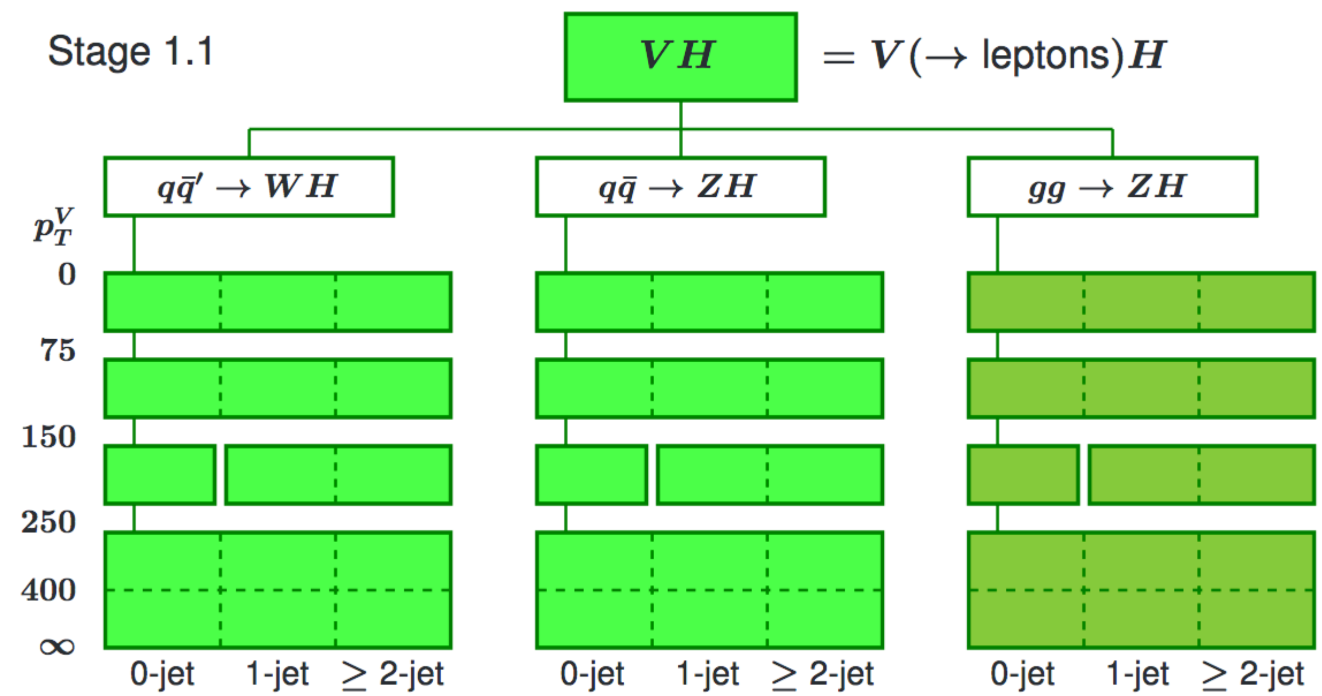

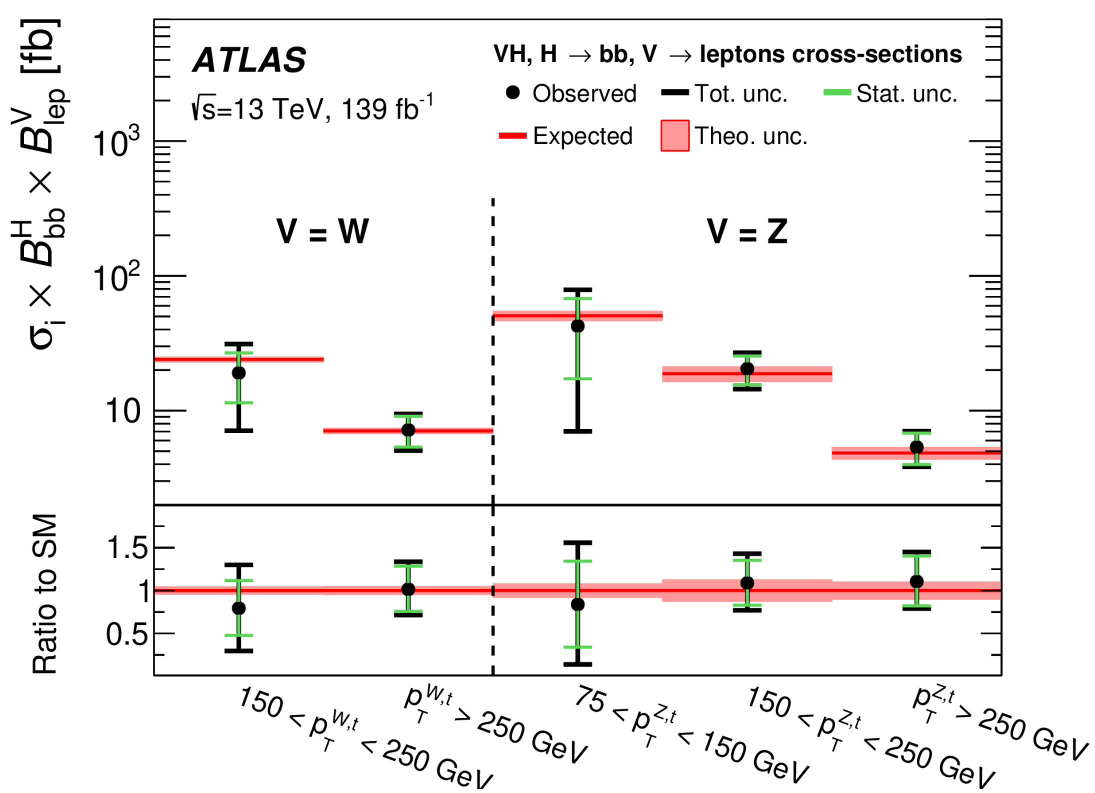

Cross-check analysis

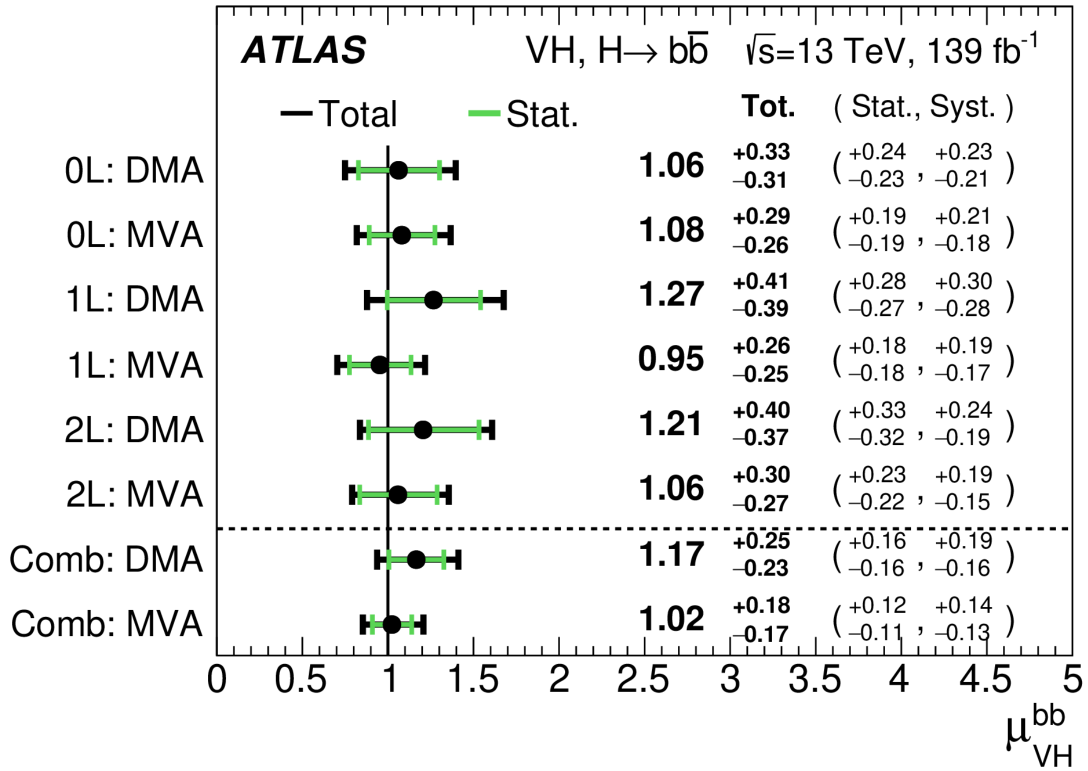

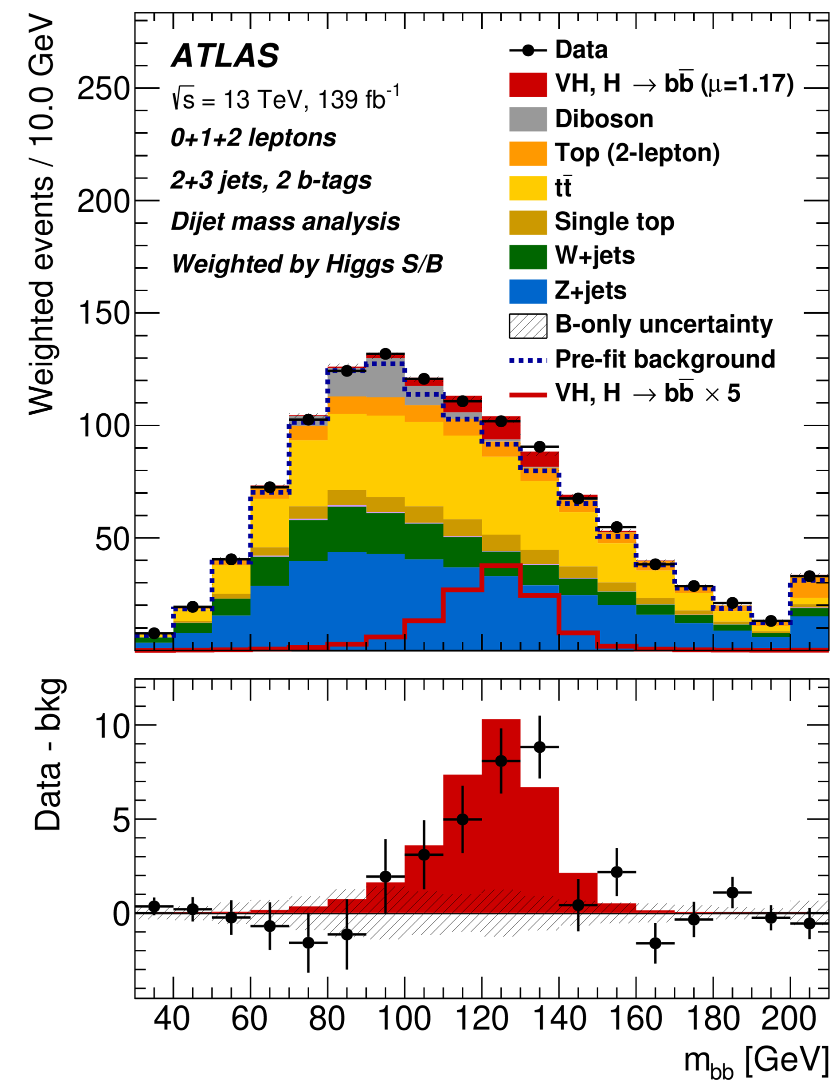

- The di-jet mass analysis is a good cross-check where the m_{bb} is fitted instead of the BDT_{VH} in the SR
  - The measurement yields an observation of the *VH* signal with a significance of 5.5σ (4.9σ expected)
  - The measurements are in good agreement with the MVA measurements in all three channels

MVA and m_{bb} compatibility

- The same events are used for the measurements in the MVA and di-jet mass analysis
    - It is interesting to quantify the compatibility between the two measurements
- Compatibility evaluated by using the bootstrap method based only on statistical fluctuations
- Generate a set of replicas of the nominal BDT_{VH} and m_{bb} **data** distributions
    - By fluctuating all the events by the same manner in both distributions using weights
- ~450 fits were performed using the data replicas to find the best fit value for each measurement
    - The results of the MVA and m_{bb} measurements were found to be in agreement within 1σ

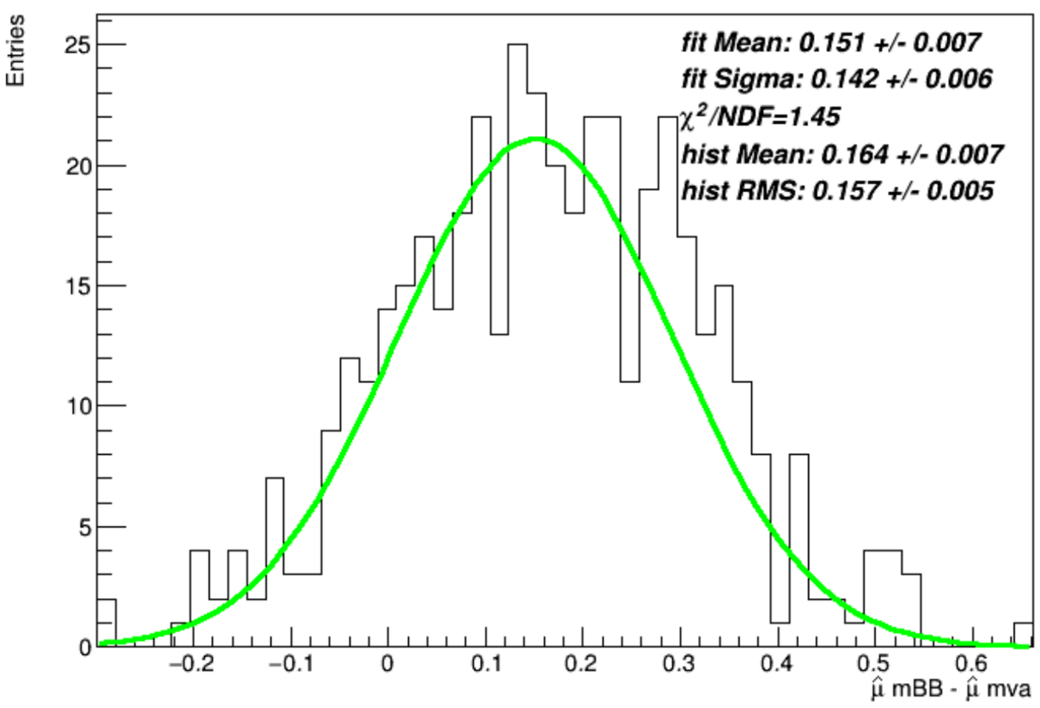

Summary

- **Characterisation of the liquid argon calorimeter pre-amplifiers for the Phase-II upgrade**
  - Evaluated the performance of two proposed prototypes, LAUROC0 and HLC1
  - The results allowed to check if they match the requirements and to identify the needed improvements
    - Mostly good linearity but high electronic noise
  - Gain simulation study allowed to validate the proposed two gain scheme
- **Measurements of the *VH, H→bb* with full Run-2 was performed:**
  - Using a new events categorisation to harmonise the analyses and better control the backgrounds
  - Multi-jet background and its uncertainties were studied and estimated in the 1-lepton channel
  - A multi-dimensional reweighting method based on BDTs implemented for the estimation of background shape uncertainties
  - Measurements yielded the observation of the *VH* and *ZH* signals and a strong evidence of the *WH* signal
  - Results of the analysis were published in a paper: arXiv:2007.02873

Back-up

Experimental setup

- Same test bench to test the LAUROC0 and HLC1 performance including:
  - **External generator** to inject signal into the setup
  - **Toy calorimeter** built with different outputs of different injector resistance to emulate the detector input signal
  - **Front-end test board (FETB)** containing an ADC driver circuit of 32 ADC channels for the signal shaping and digitisation
    - It include also a CR-(RC)2 filter since LAUROC0 does not include one
  - **Digital readout Xilinx ZC706 board** to read the signals sent by the FETB
  - **Host computer** to configure the ASICs and to store the measurements for offline processing

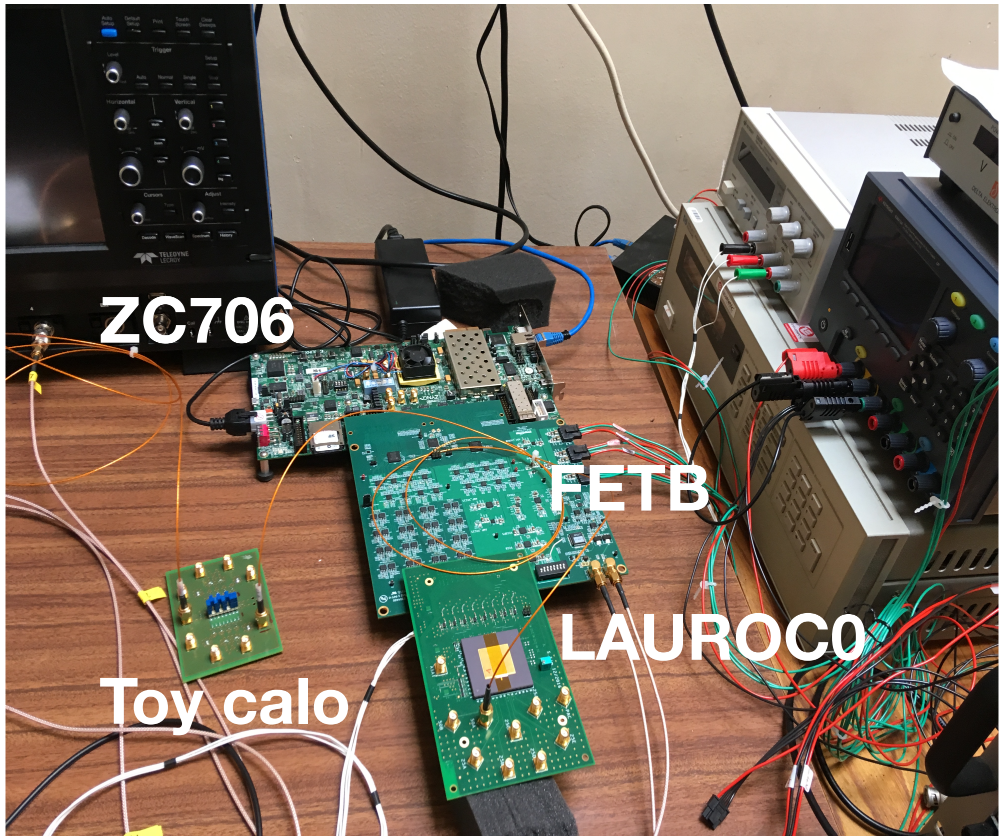

Input impedance tuning

- The input impedance is first adjusted for each channel to limit the signal reflexions
- LAUROC0 input impedance tuned through set of capacitor
  - Coded over 9-bits for the 25_50 channel from 31.5fF to 16pF with a step of 31.5 fF
- HLC1 input impedance is configurable over 3-bits
  - For a range of 24.4-28.9Ω with a step of 0.65Ω (25Ω channel) and a range of 47.6-56.0Ω with a step of 1.20Ω (50Ω channel)
- The input impedance is calculated by injecting a know current and measuring the amplitude of the signal at the input of the PA
  - All the configurations were tested to find the most adapted one
- The tuning works well for both LAUROC0 and HLC1
  - Difference between the LAUROC0 expected and measured values coming from the LSB true value (from process variation)

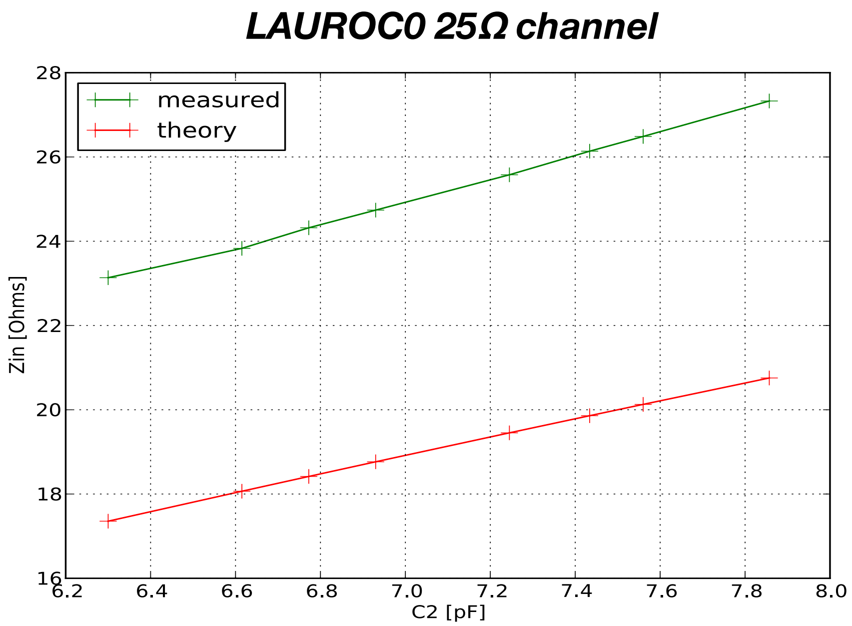

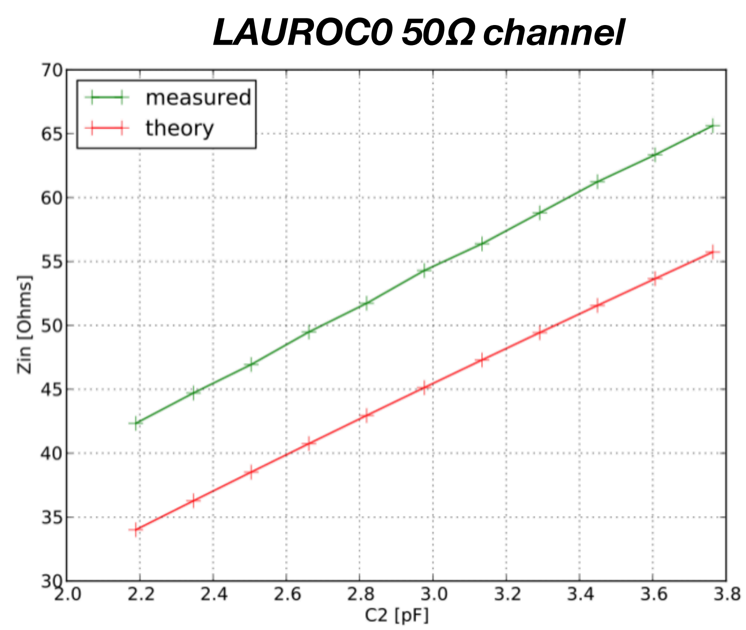

HLC1 input impedance tuning

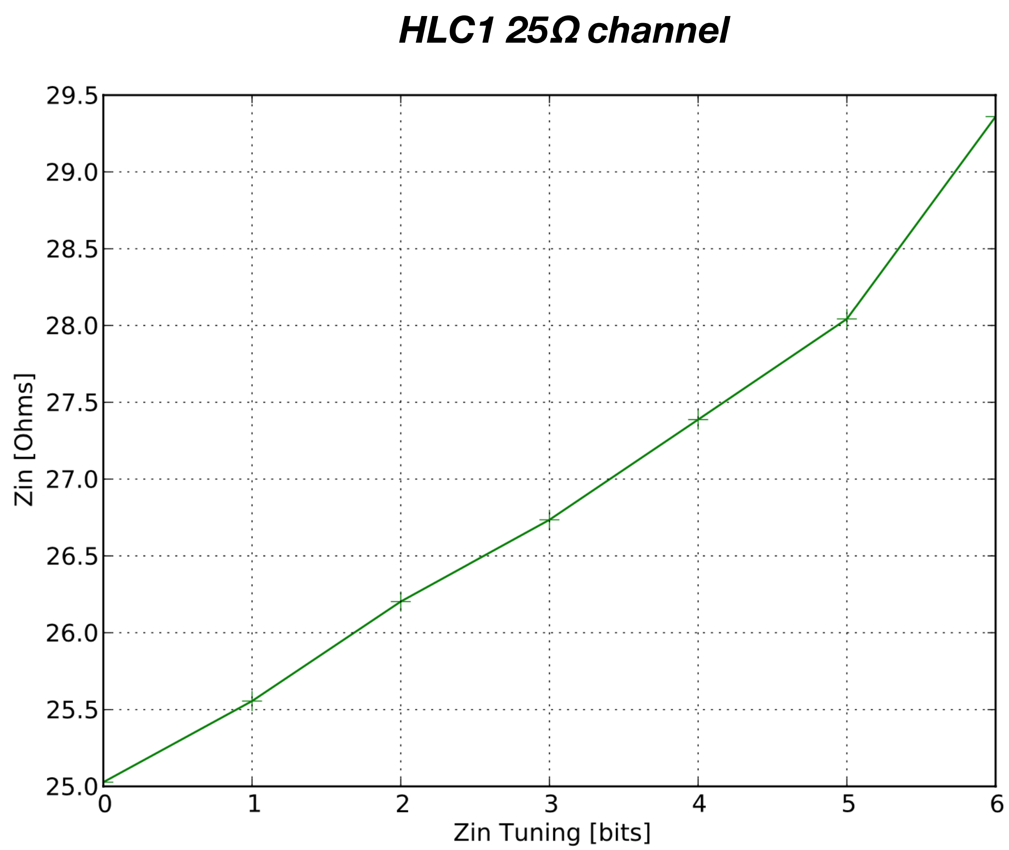

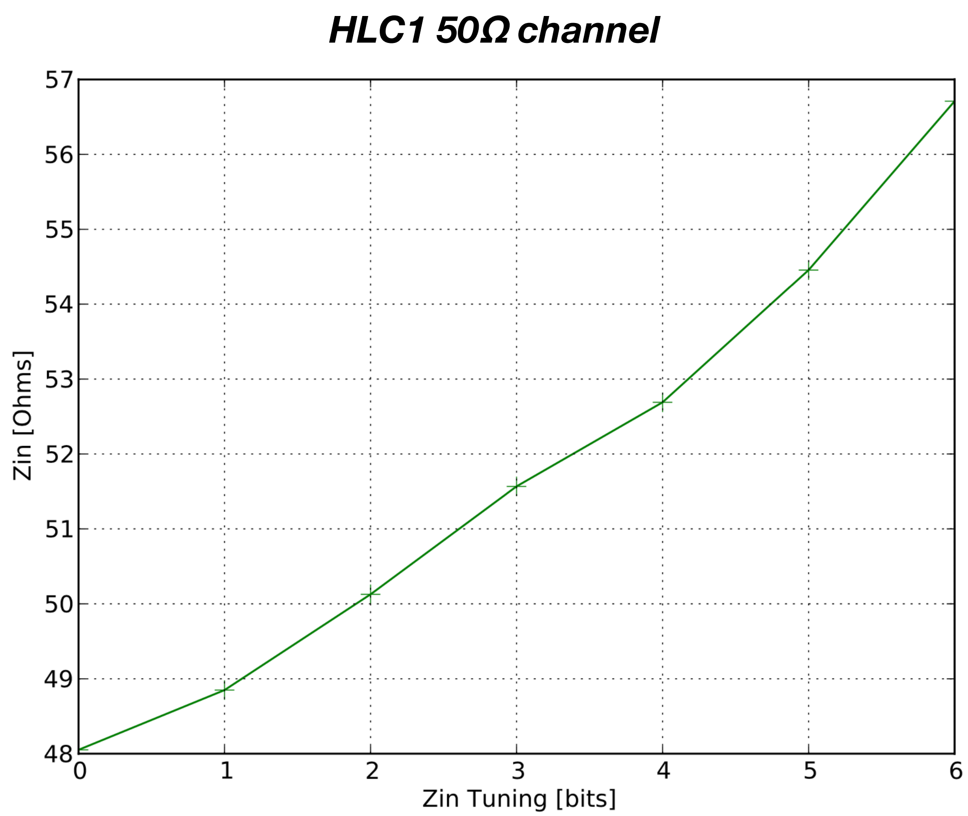

- Tuning works well

Characterisation of LAUROC0 discriminator

- The LAUROC0 include a discriminator to be triggered to cut the HG output when it saturates and only measure the LG output
    - It is controlled by a threshold on the LG tuned over 10-bits
- The most adapted threshold value should be chosen to trigger the switch just before the HG saturation
    - Different configuration were tested and Vth = 700 (DAC) was found to be the most adapted
- Need to quantify the impact of the discriminator triggering the physics performance
    - It has an impact on the LG pulse amplitude with a local impact on the INL of 1%
- This was improved in the LAUROC1 iteration, where the LG is a copy of the HG similarly to the HLC1 design

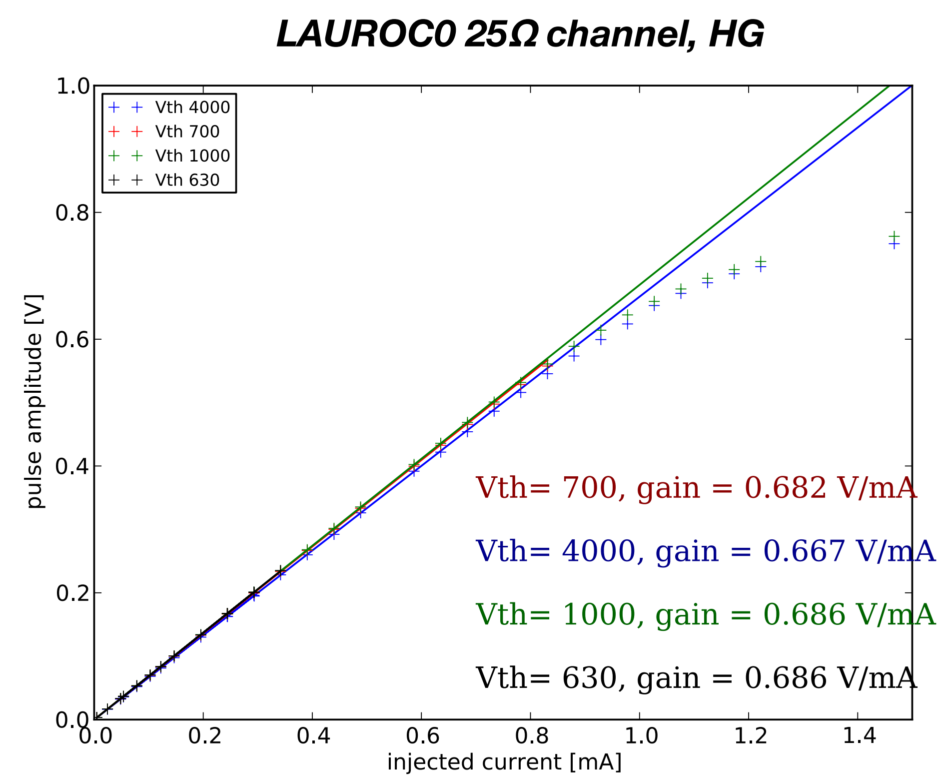

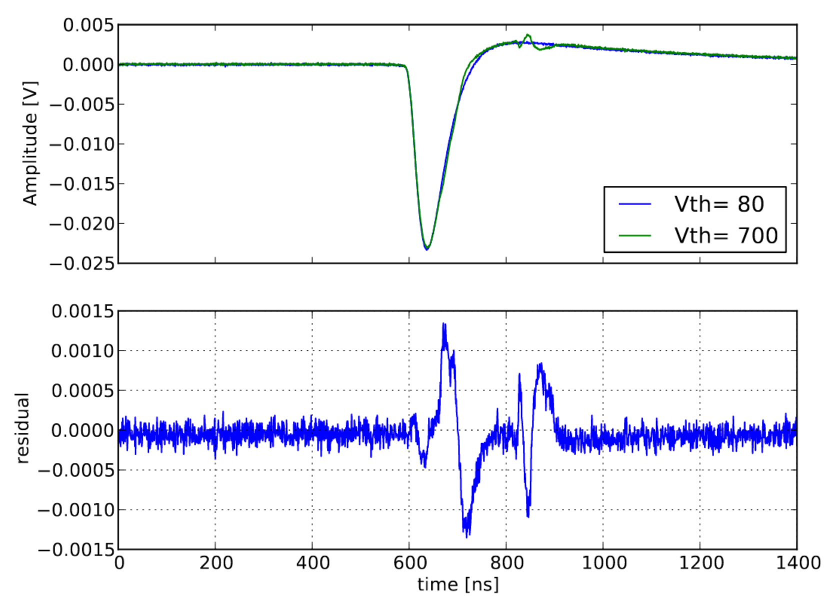

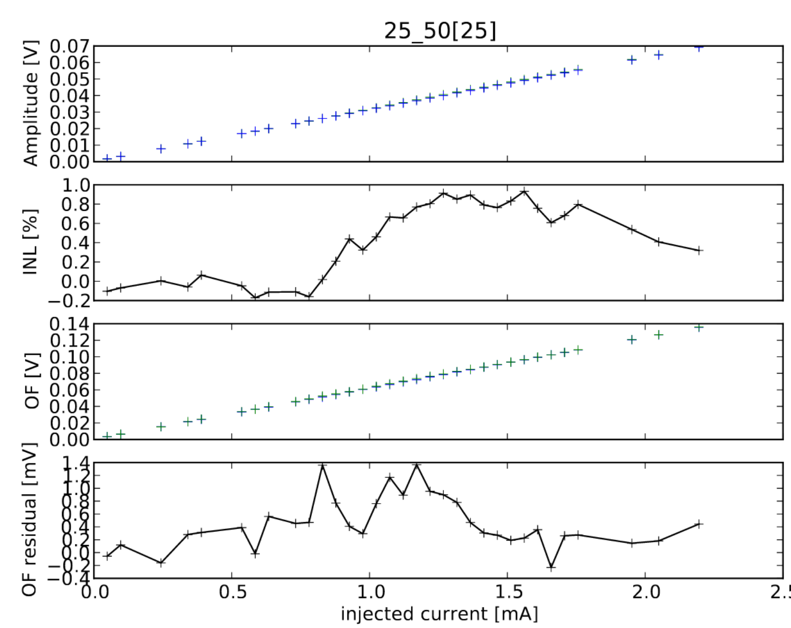

Linearity measurements

- The measured amplitudes are for each current value are fitted up to the end of the expected dynamic range to compute the non-linearity integral (INL)
- The 25Ω (50Ω) channels are expected to have a good linearity up to 10 (2) mA

LAUROC0

- 25Ω LG: INL< 0.15% up to 7 mA and and 1% beyond this value
- 25Ω HG: INL< 0.15% in the whole dynamic range
- 50Ω LG: INL< 0.25% up to 1 mA and few percents beyond this value
- 50Ω HG: INL< 0.1% in the whole dynamic range

HLC1

- 25Ω LG: INL< 0.5% up to 8 mA
- 25Ω HG: INL< 0.15% in the whole dynamic range
- 50Ω LG: INL< 0.3% up to 1.7 mA
- 50Ω HG: INL< 0.2% in the whole dynamic range

- Mostly **good linearity** in all channels and the range of the 50Ω channel in LAUROC0 was **fixed** in the next iteration

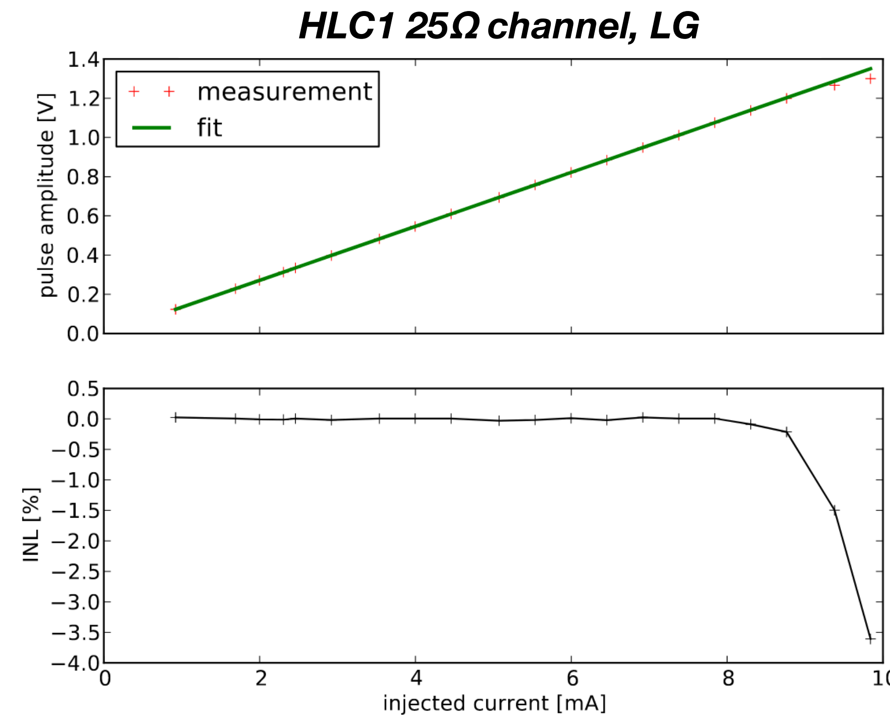

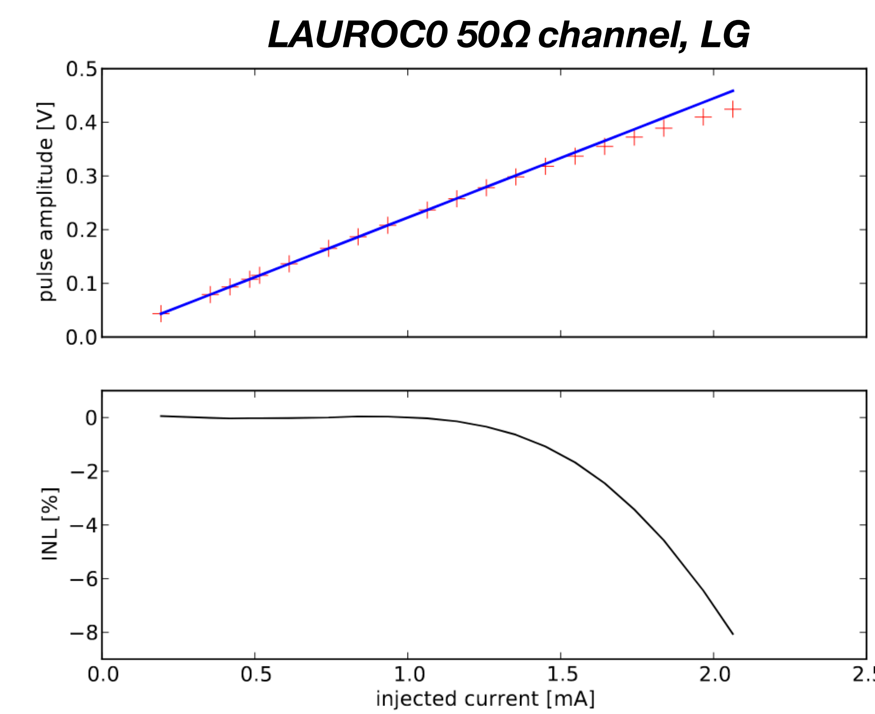

Linearity: LAUROC0 25Ohm channel

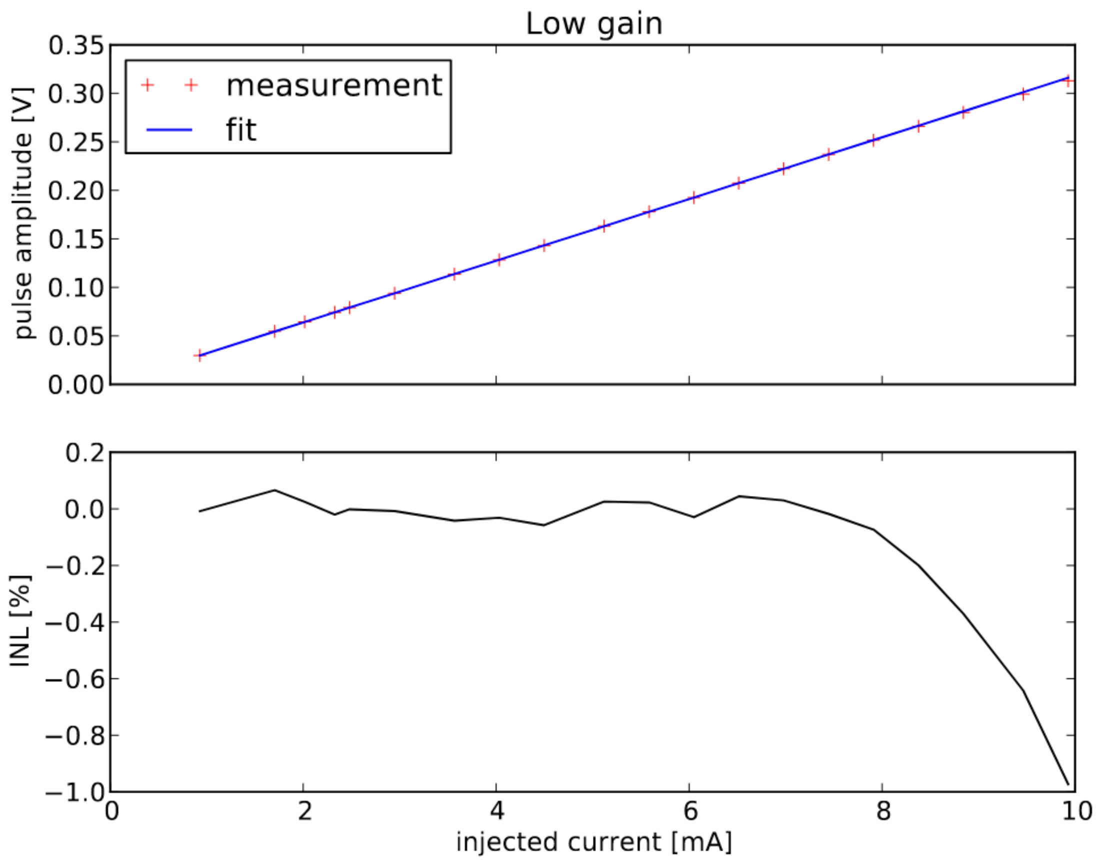

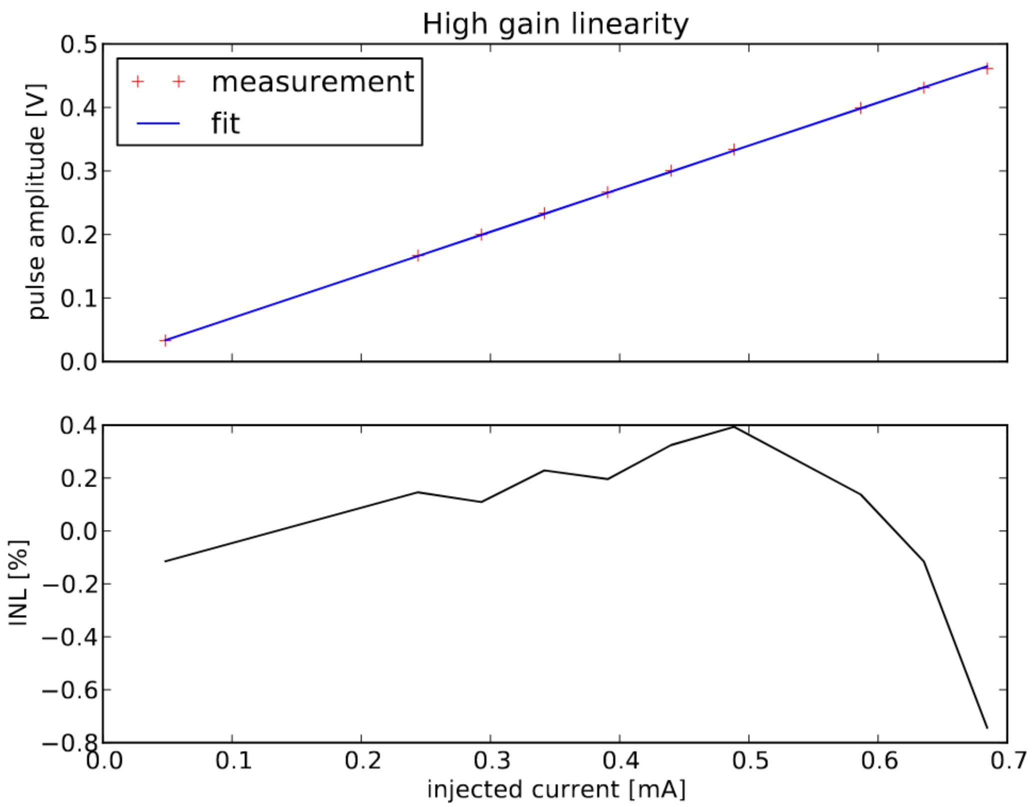

- LG: INL< 0.15% up to 7mA and and 1% beyond this value
- HG: INL< 0.15% in the whole dynamic range

Linearity: LAUROC0 50Ohm channel

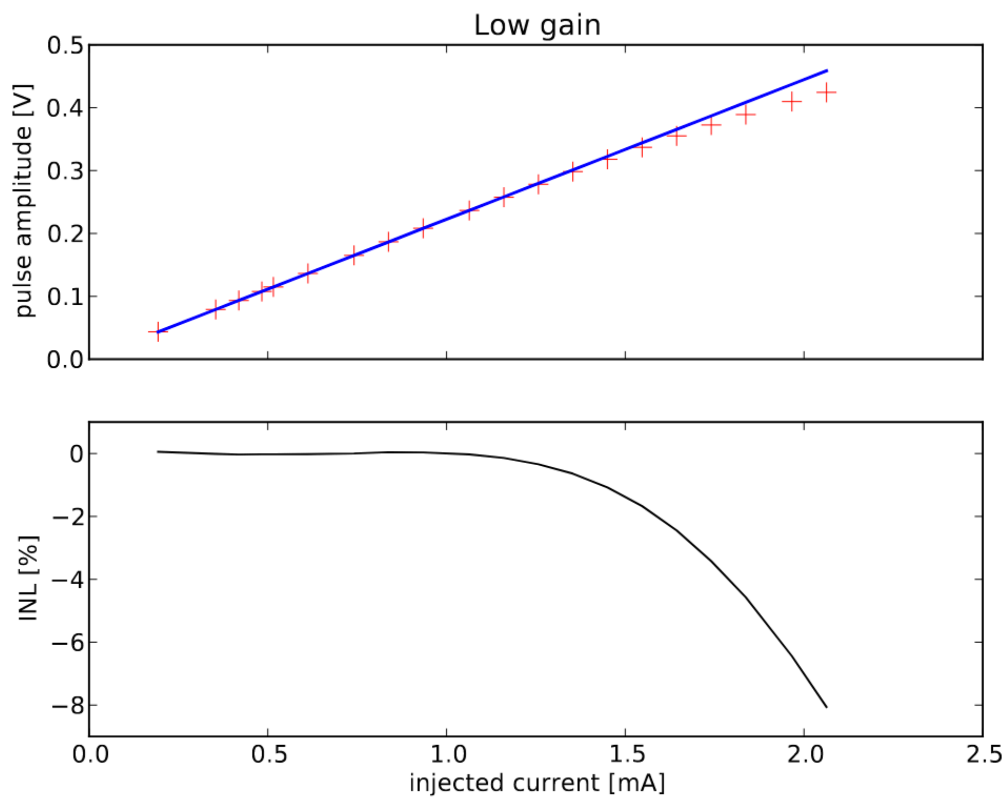

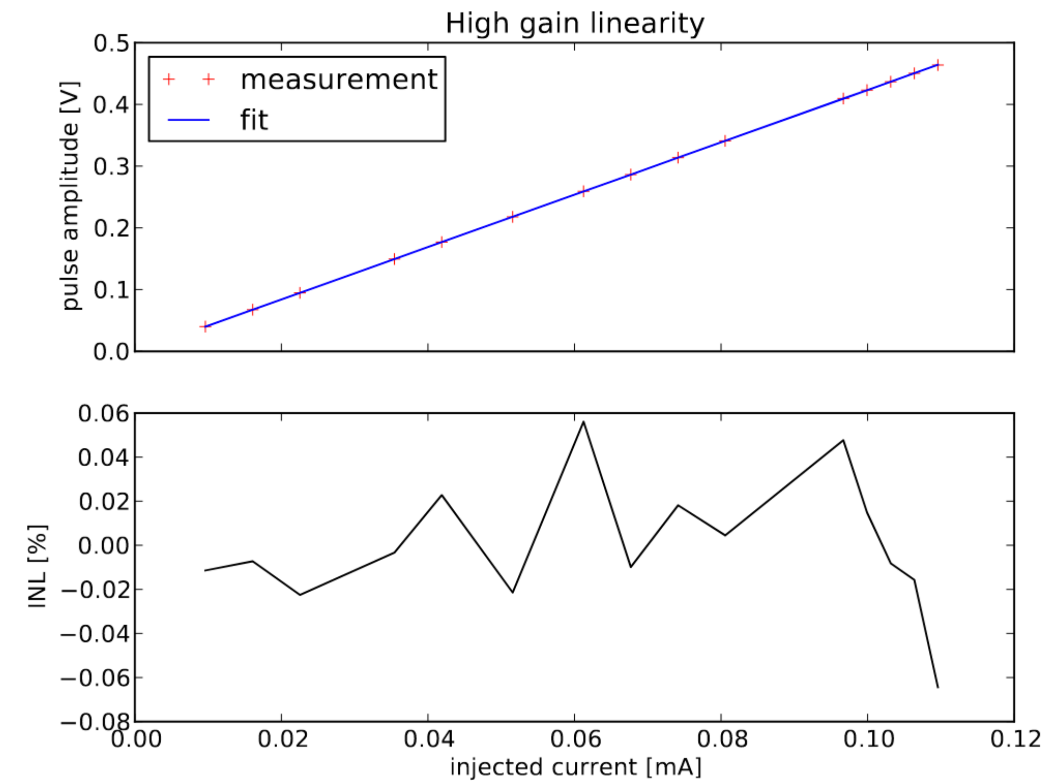

- LG: INL< 0.25% up to 1mA and few percents beyond this value
- HG: INL< 0.1% in the whole dynamic range

Linearity: HLC1 25Ohm channel

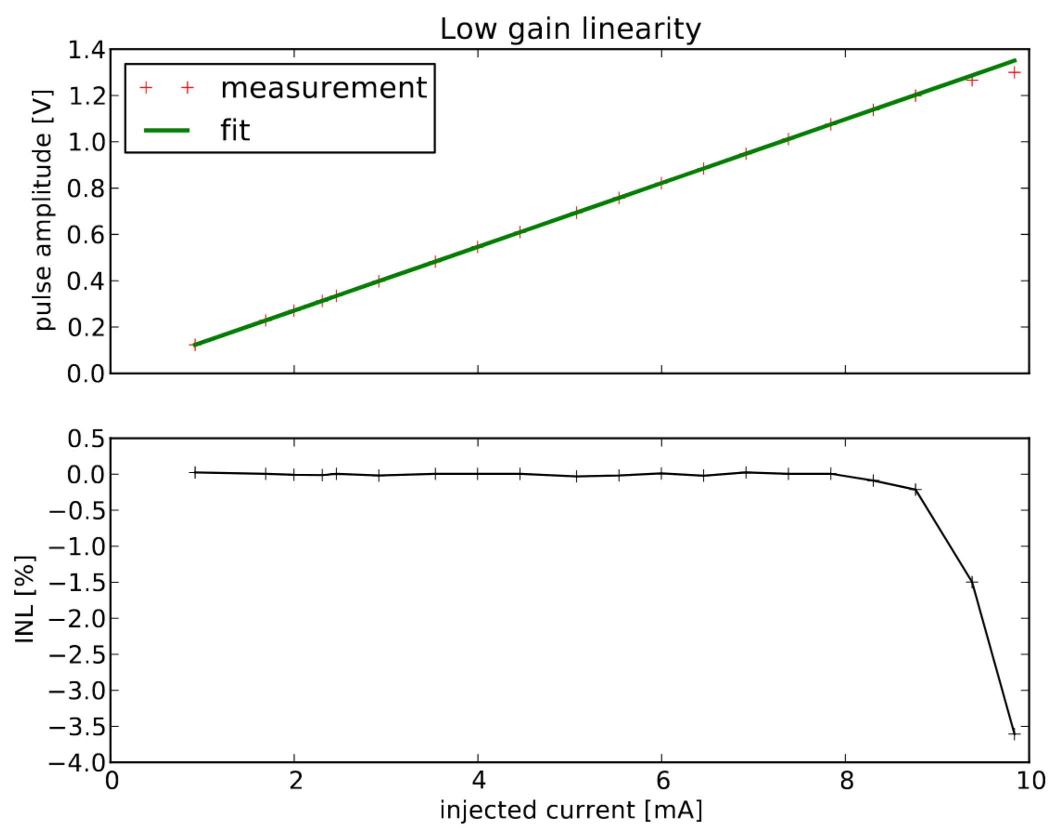

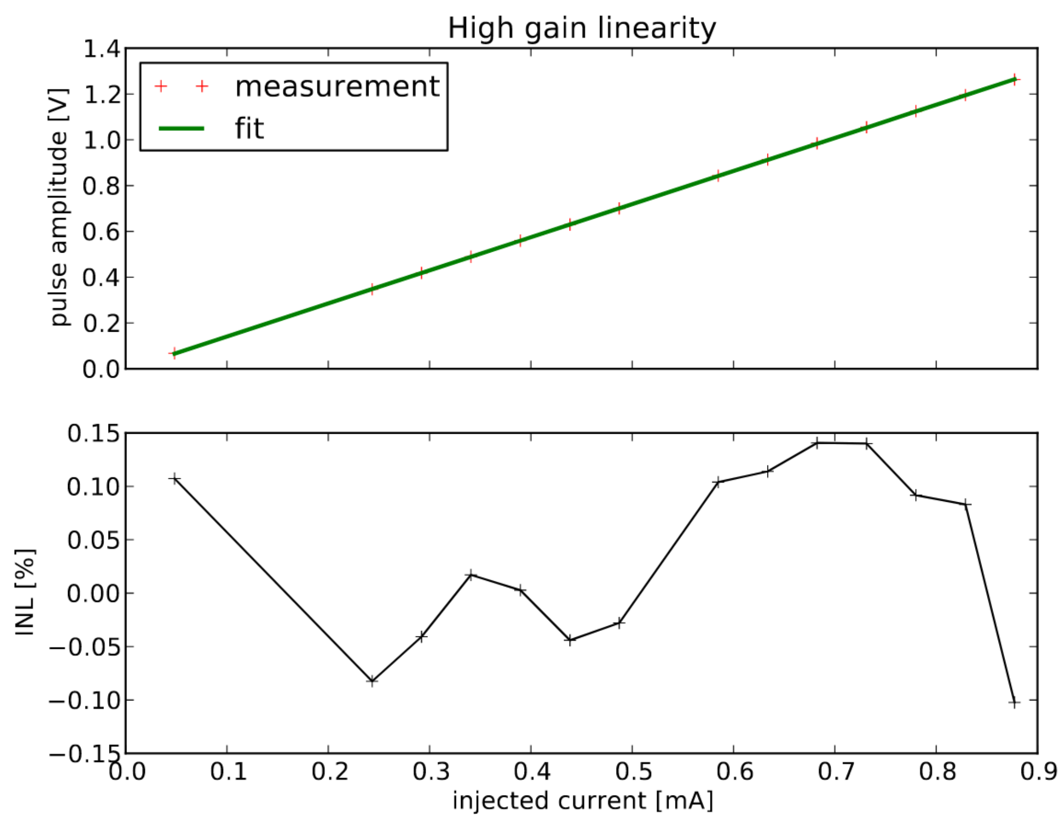

- LG: INL< 0.5% up to 8mA
- HG: INL< 0.15% in the whole dynamic range

Linearity: HLC1 50Ohm channel

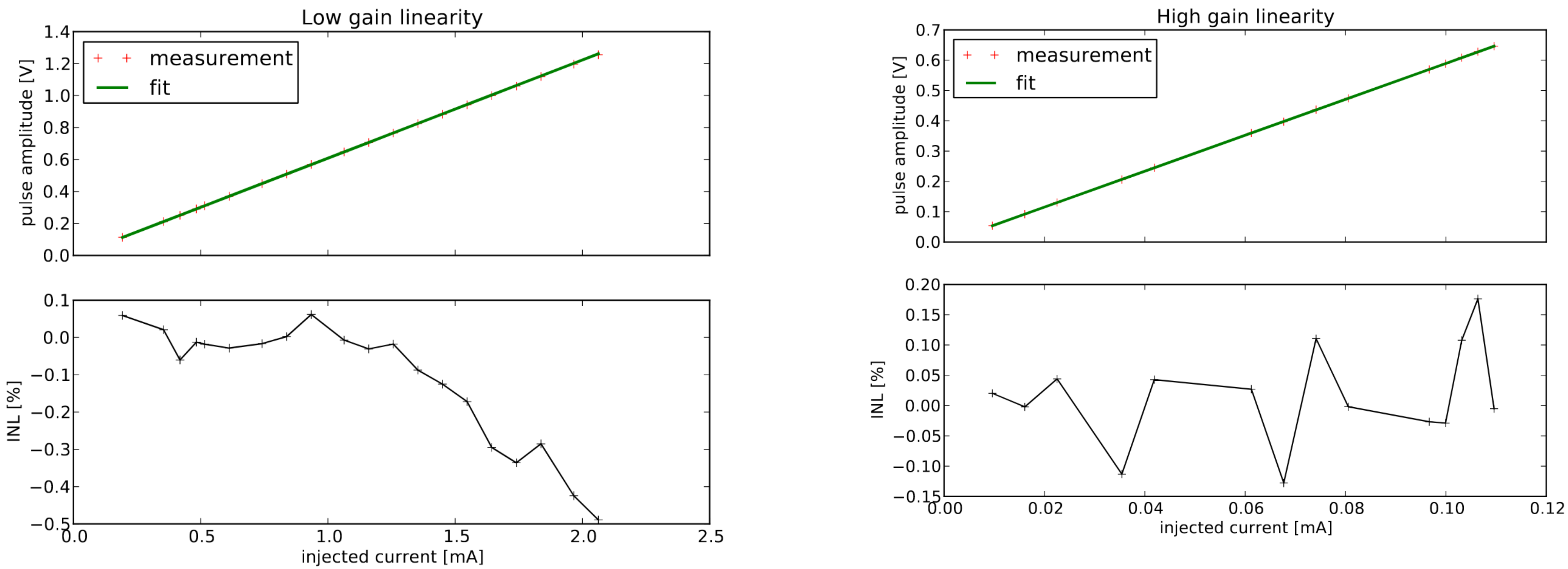

- LG: INL< 0.3% up to 1.7mA
- HG: INL< 0.2% in the whole dynamic range

Quantisation noise at gain switching

- The gain switching occurs when the HG reaches the end of the dynamic range and thereby only the LG can be measured
- The choice of the high gain and the low gain should meet the following requirement:
  - At gain switching energy the quantisation noise is less than the Liquid Argon resolution to not degrade the total resolution
- Digitisation is done using an ideal 14-bits range ADC with noise= LSB/2
  - 1/4 of the dynamic range is reserved for negative part of the signal
- A simulation study have been conducted to test the typical gain ratio between the low and the high gain of 23 (19) for the 25Ω (50Ω) channel
  - Quantisation noise is an order of magnitude lower than the LAr resolution: $10\%/\sqrt{E} + 0.2\%$

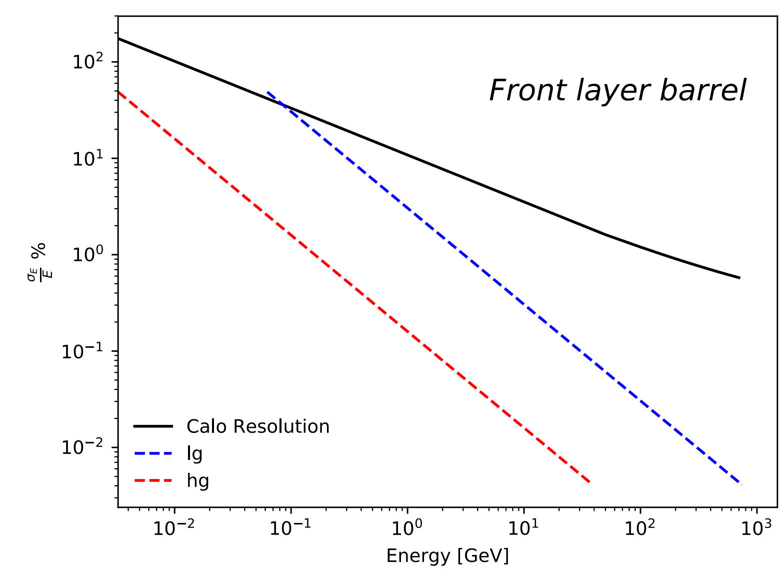

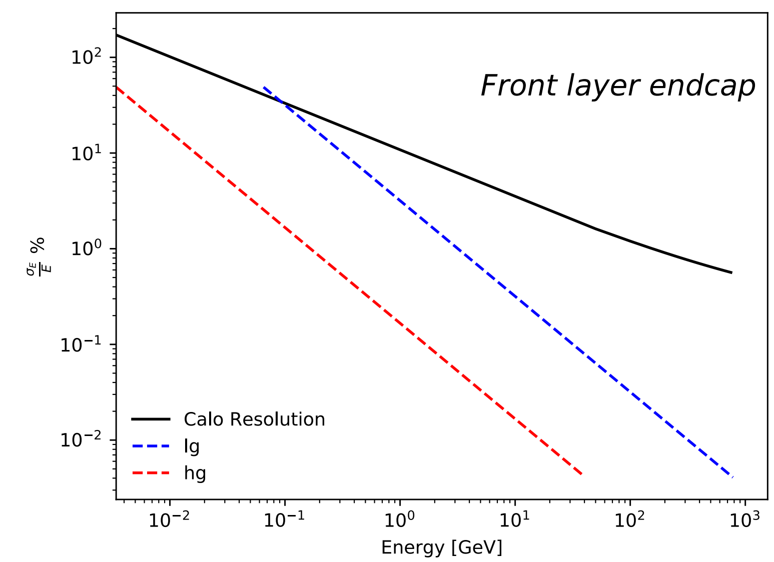

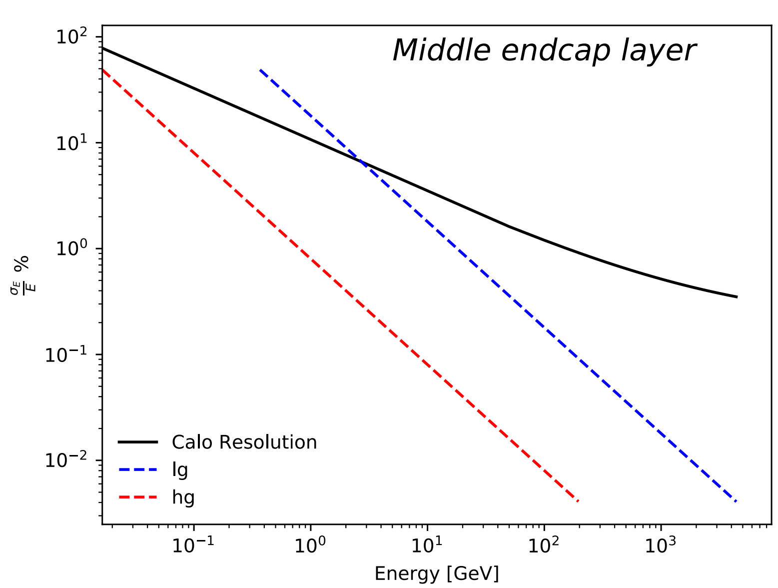

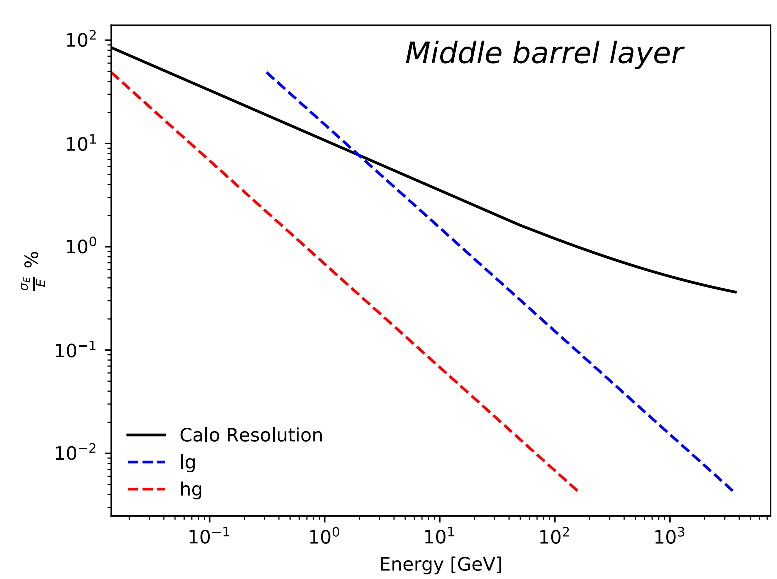

Conclusion and outlook

- LAUROC0 and HLC1 pre-amplifier prototypes have been proposed for the LAr Phase-II upgrade
- Results of the measurements allowed to check if the prototypes match the requirements and to identify the needed improvements
    - Good input impedance tuning, mostly good linearity over the whole dynamic range
    - The electronic noise needs to be improved in both designs
- LAUROC1 is the second ASIC generation
    - The dynamic range was improved to reach 2mA and electronic noise was lowered to ~250nA
- ALFE0 is the upgraded prototype of HLC1
    - Good linearity in the whole dynamic range and electronic noise similar to the current electronics
- LAUROC2 and ALFE1 are the final ASIC prototypes
    - The specification measurements will be conducted to decide on a single design

BDT_{VH} training

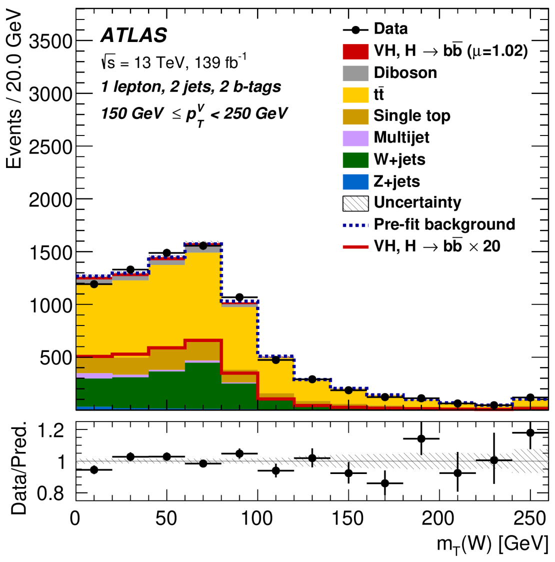

+

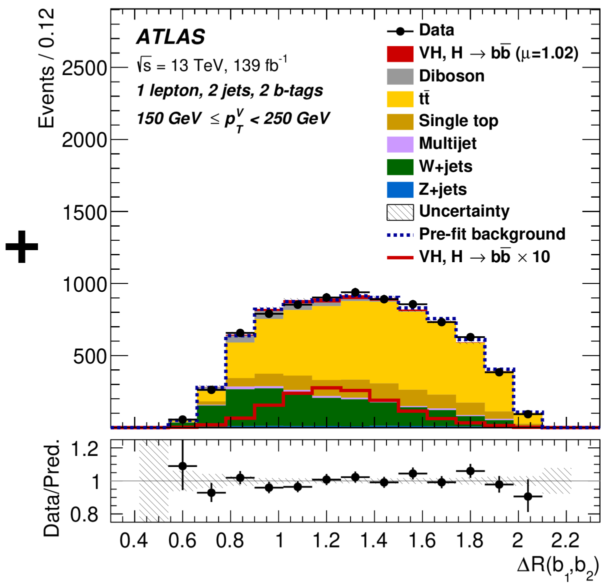

+

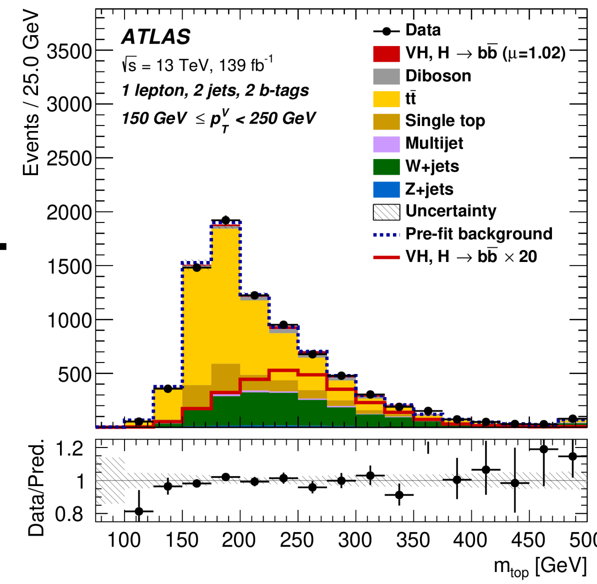

+ .... =

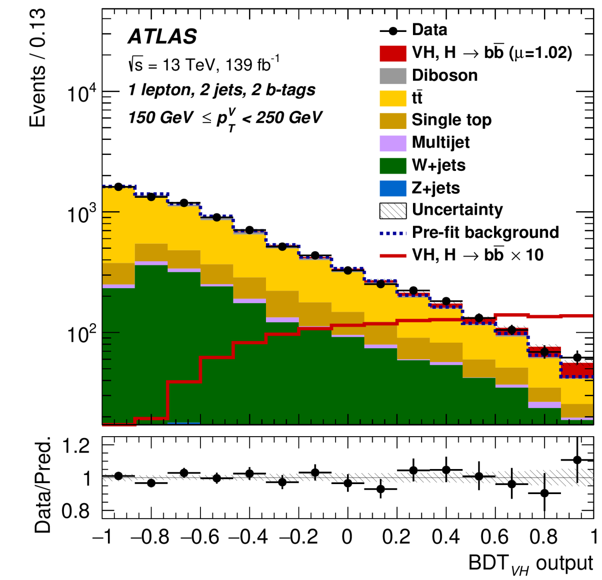

Variable	Description	0-lepton	1-lepton	2-lepton
m_{jj}	Invariant mass of two Higgs boson candidate jets	✓	✓	✓
$\Delta R(jet_1, jet_2)$	Distance between the two Higgs boson candidate jets	✓	✓	✓
p_T^{jet1}	Transverse momentum of the leading b-tagged jet	✓	✓	✓
p_T^{jet2}	Transverse momentum of the sub-leading b-tagged jet	✓	✓	✓
p_T^V	Transverse momentum of the vector boson	✓	✓	✓
E_T^{miss}	Missing transverse energy	$\equiv p_T^V$	✓	
$\Delta\phi(V, H)$	Distance in ϕ between the vector boson and the Higgs boson candidate	✓	✓	✓
binned MV2c10(jet$_1$)	MV2c10 binned distribution of the leading jet	✓	✓	
binned MV2c10(jet$_2$)	MV2c10 binned distribution of the sub-leading jet	✓	✓	
$\|\Delta\eta(jet_1, jet_2)\|$	Distance in η between the two Higgs boson candidate jets	✓		
M_{eff}	Scalar sum of E_T^{miss} and selected jets	✓		
track based soft E_T^{miss} term	Vectorial sum of the transverse momentum of all tracks not reconstructed in the event	✓		
$\min(\Delta\phi(l, jet))$	Distance in ϕ between the lepton and the closest b-tagged jet		✓	
m_T^W	Transverse mass of the W boson		✓	
$\Delta Y(W, H)$	Difference in rapidity between the W boson and the Higgs boson candidate		✓	
m_{top}	Mass of the top quark decaying leptonically		✓	
E_T^{miss} significance	Quasi-significance of E_T^{miss} defined as $E_T^{miss}/\sqrt{S_T}$			✓
$\Delta\eta(V, H)$	Difference in η between the vector boson and the Higgs boson candidate			✓
m_{ll}	Invariant mass of the dilepton			✓
$\cos\theta(l^-, Z)$	Angle between the negatively charged lepton and the Z boson flight direction in the Z boson rest frame			✓
	Only in 3-jet events			
$p_T^{\text{jet}_3}$	Transverse momentum of the leading un-tagged jet	✓	✓	✓
m_{jjj}	Invariant mass of the two tagged jets and the leading un-tagged jet	✓	✓	✓

BDT$_{VH}$ tuning

	BDT-1	BDT-2
Training	fold-1	fold-2
Evaluation	fold-2	fold-1
Over-training test	fold-1	fold-2

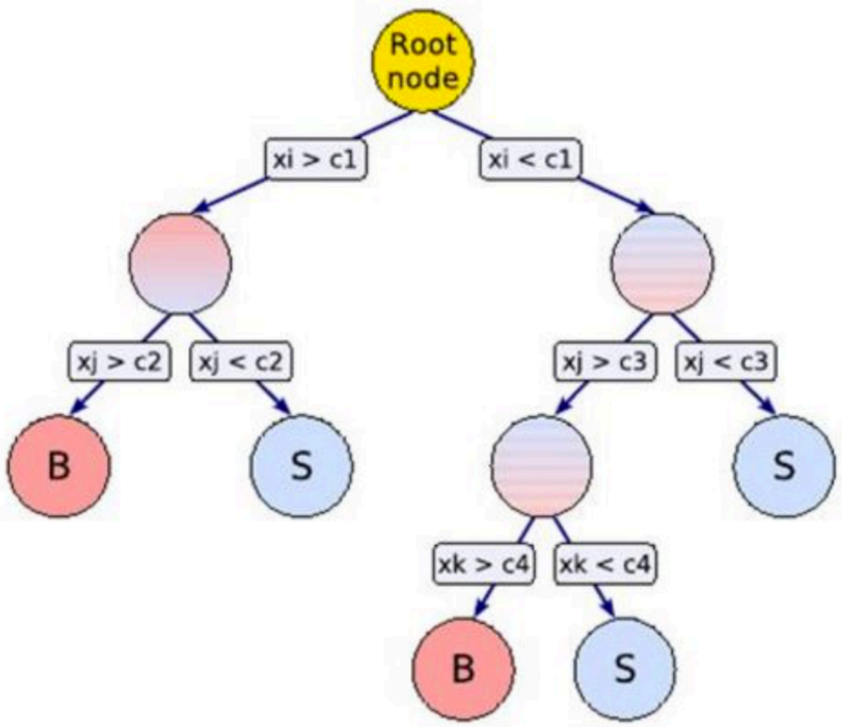

Training Setting	Value	Definition
BoostType	gradient boosting	Boost procedure
Shrinkage	0.5	Learning rate
SeparationType	Gini index	Node separation gain
PruneMethod	No Pruning	Pruning method
NTrees	200 (600 for 1-lepton VH)	Number of trees
MaxDepth	4 (2 for 1-lepton diboson)	Maximum tree depth
nCuts	100	Number of equally spaced cuts tested per variable per node
nEventsMin	5%	Minimum number of events in a node (% of total events)

BDT plots: 0-lepton

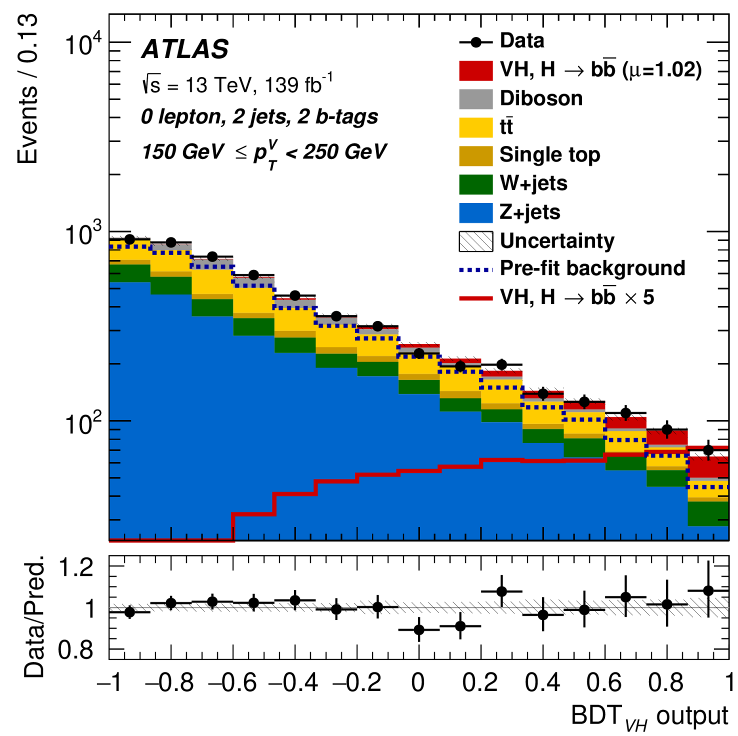

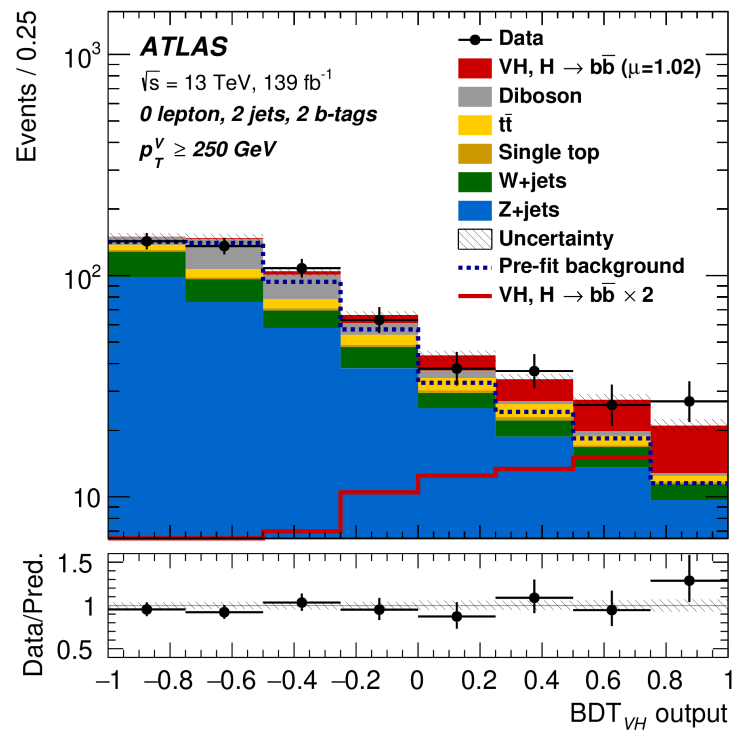

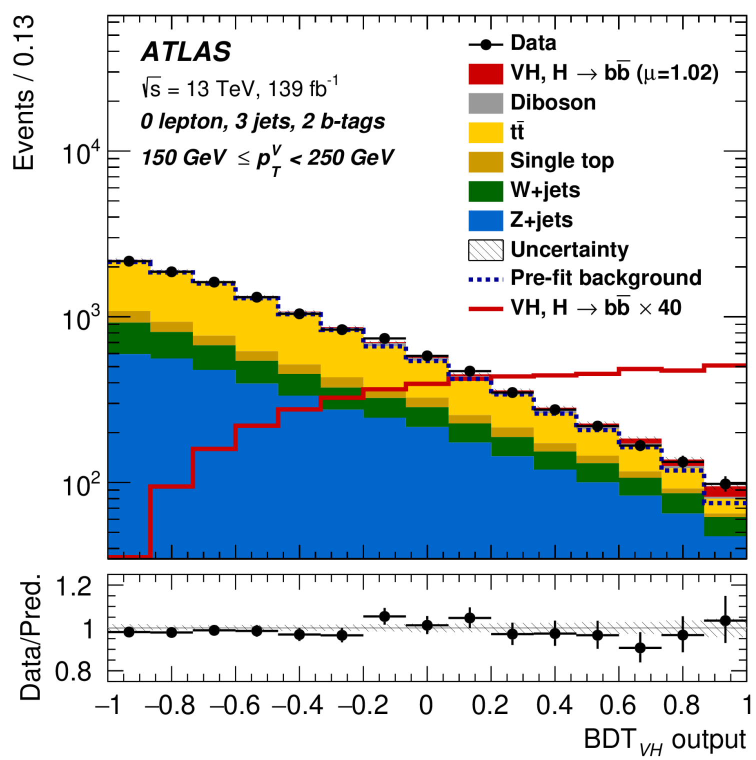

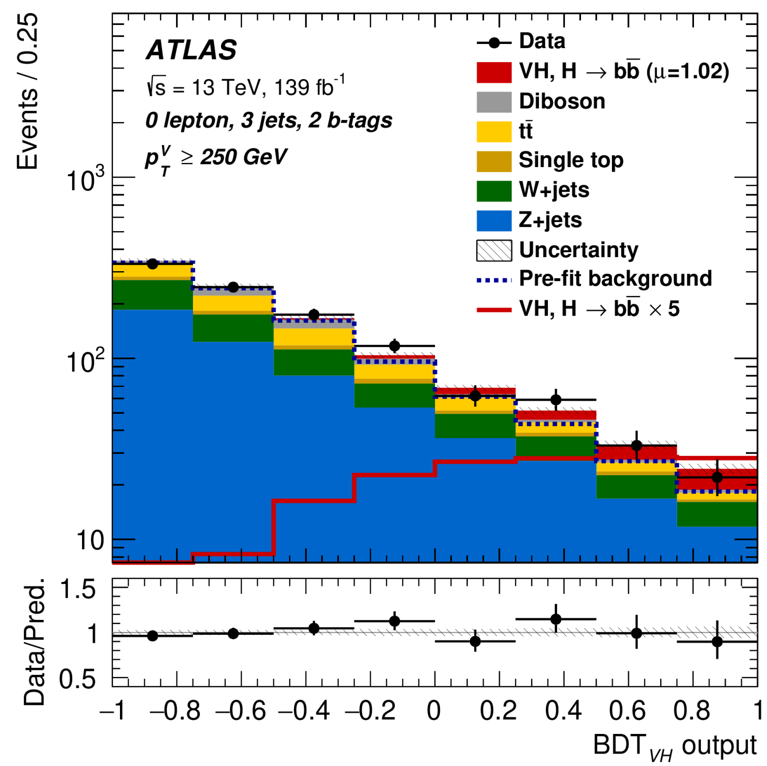

BDT plots: 1-lepton

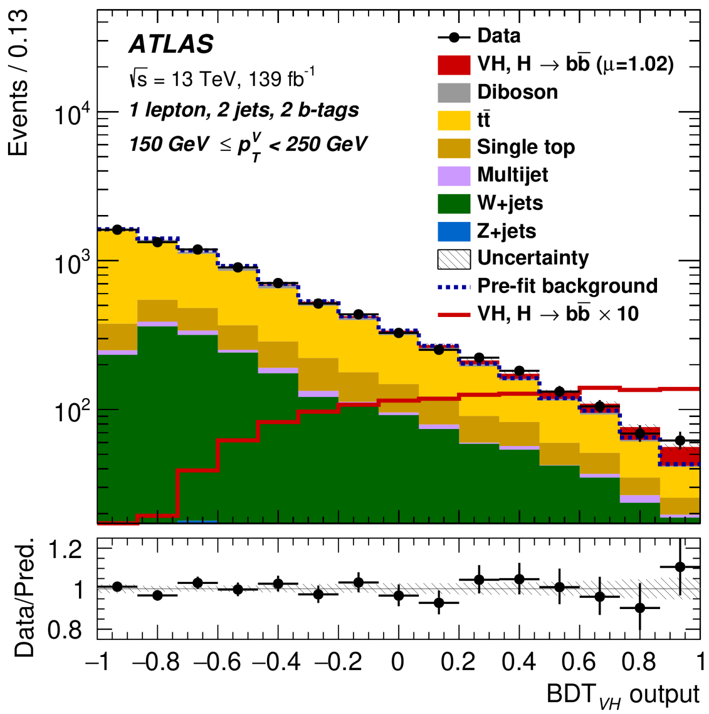

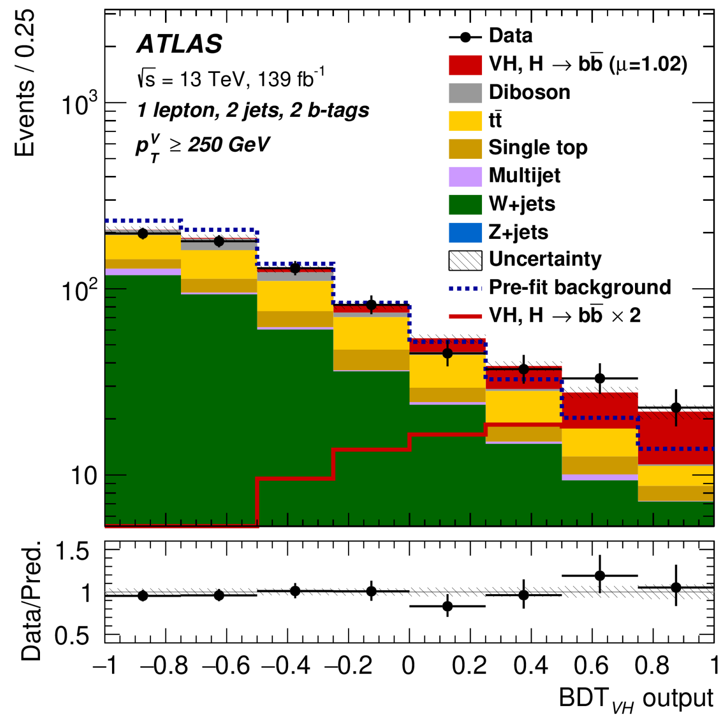

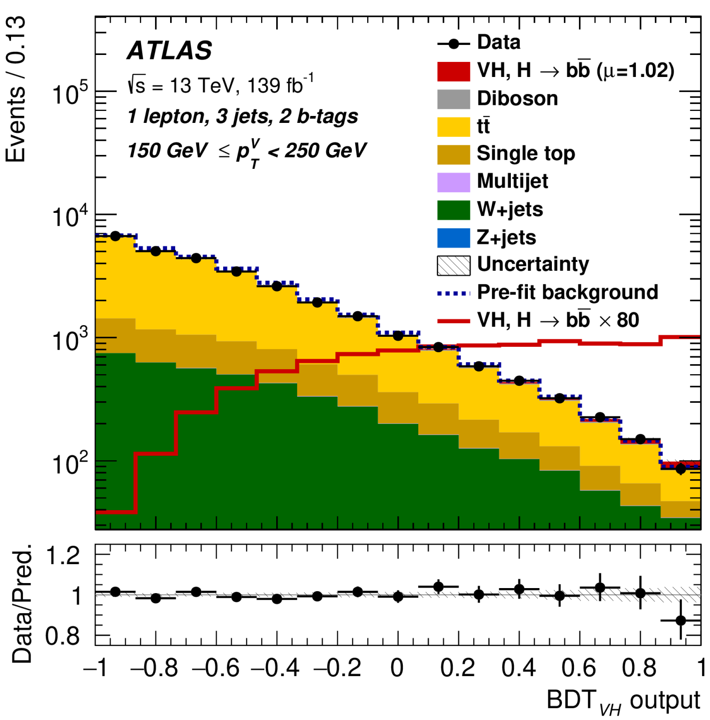

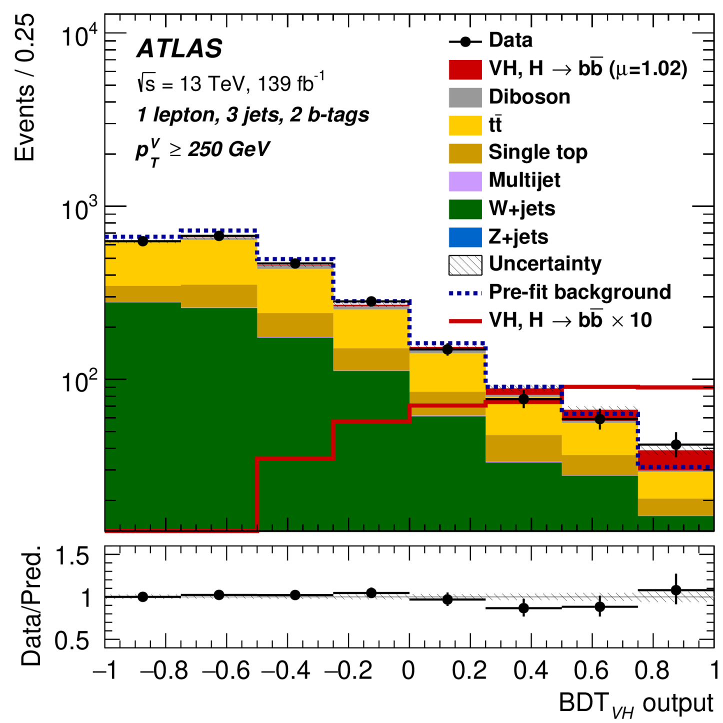

BDT plots: 2-lepton

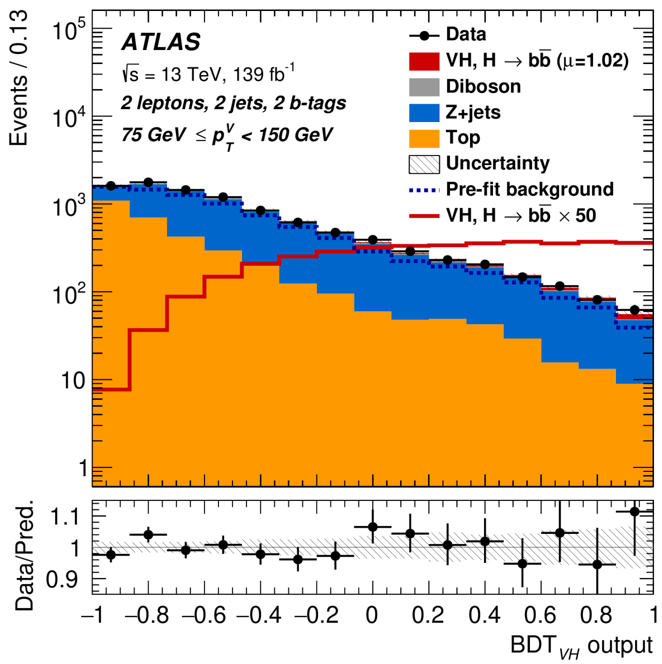

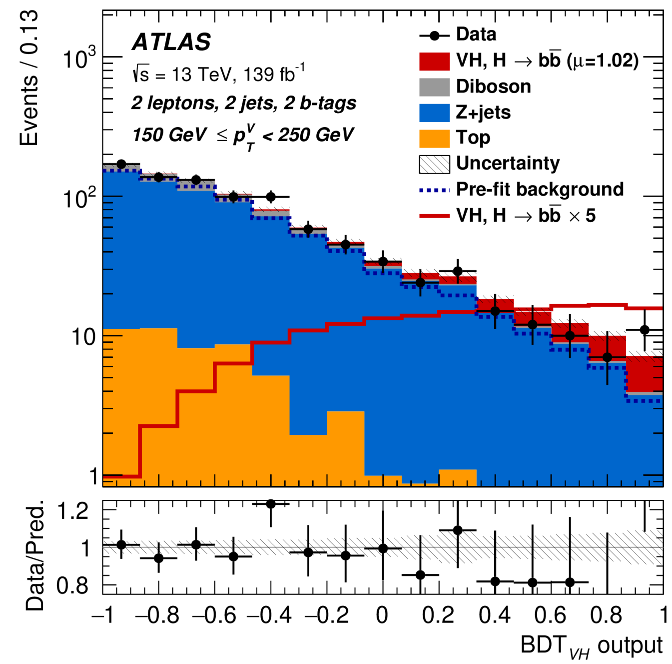

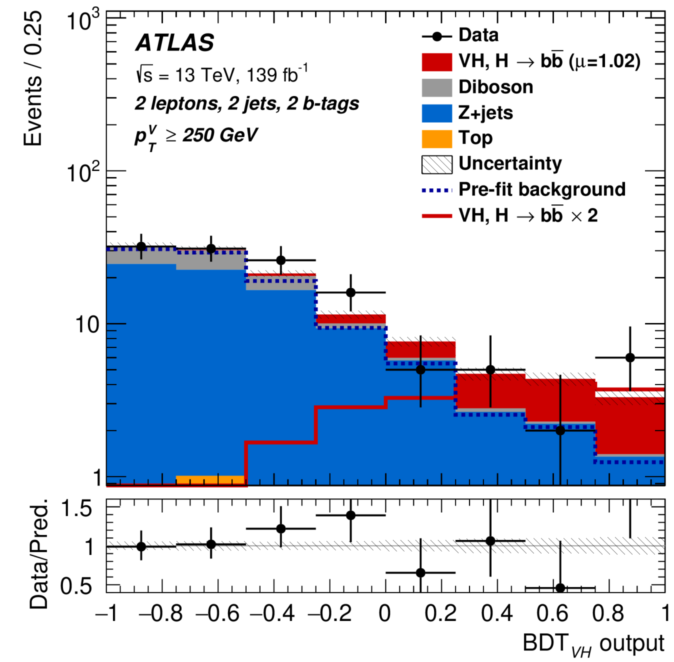

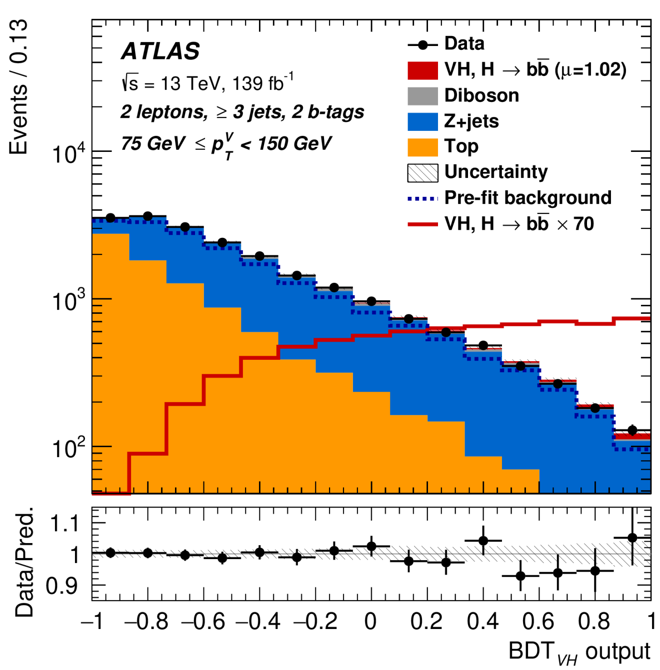

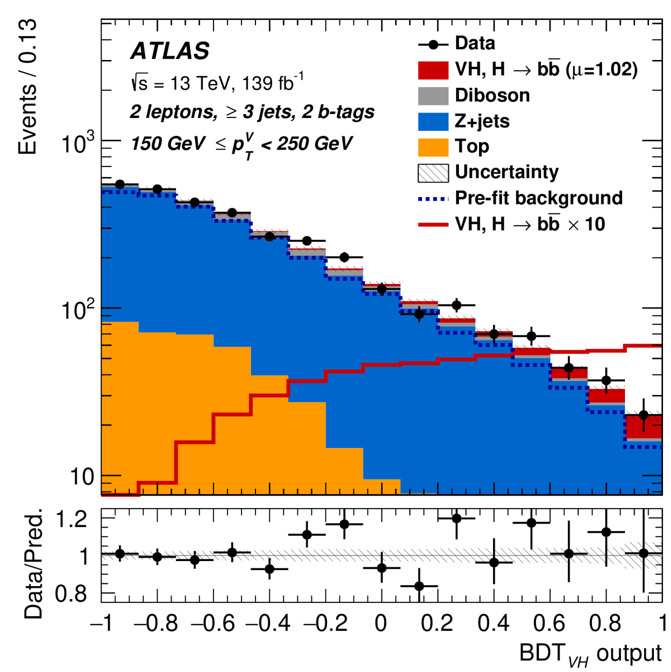

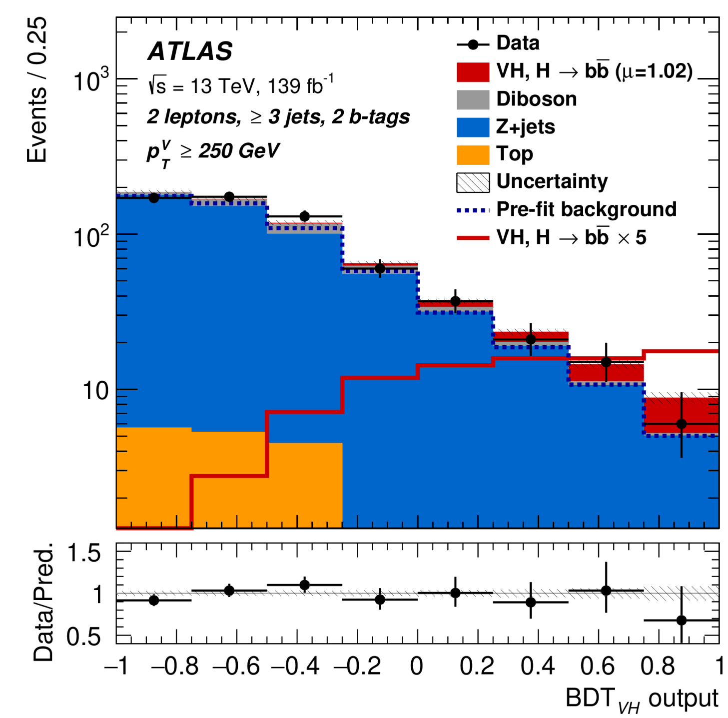

Statistical fluctuations in the BDT output

Correct folds

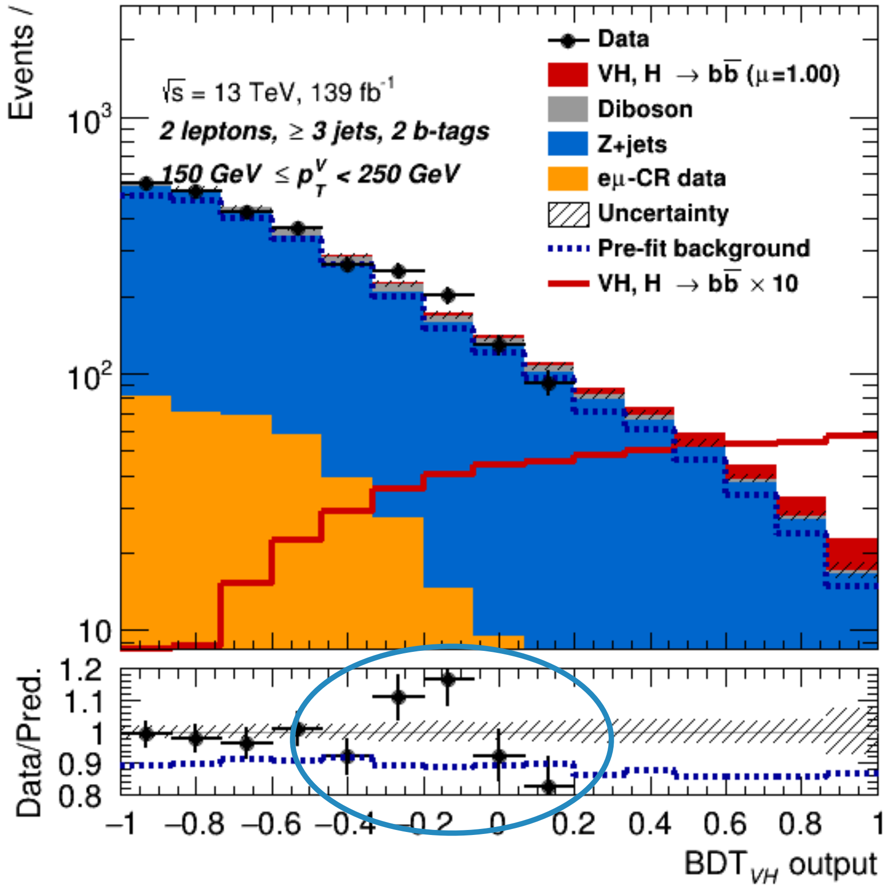

Inverted folds

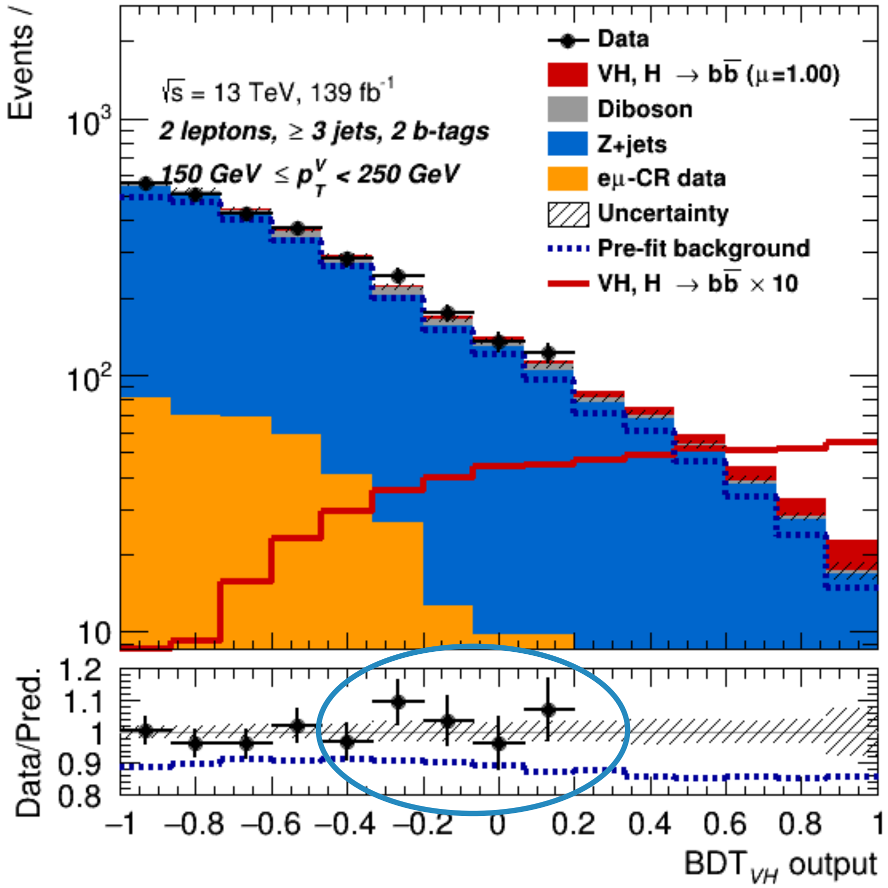

- Disagreement between data and MC in some bins
- Reproduced data histograms by inverting the BDT folds in the application
  - The data/MC disagreement in this regions is due to fluctuations in the BDT distribution
  - No impact on the systematics was observed

Postfit plots: 0-lep

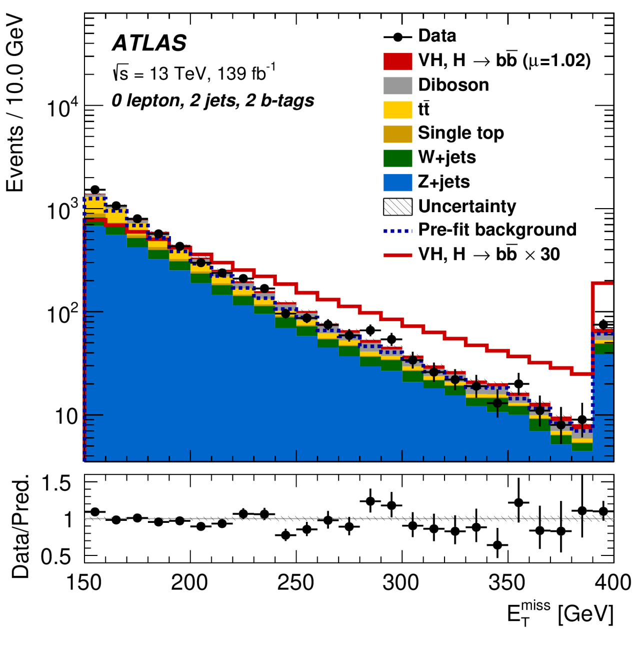

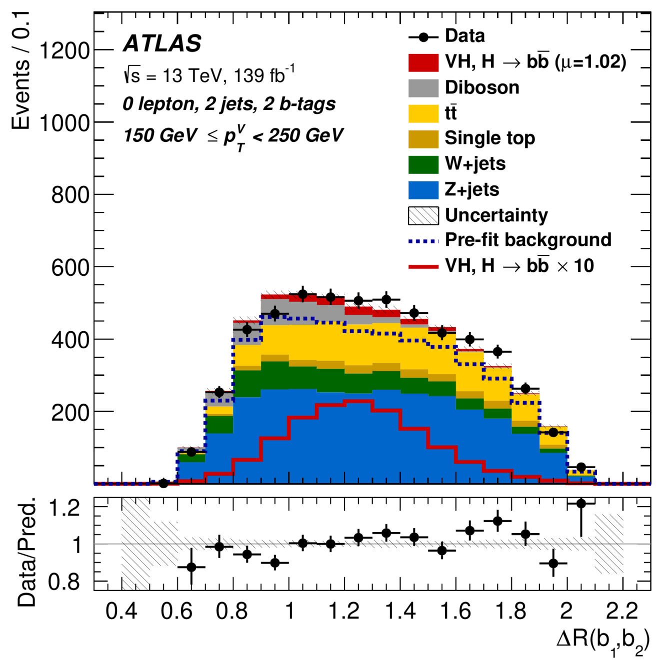

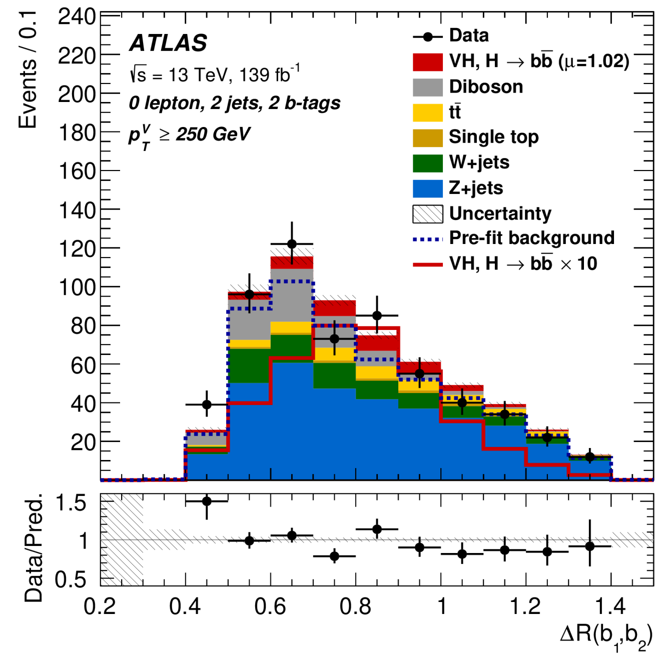

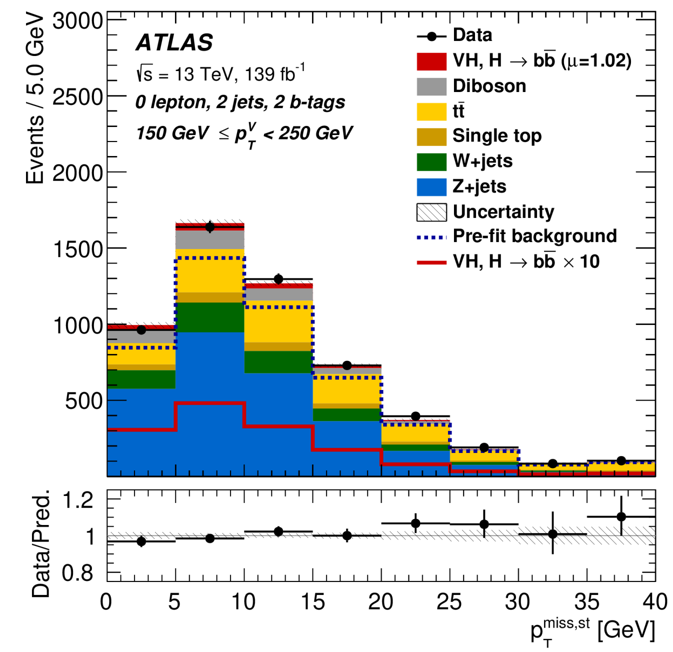

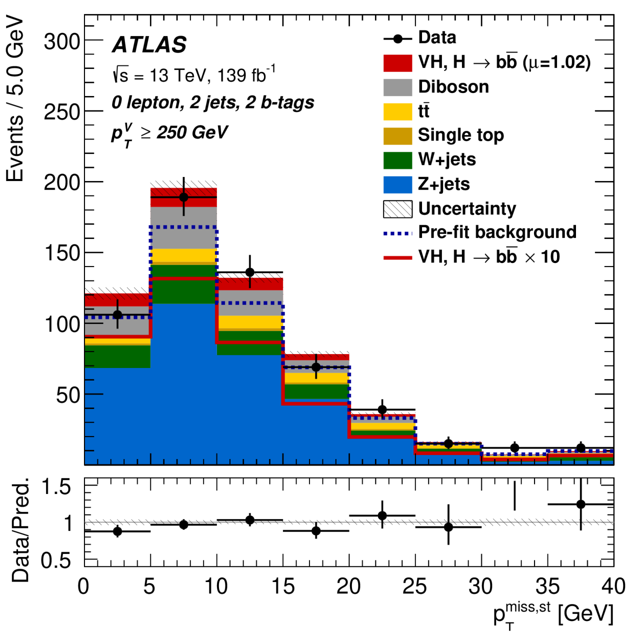

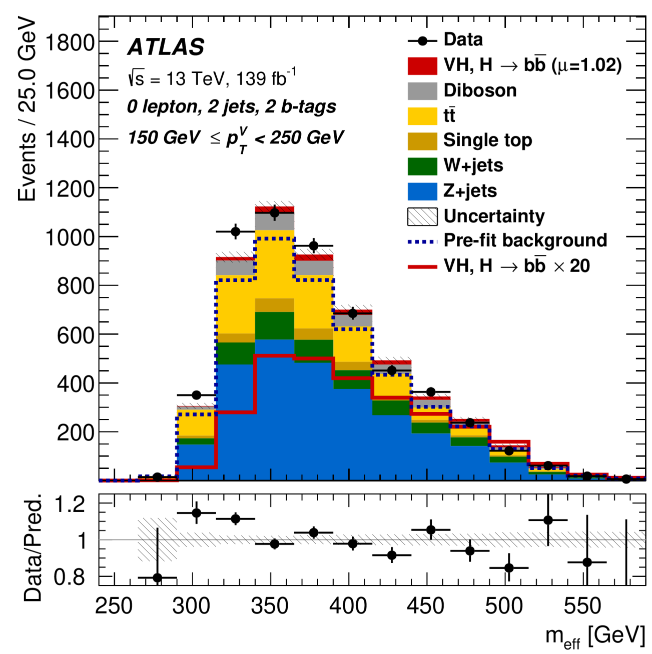

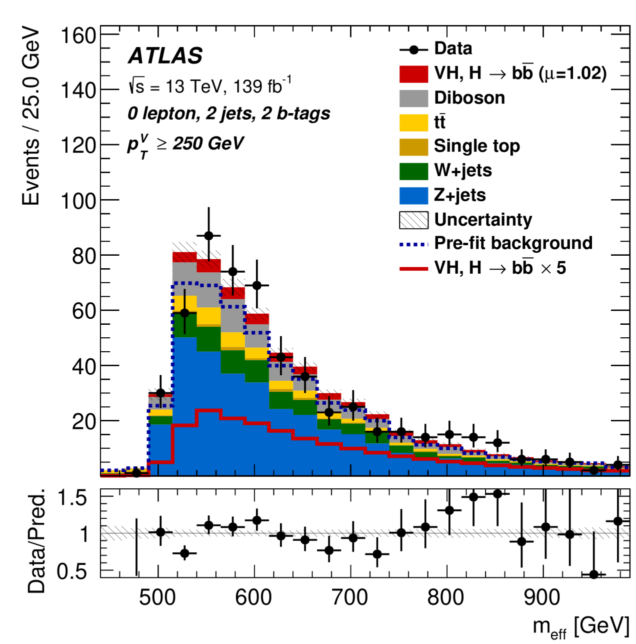

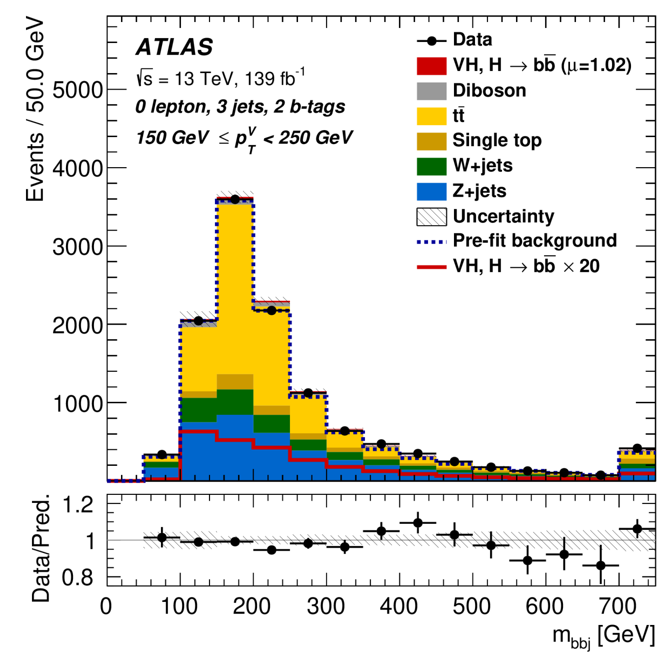

Postfit plots: 1-lep

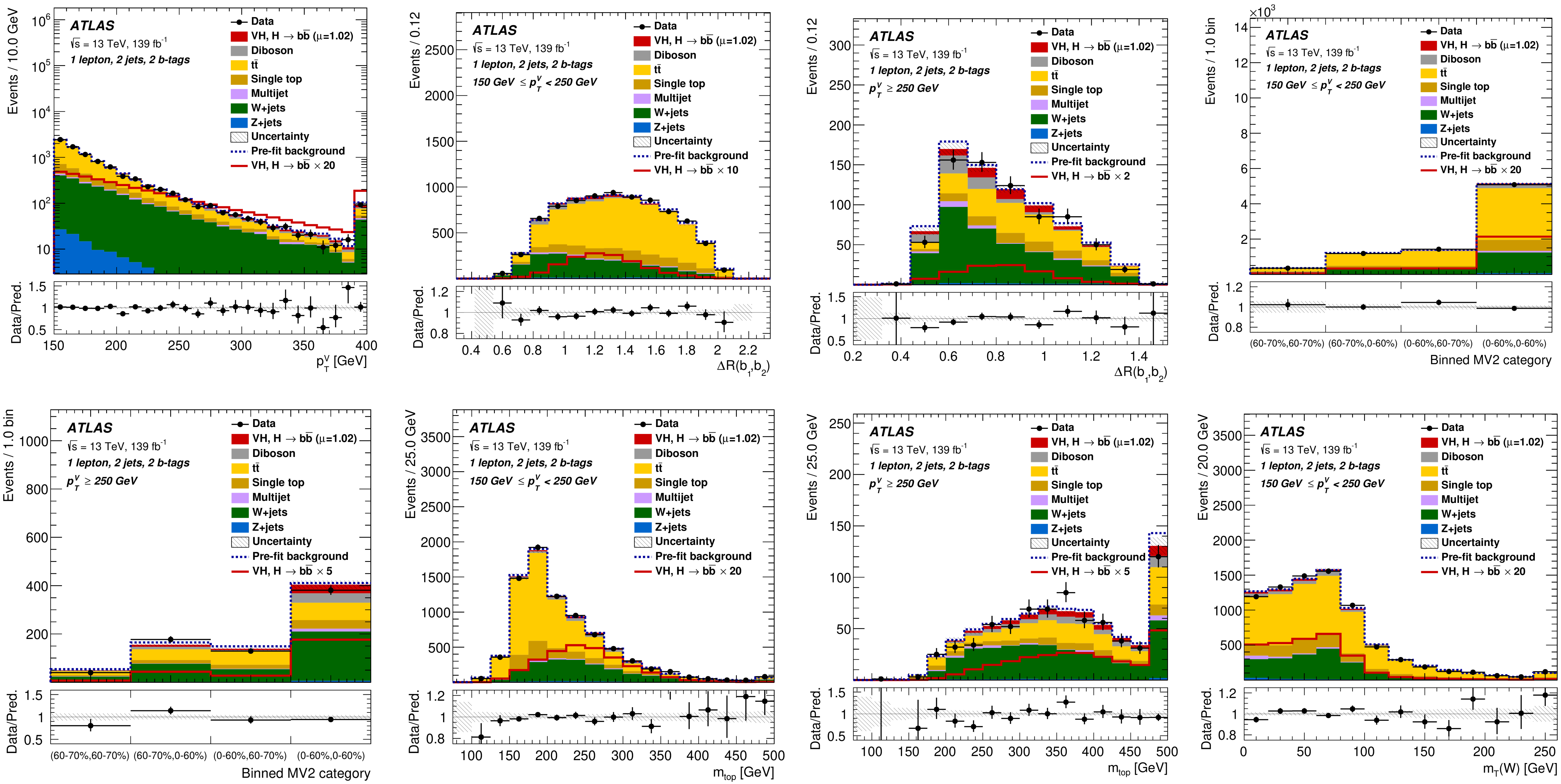

Postfit plots: 2-lep

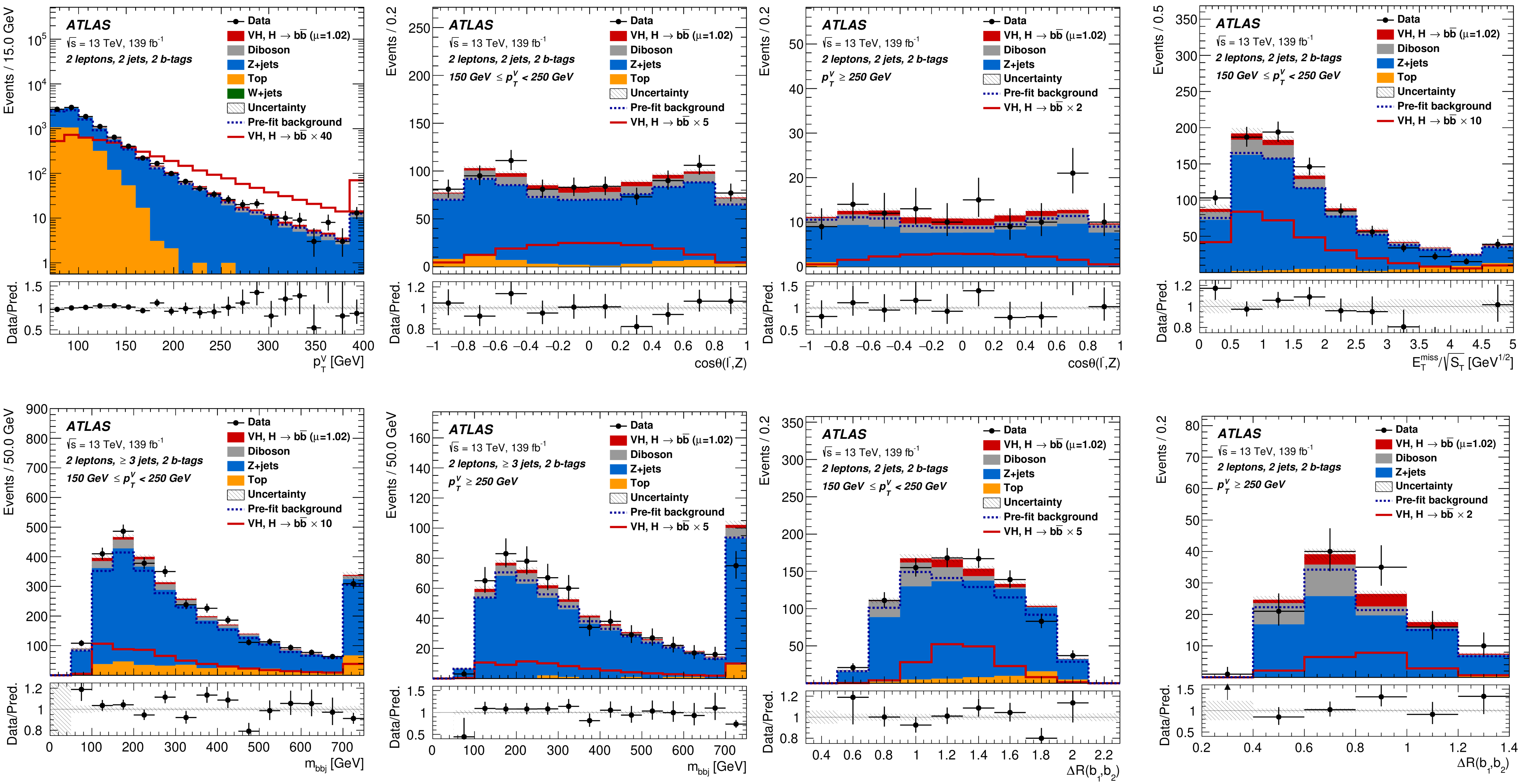

ΔR_{bb}-p_T^V cuts:0-lepton channel

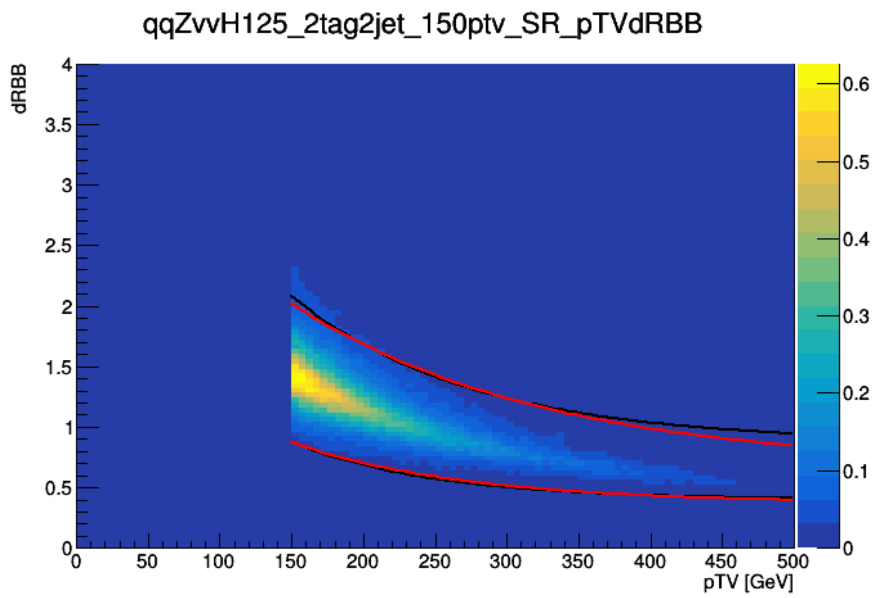

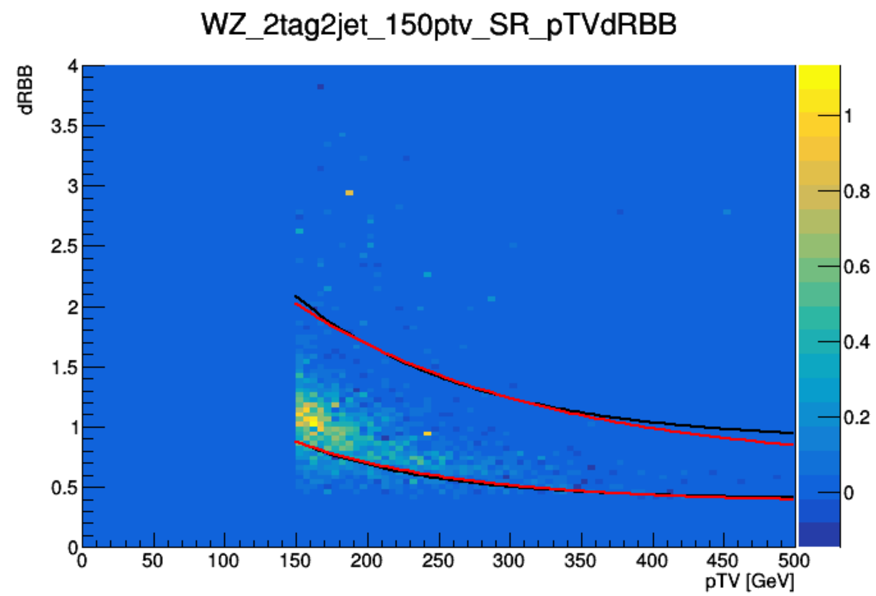

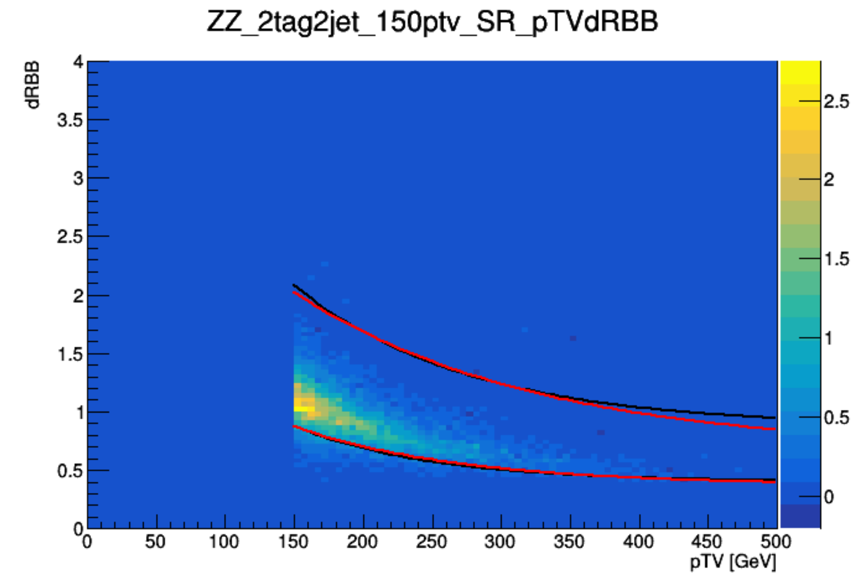

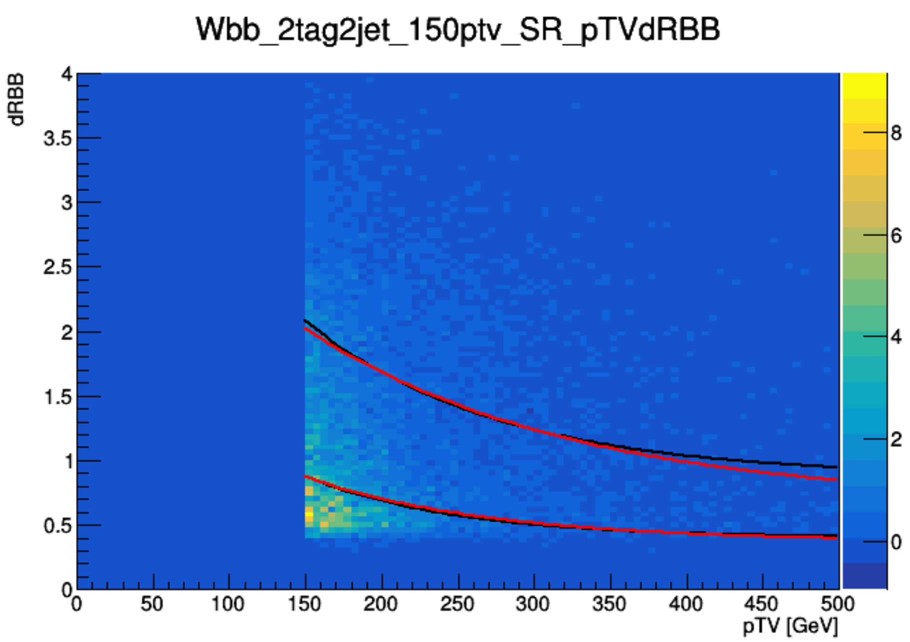

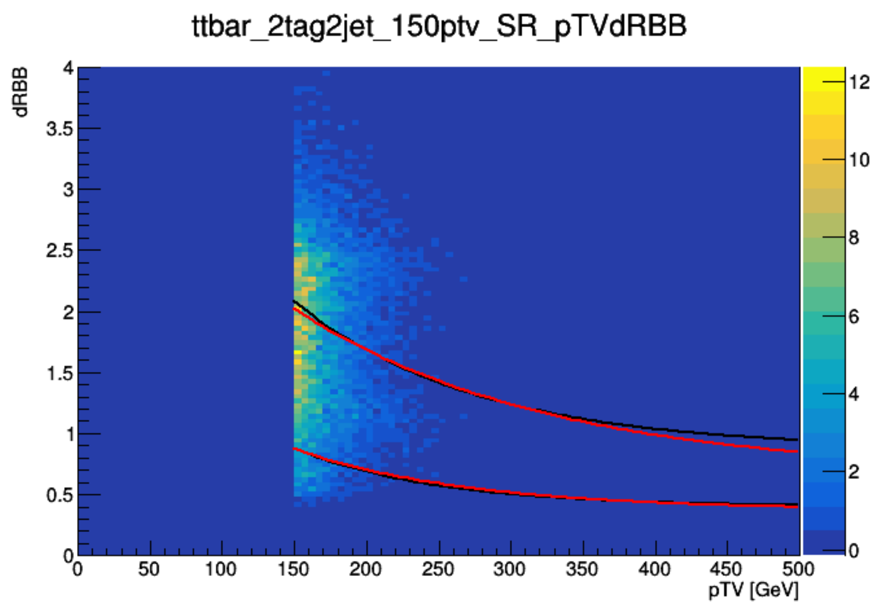

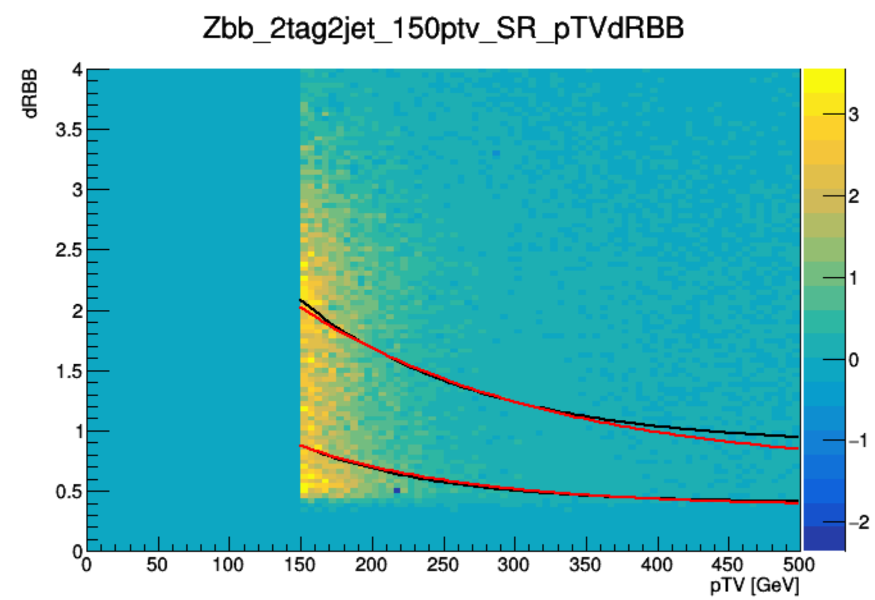

ΔR_{bb}-p_T^V cuts: 1-lepton channel

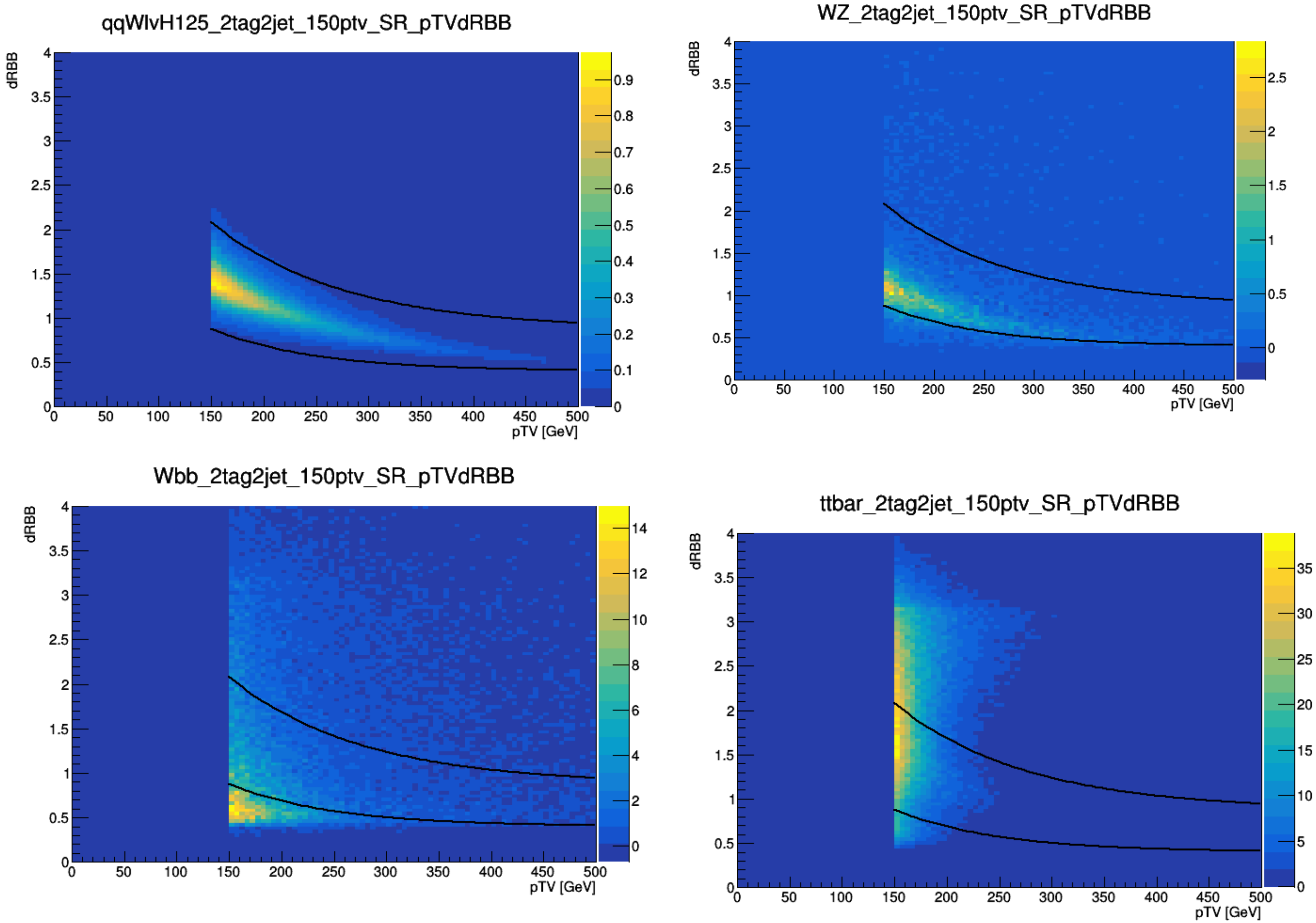

ΔR_{bb}-p_T^V cuts: 2-lepton channel

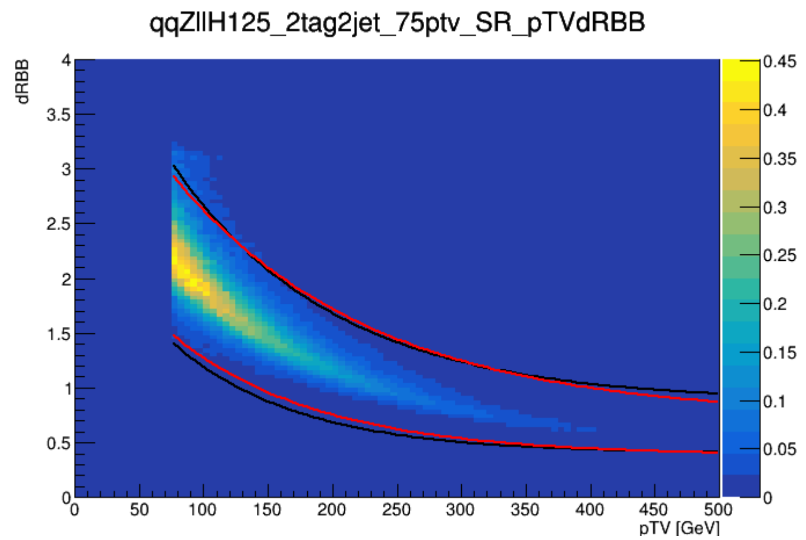

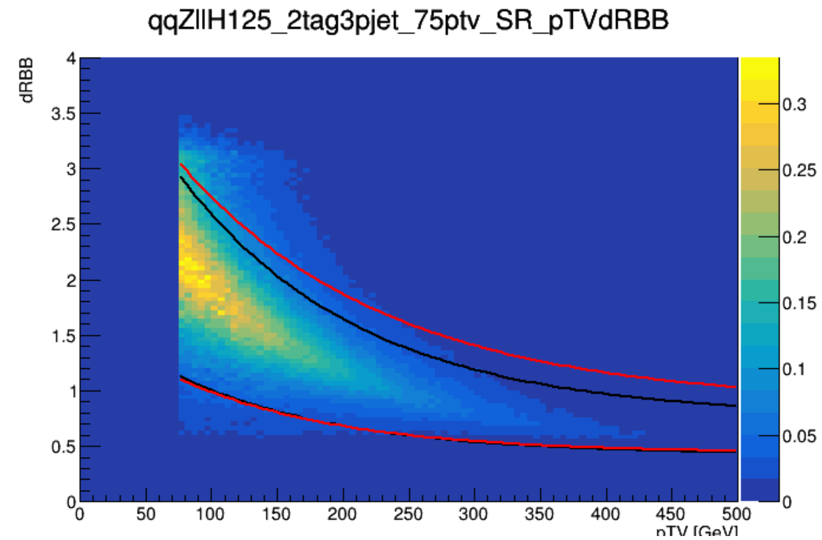

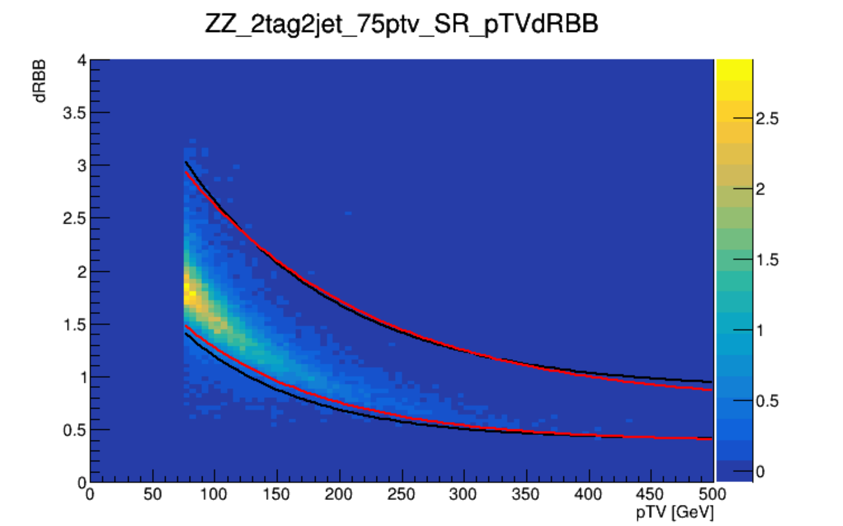

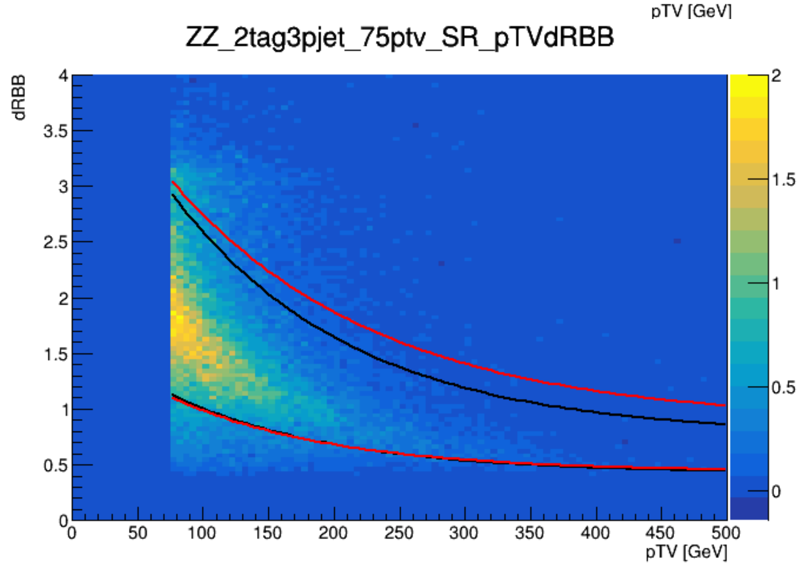

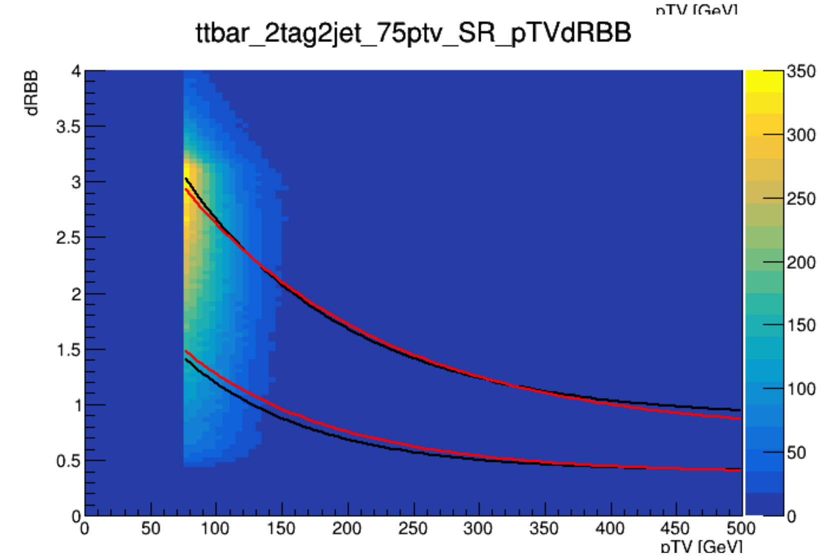

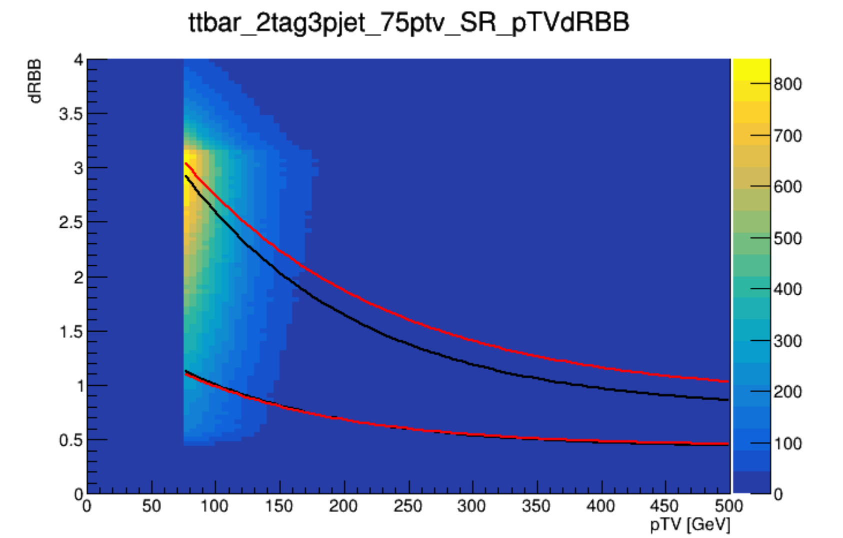

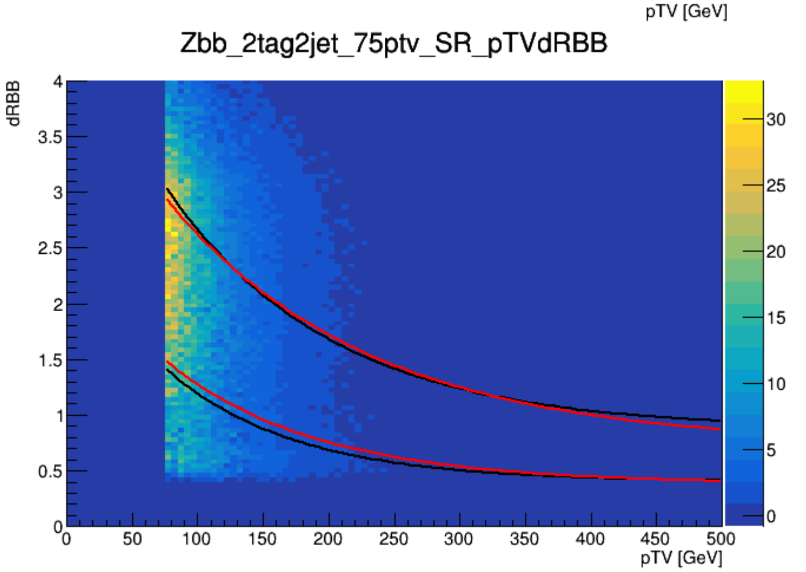

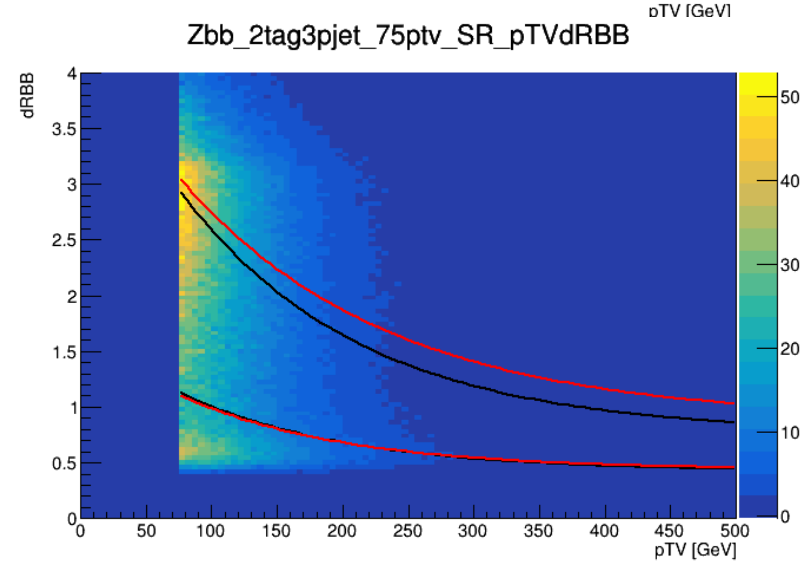

Pre-fit plots, 2-jet, pTV>150GeV

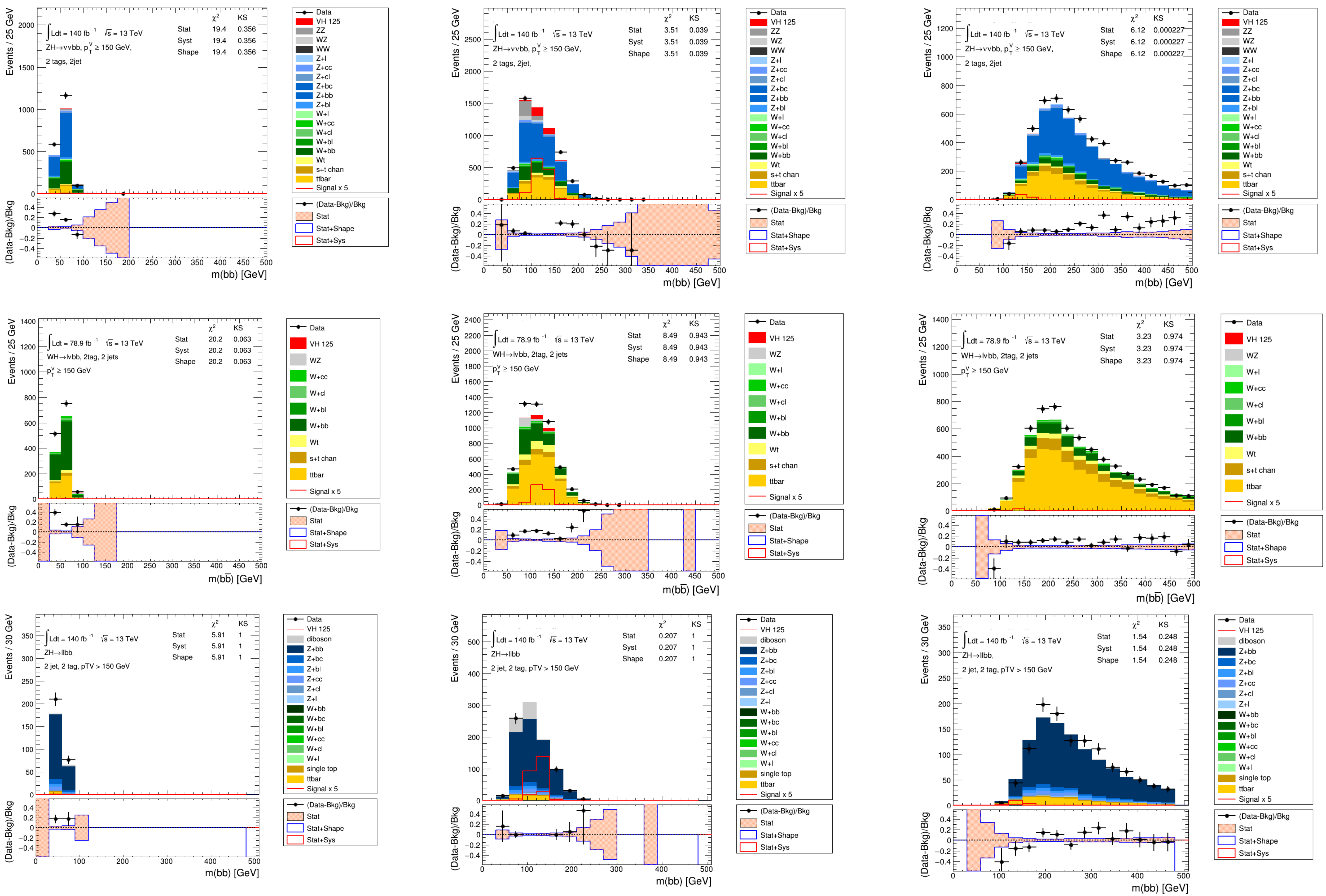

BDT distribution after categorisation

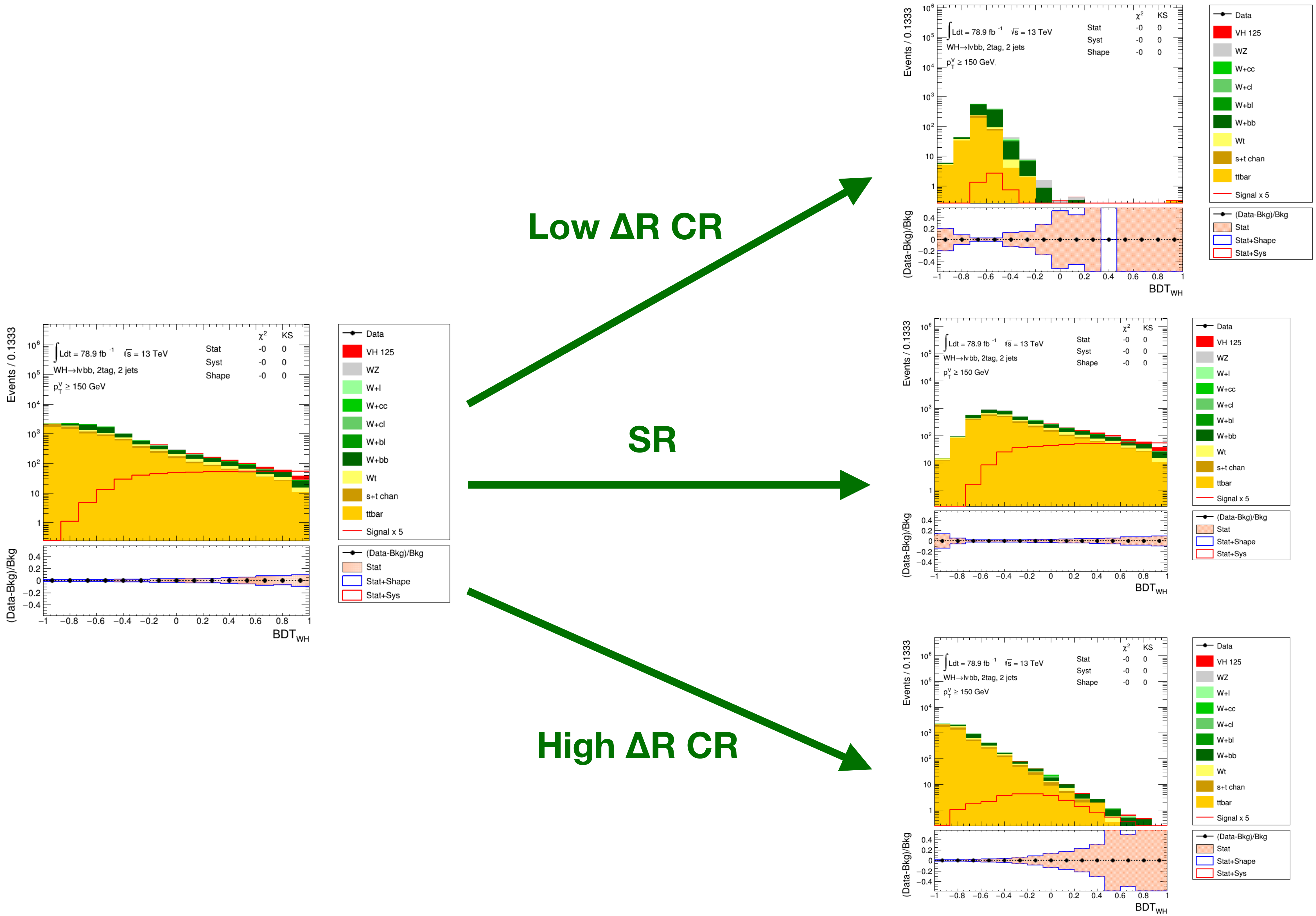

Constrains: MVA vs Mbb vs VZ

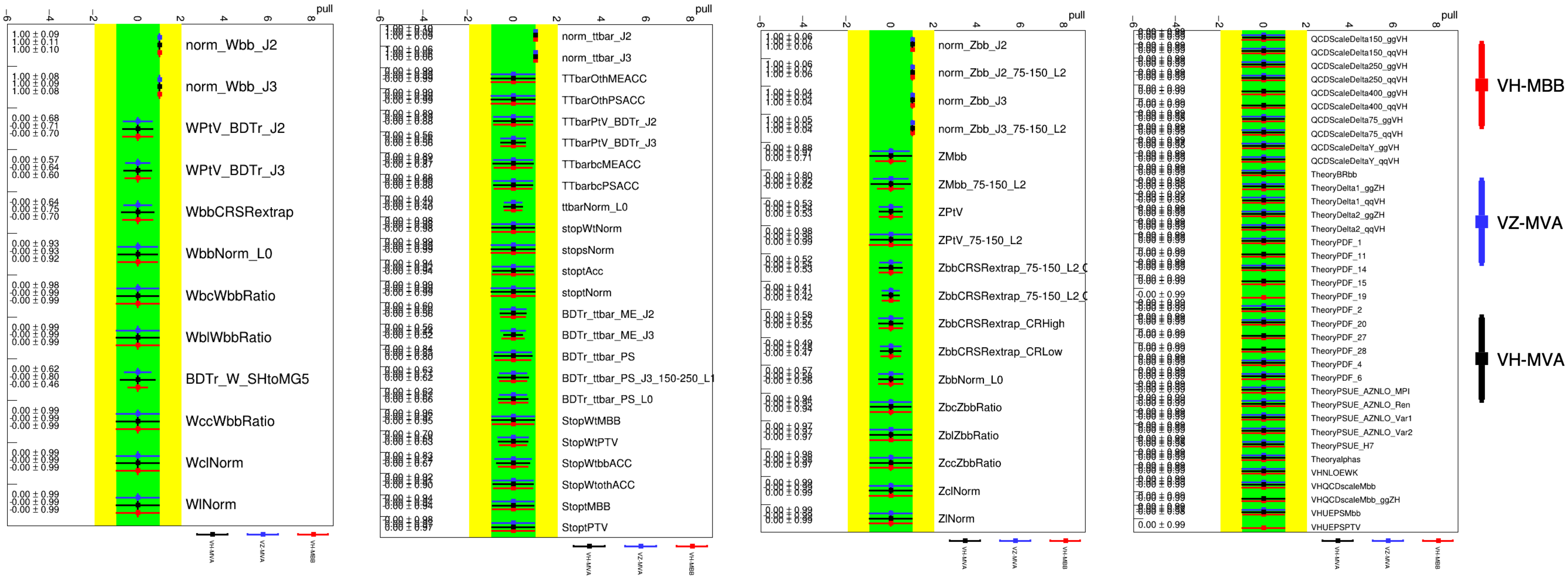

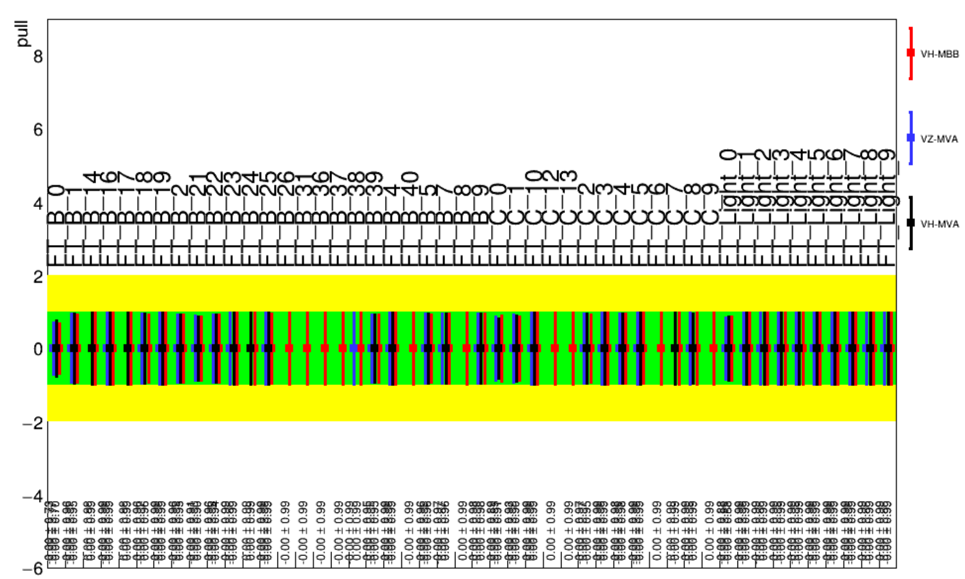

Constrains: nominal vs NoCRs

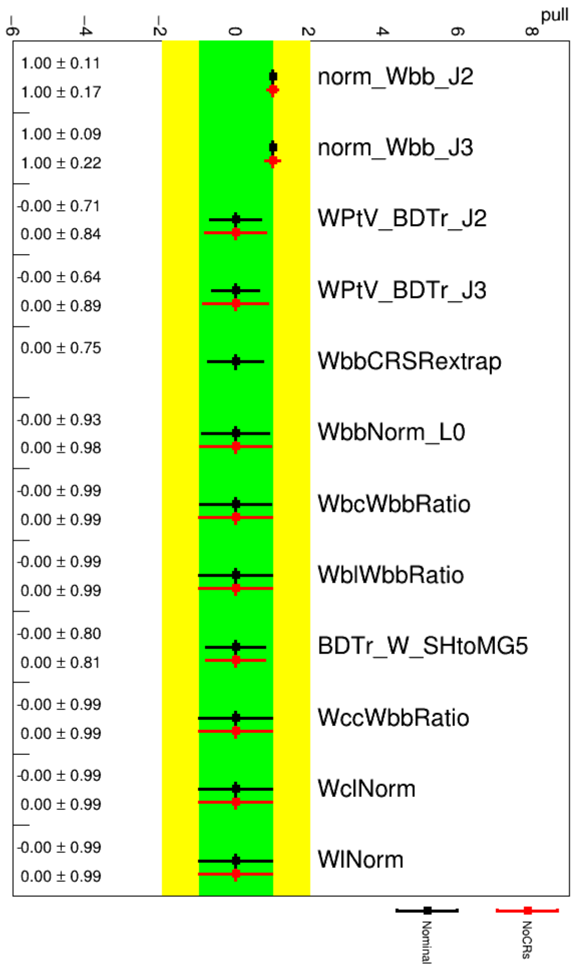

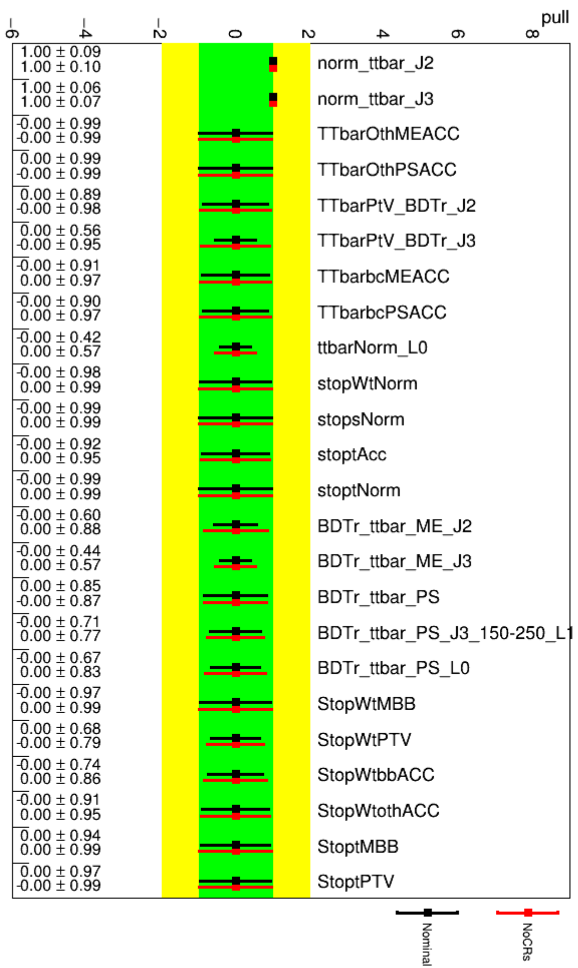

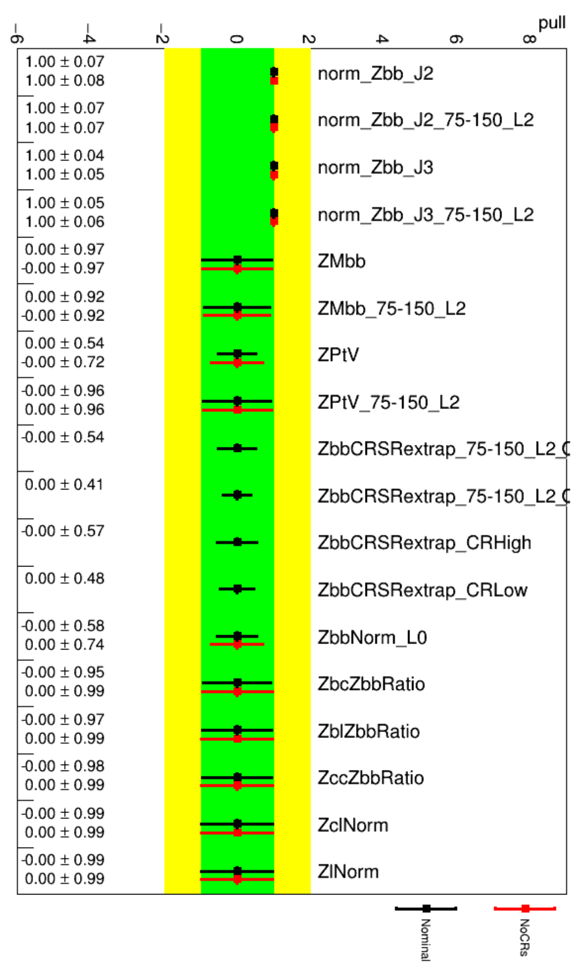

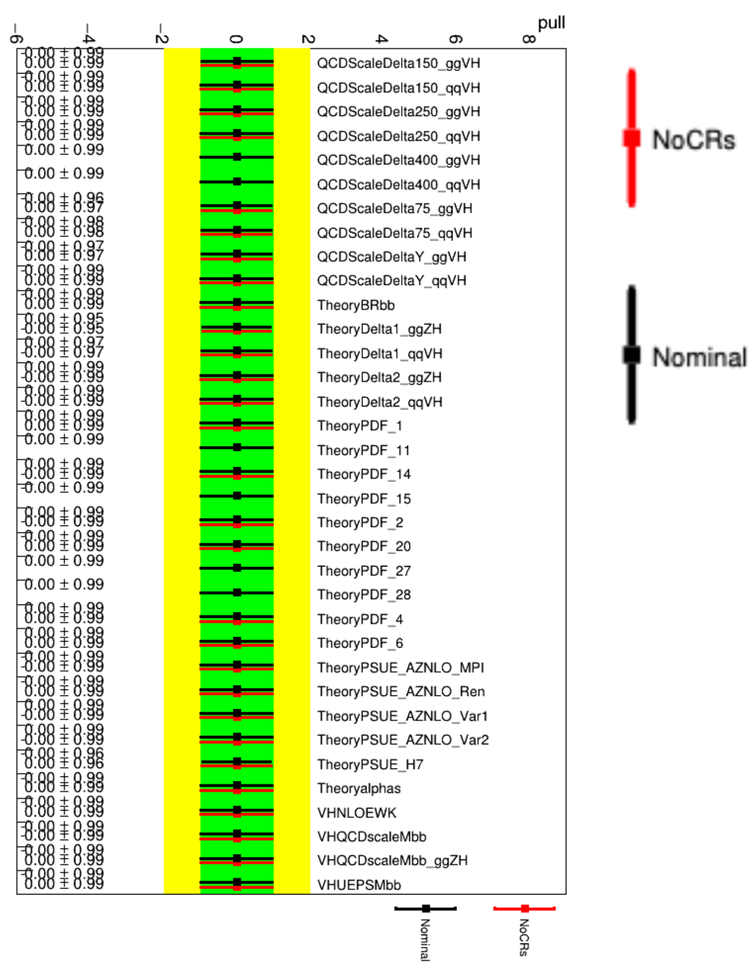

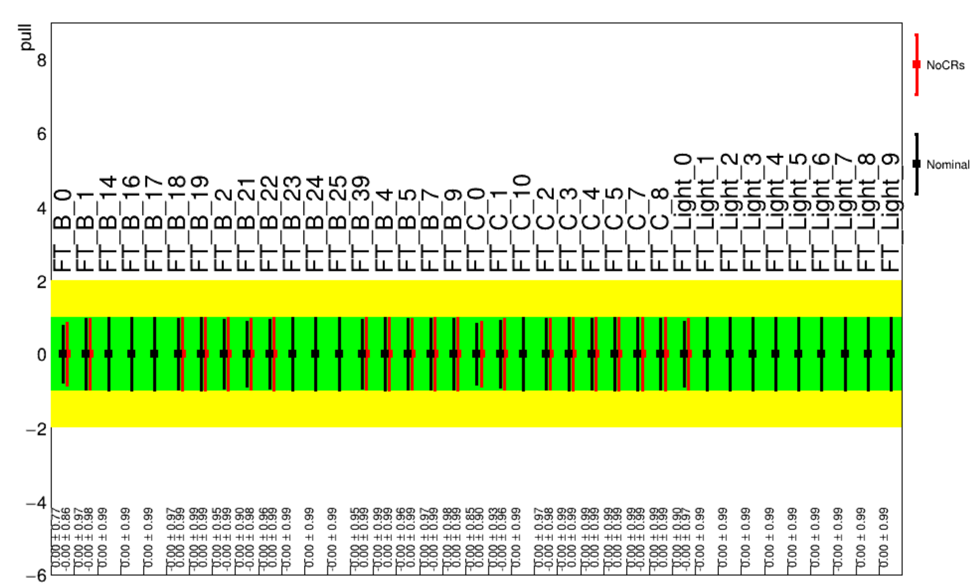

Constrains: discriminant in CRs

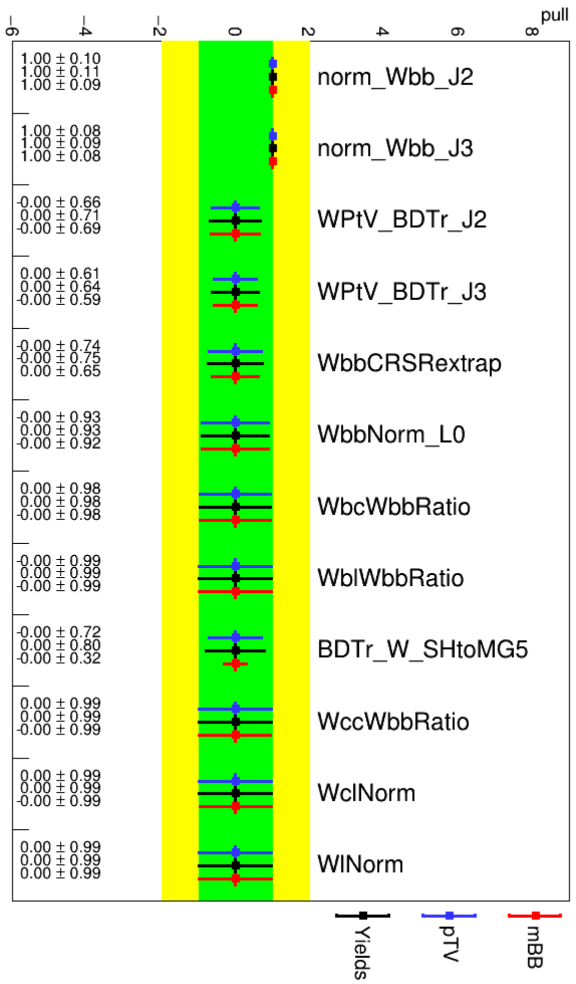

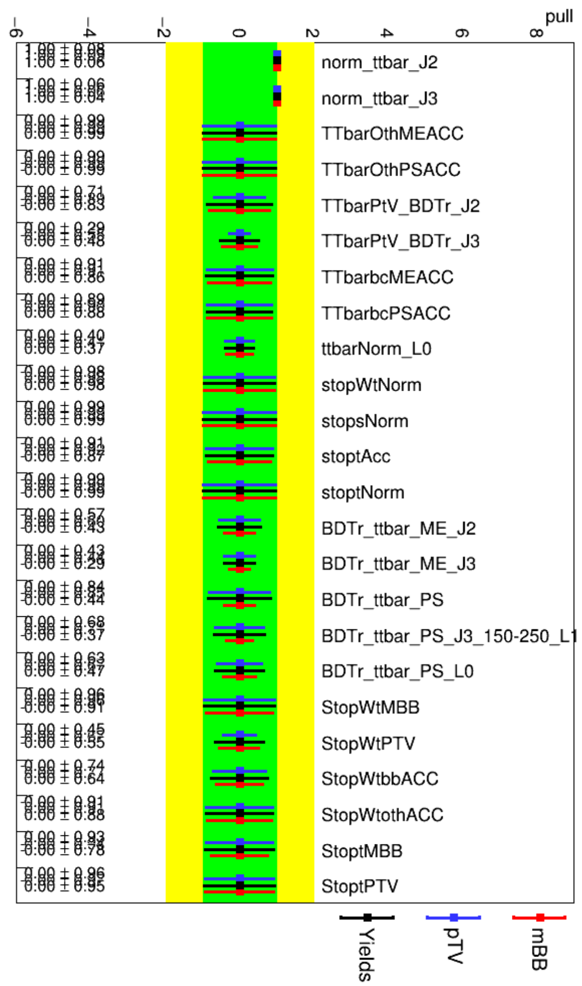

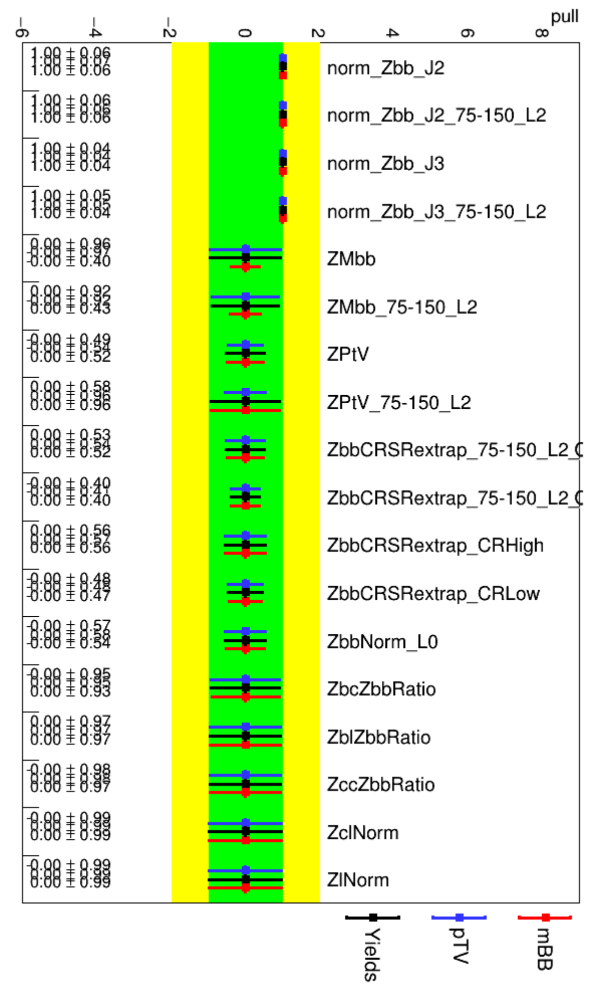

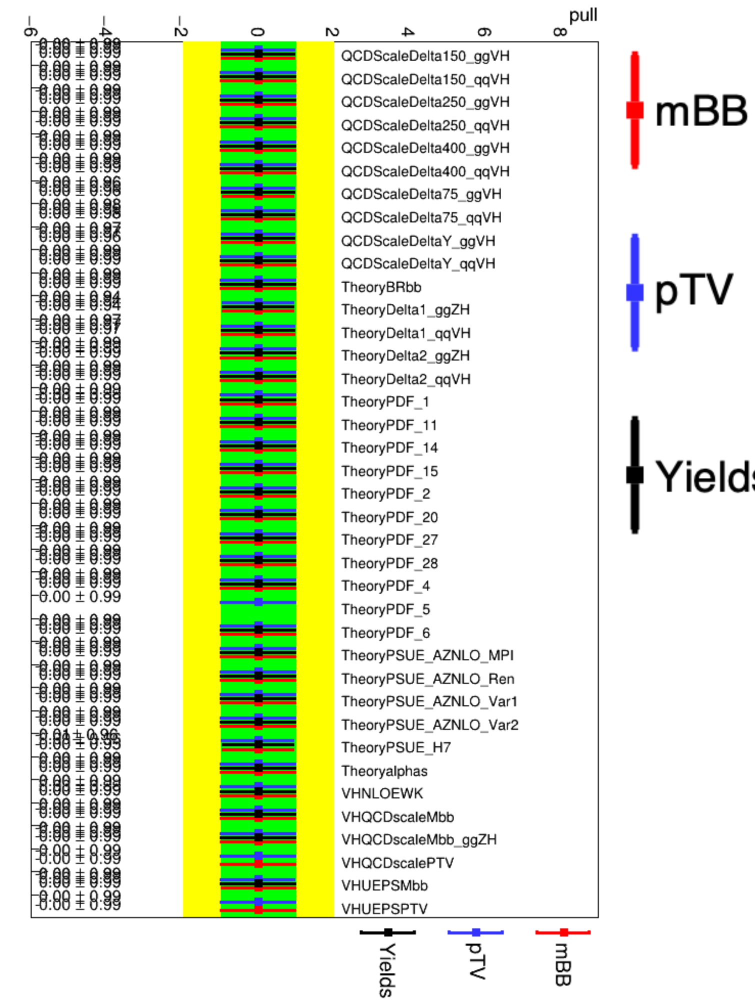

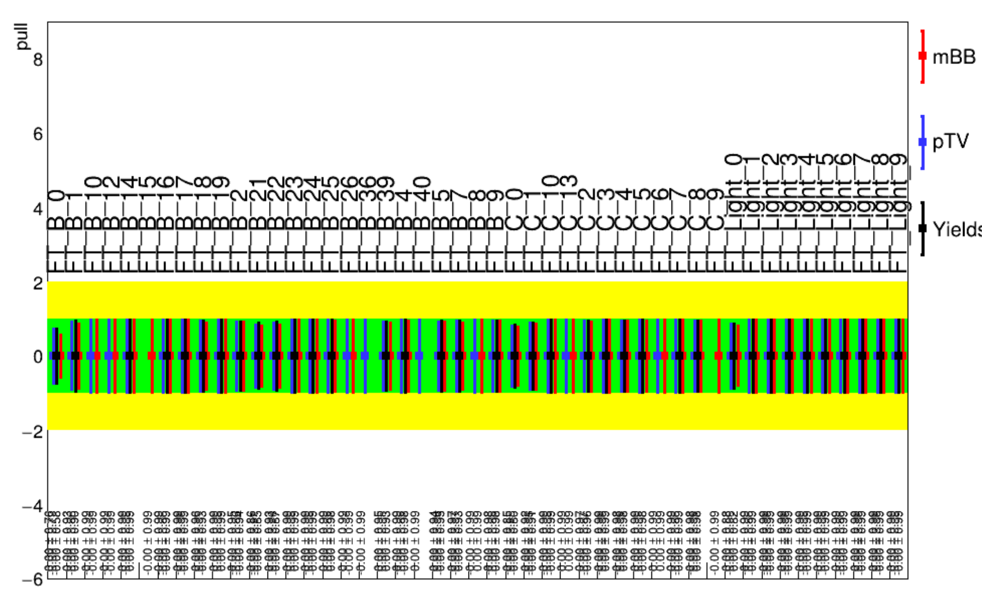

Asimov: Breakdown of systematics

- Combined fit with 139fb^{-1}

POI SigXsecOverSM	Central Value 1	Central Value 1	Central Value 1
Set of nuisance	Yields	p_T^V	m_{bb}
Total	±0.179	±0.178	±0.167
DataStat	±0.116	±0.116	±0.115
FullSyst	±0.137	±0.135	±0.121
Data stat only	±0.108	±0.108	±0.107
Top-emu CR stat	±0.016	±0.017	±0.018
Floating normalizations	±0.036	±0.035	±0.033
Modelling: VH	±0.051	±0.050	±0.048
Modelling: Background	±0.068	±0.067	±0.070
Multi Jet	±0.006	±0.006	±0.007
Modelling: single top	±0.022	±0.022	±0.030
Modelling: ttbar	±0.020	±0.020	±0.023
Modelling: W+jets	±0.037	±0.036	±0.022
Modelling: Z+jets	±0.032	±0.032	±0.030
Modelling: Diboson	±0.039	±0.038	±0.040
MC stat	±0.029	±0.030	±0.029
Experimental Syst	±0.076	±0.076	±0.062
Detector: lepton	±0.004	±0.007	±0.005
Detector: MET	±0.014	±0.015	±0.017
Detector: JET	±0.045	±0.044	±0.032
Detector: FTAG (b-jet)	±0.045	±0.044	±0.023
Detector: FTAG (c-jet)	±0.036	±0.036	±0.034
Detector: FTAG (l-jet)	±0.011	±0.010	±0.008
Detector: FTAG (extrap)	±0.000	±0.000	±0.000
Detector: PU	±0.005	±0.006	±0.010
Lumi	±0.016	±0.015	±0.016

Comparison with ICHEP MVA results

	ICHEP	ICHEP_pTV	2CRs	3CRs
Total	0.454	0.435	0.442	0.433
DataStat	0.267	0.267	0.269	0.269
FullSyst	0.367	0.343	0.350	0.339
Floating normalizations	0.071	0.037	0.046	0.069
Multi Jet	0.000	0.000	0.000	0.000
Modelling : single top	0.093	0.088	0.090	0.093
Modelling : ttbar	0.078	0.066	0.086	0.066
Modelling : W+jets	0.145	0.075	0.111	0.088
Modelling : Z+jets	0.000	0.000	0.000	0.000
Modelling : Diboson	0.056	0.055	0.058	0.067
Modelling : VH	0.125	0.124	0.122	0.120
Detector : lepton	0.007	0.005	0.003	0.003
Detector : MET	0.004	0.004	0.005	0.001
Detector : JET	0.052	0.053	0.075	0.071
Detector : FTAG (b-jet)	0.059	0.064	0.070	0.050
Detector : FTAG (c-jet)	0.111	0.113	0.128	0.115
Detector : FTAG (l-jet)	0.014	0.007	0.015	0.005
Detector : FTAG (extrap)	0.021	0.021	0.018	0.022
Detector : PU	0.004	0.003	0.018	0.014
Lumi	0.018	0.017	0.017	0.016
MC stat	0.166	0.165	0.164	0.163

- Asimov fit results in the 1-lepton channel
  - Compare the ICHEP results with ~80fb^{-1} with new analysis categorisation

Comparison with old categorisation

- Asimov fit results in the 0-lepton channel
  - Compare the previous analysis categorisation with 139fb[-1]

	default	New Model
Total	0.317	0.310
DataStat	0.206	0.207
FullSyst	0.241	0.231
Data stat only	0.191	0.193
Floating Normalisations	0.032	0.022
Modelling : VH	0.095	0.090
Modelling Background	0.158	0.138
Multi Jet	0.000	0.000
Modelling : single top	0.040	0.034
Modelling : ttbar	0.028	0.027
Modelling : W+jets	0.050	0.042
Modelling : Z+jets	0.064	0.042
Modelling : Diboson	0.081	0.069
MC stat	0.088	0.089
Experimental Syst	0.151	0.157
Detector : lepton	0.000	0.000
Detector : MET	0.013	0.020
Detector : JET	0.098	0.085
Detector : FTAG (b-jet)	0.088	0.104
Detector : Ftag (c-jet)	0.057	0.061
Detector : Ftag (l-jet)	0.011	0.010
Detector : Ftag (extrap)	0.000	0.003
Detector : PU	0.006	0.005
Lumi	0.018	0.016

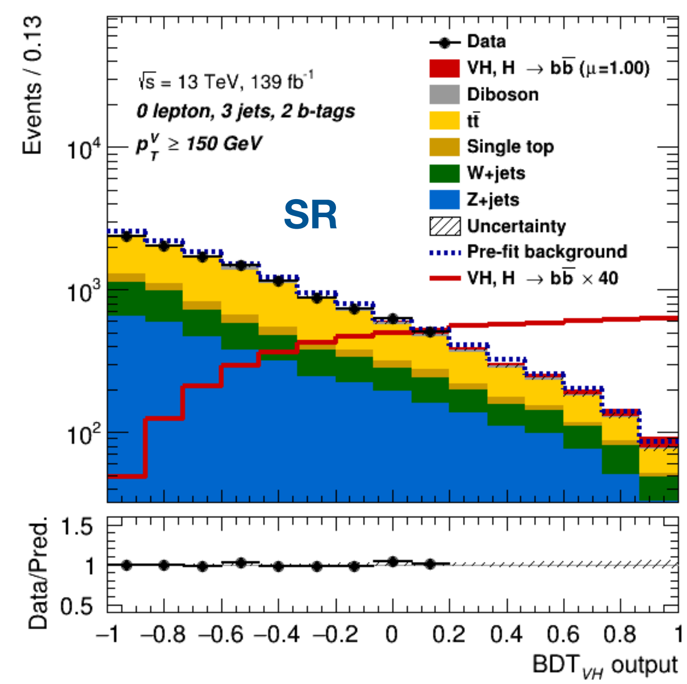

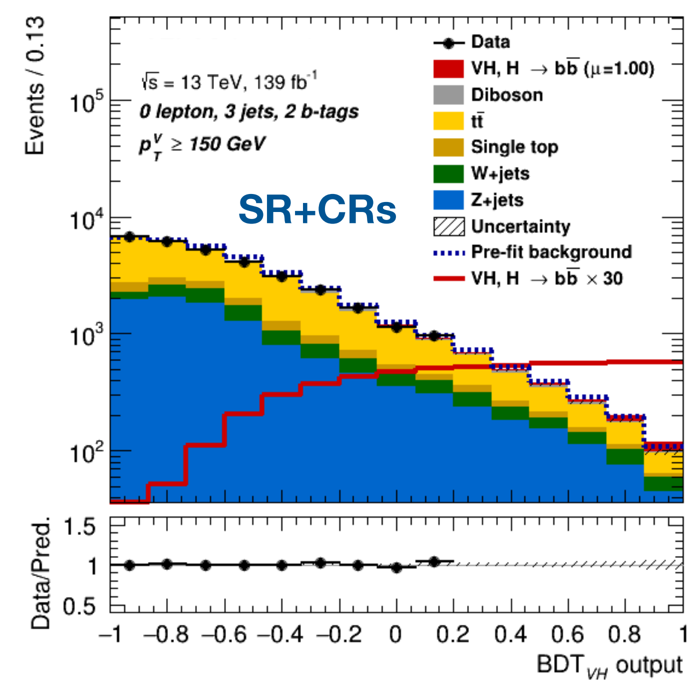

Comparison with old categorisation

- Asimov fit results in the 2-lepton channel
  - Compare the previous analysis categorisation with 139fb^{-1}
  - Including the previous eμ control region

	default	New Model
Total	0.281	0.276
DataStat	0.205	0.209
FullSyst	0.192	0.180
Data stat only	0.190	0.195
Floating normalizations	0.055	0.059
Modelling : VH	0.115	0.114
Modelling : Background	0.108	0.099
Multi Jet	0.000	0.000
Modelling : single top	0.012	0.012
Modelling : ttbar	0.039	0.058
Modelling : W+jets	0.000	0.000
Modelling : Z+jets	0.075	0.054
Modelling : Diboson	0.033	0.026
MC stat	0.057	0.055
Experimental Syst	0.109	0.108
Detector : lepton	0.013	0.011
Detector : MET	0.006	0.017
Detector : JET	0.069	0.059
Detector : FTAG (b-jet)	0.060	0.078
Detector : FTAG (c-jet)	0.024	0.018
Detector : FTAG (l-jet)	0.028	0.025
Detector : FTAG (extrap)	0.000	0.000
Detector : PU	0.008	0.012
Lumi	0.017	0.017

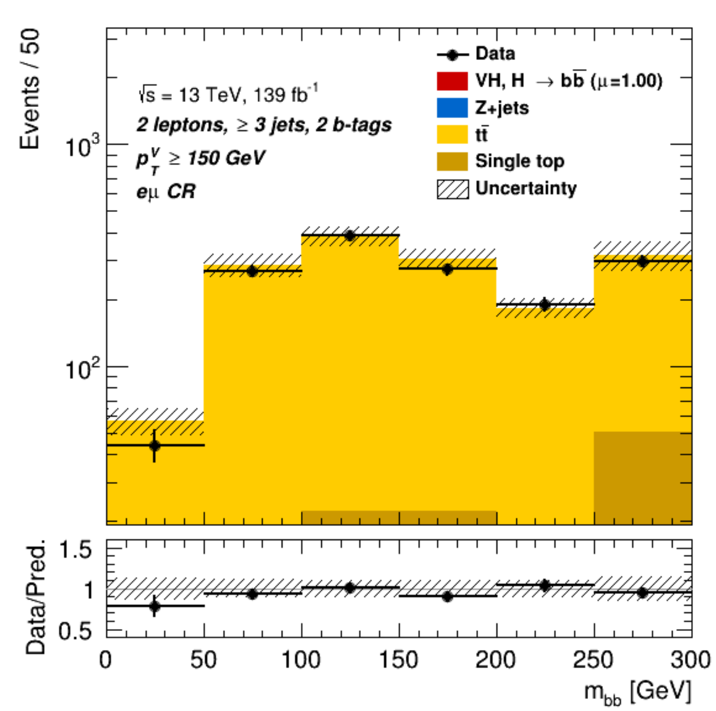

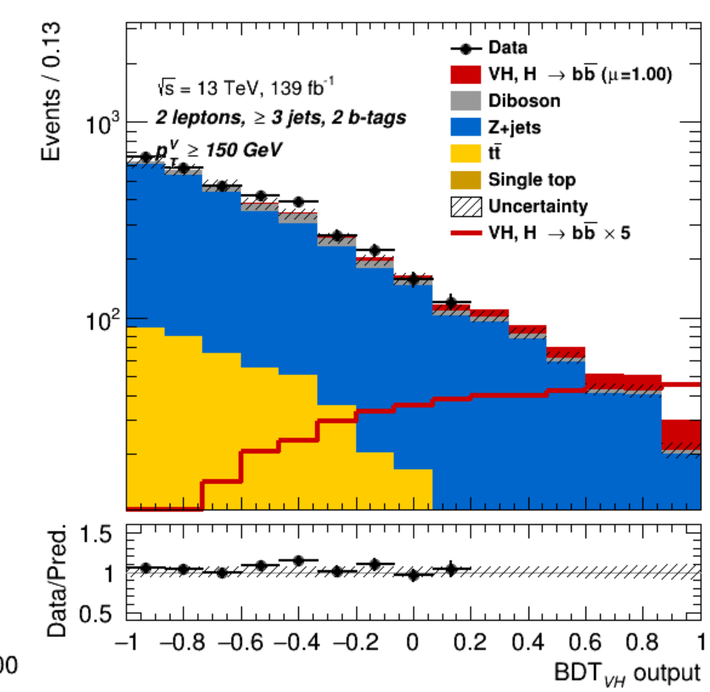

Multi-jet inverted isolation region

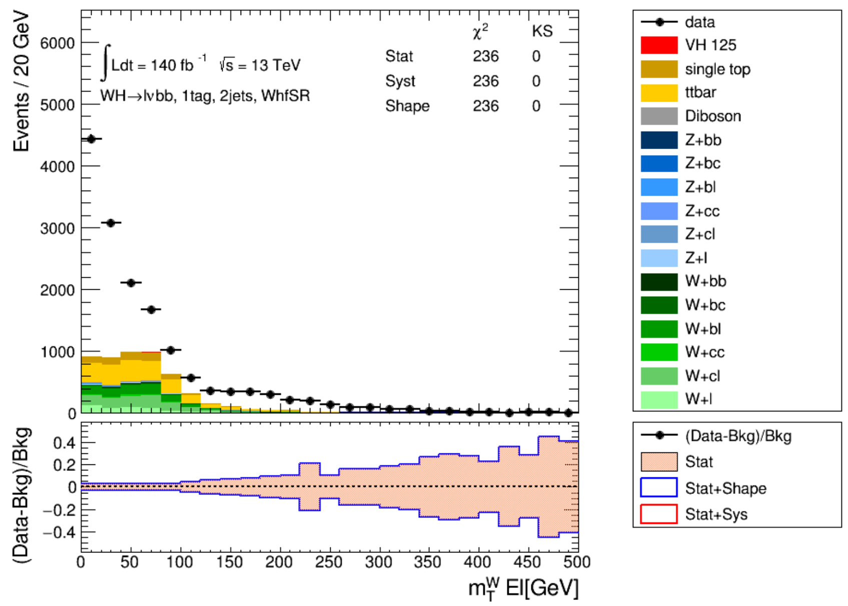

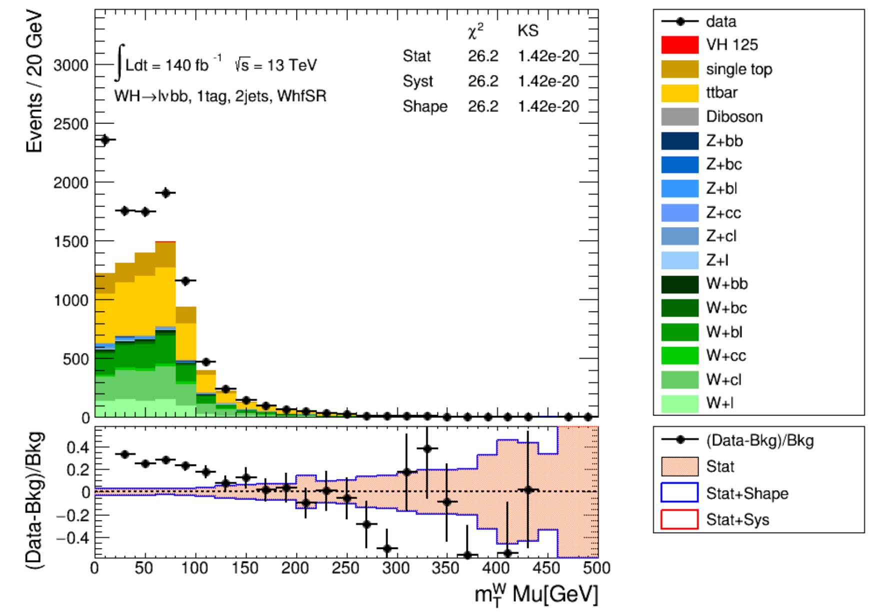

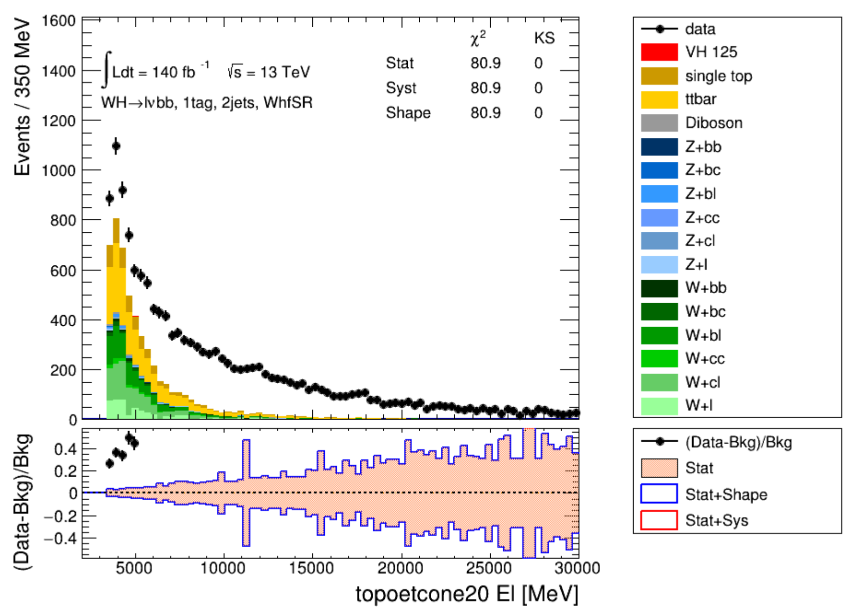

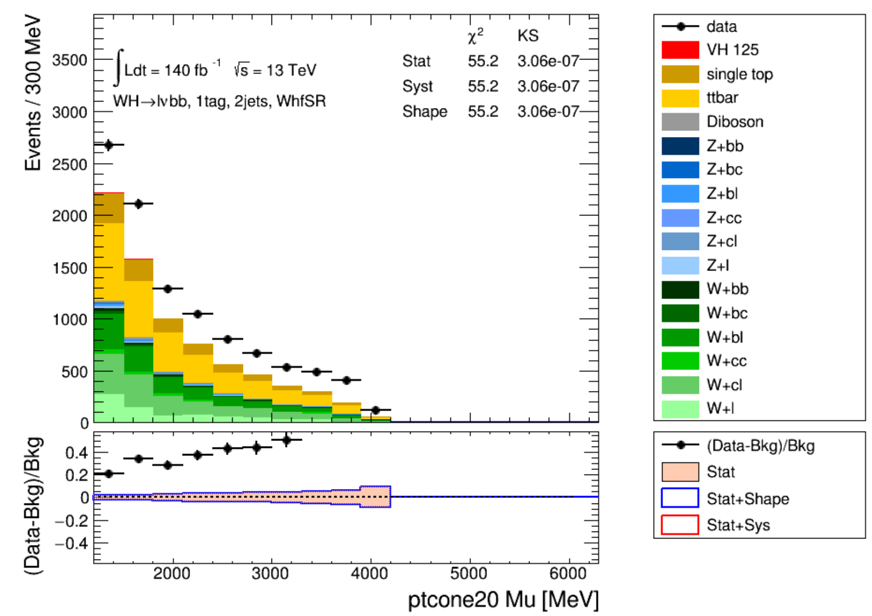

	Isolated Region	Inverted Isolation Region
Electron	FCLoose topoEtCone20 $<$ max(0.015 p_T^l,3.5) GeV	FCLoose topoEtCone20 $>$ max(0.015 p_T^l,3.5) GeV
Muon	FixedCutLoose PtCone20 $<$ 1.25 GeV	FixedCutLoose PtCone20 $>$ 1.25 GeV PtCone20 $<$4 GeV

Fit Performance: 2jet High Ptv

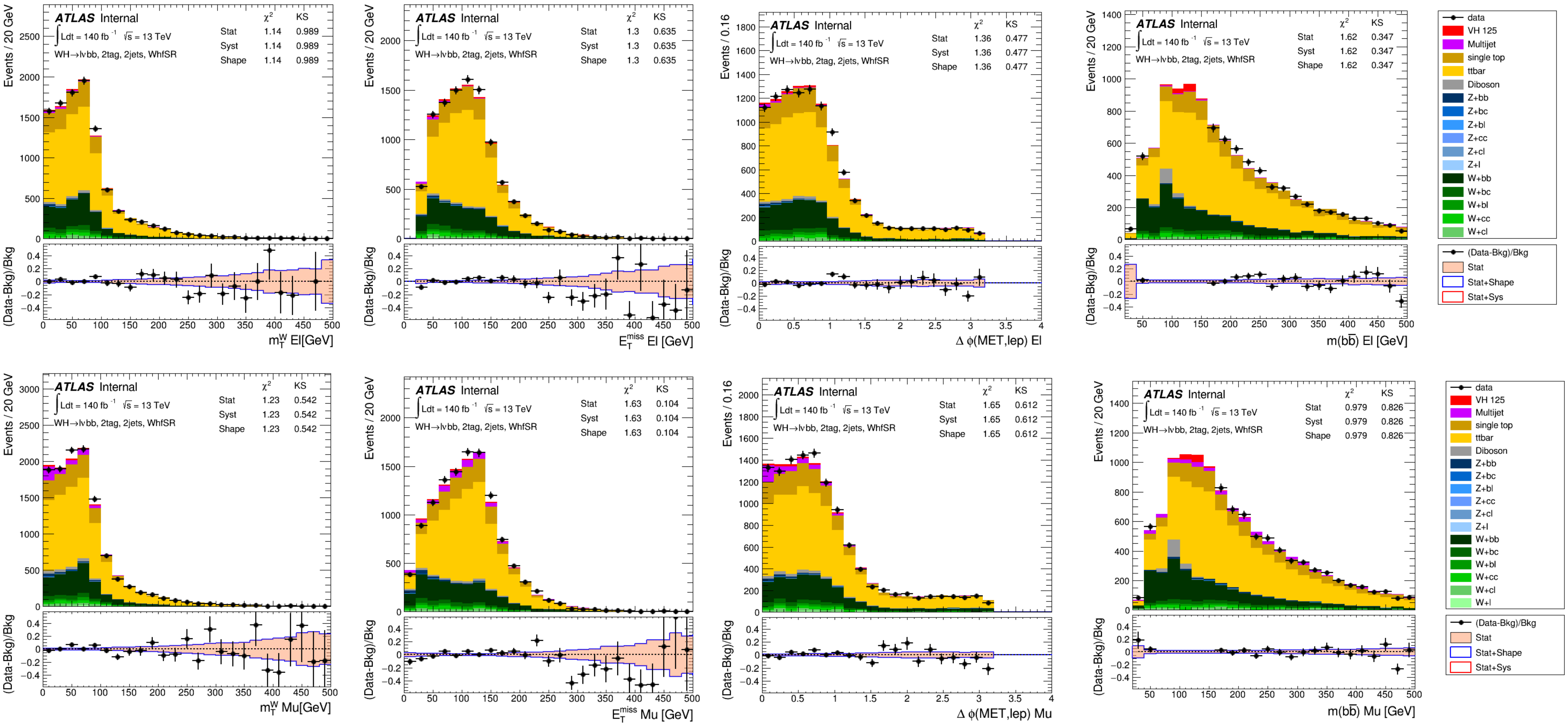

- Less MJ in the electron channel and more in the muon channel with the new fit: MJ fraction in El is 0.7% and 3.8% in Mu
- data/MC agreement is good with the new fit

Multi-jet template Fit: 2jet, $p_T^V>150$GeV

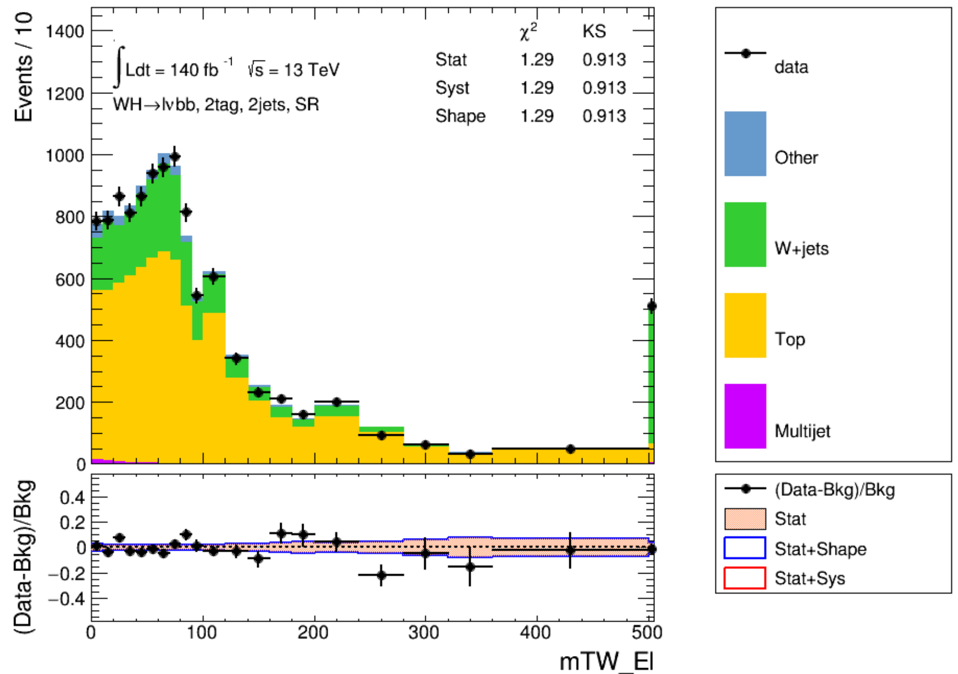


```
 Constant Parameter     Value
--------------------   ------------
   Others_SR_Nevents    3.5729e+02
        Others_scale    1.0000e+00
      Top_SR_Nevents    8.4063e+03
        W_SR_Nevents    2.2160e+03
multijetEl_SR_Nevents     1.0764e+04

 Floating Parameter    InitialValue     FinalValue (+HiError,-LoError)
--------------------   ------------   ------------------------------------
           Top_scale    1.0000e+00    8.9206e-01 (+2.28e-02,-2.30e-02)
             W_scale    1.0000e+00    1.3253e+00 (+7.42e-02,-7.33e-02)
     multijetEl_scale    1.0000e+00    7.2818e-03 (+1.34e-02,--0.00e+00)
```

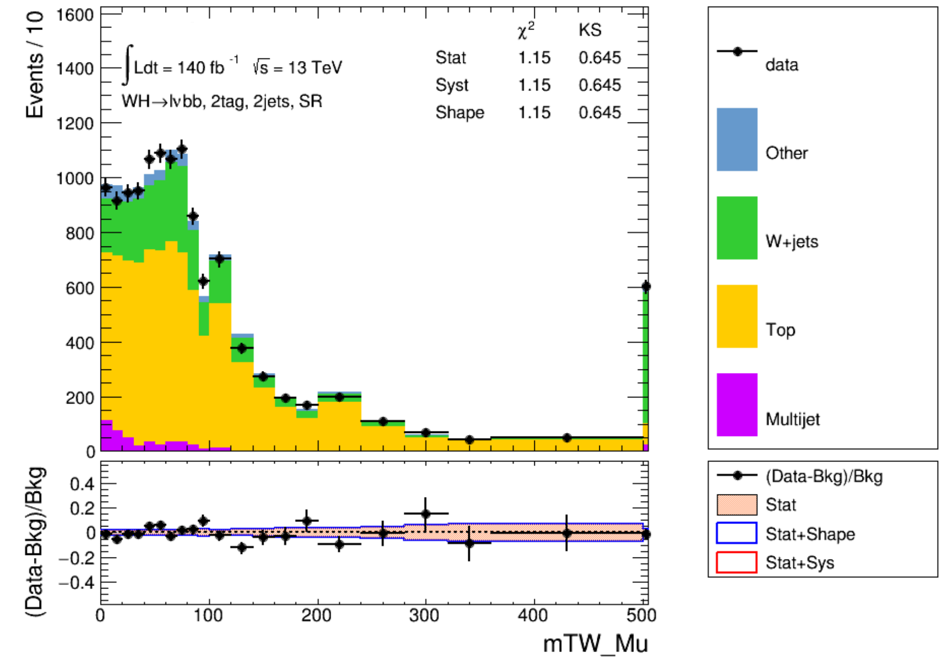


```
 Constant Parameter     Value
--------------------   ------------
   Others_SR_Nevents    5.1065e+02
        Others_scale    1.0000e+00
      Top_SR_Nevents    9.5696e+03
        W_SR_Nevents    2.9264e+03
multijetMu_SR_Nevents     2.7773e+03

 Floating Parameter    InitialValue     FinalValue (+HiError,-LoError)
--------------------   ------------   ------------------------------------
           Top_scale    1.0000e+00    8.5869e-01 (+2.12e-02,-2.11e-02)
             W_scale    1.0000e+00    1.0874e+00 (+6.02e-02,-5.94e-02)
     multijetMu_scale    1.0000e+00    1.6854e-01 (+4.94e-02,-4.86e-02)
```

- mTW distribution into mTW_El and mTW_Mu
- 6 SF: Top_El, W_El, MJ_El, Top_Mu, W_Mu, MJ_Mu
- Top and W scales are different in the two channels
- MJ fraction in El is 0.7% and 3.8% in Mu

Fit Performance: 2jet High Ptv

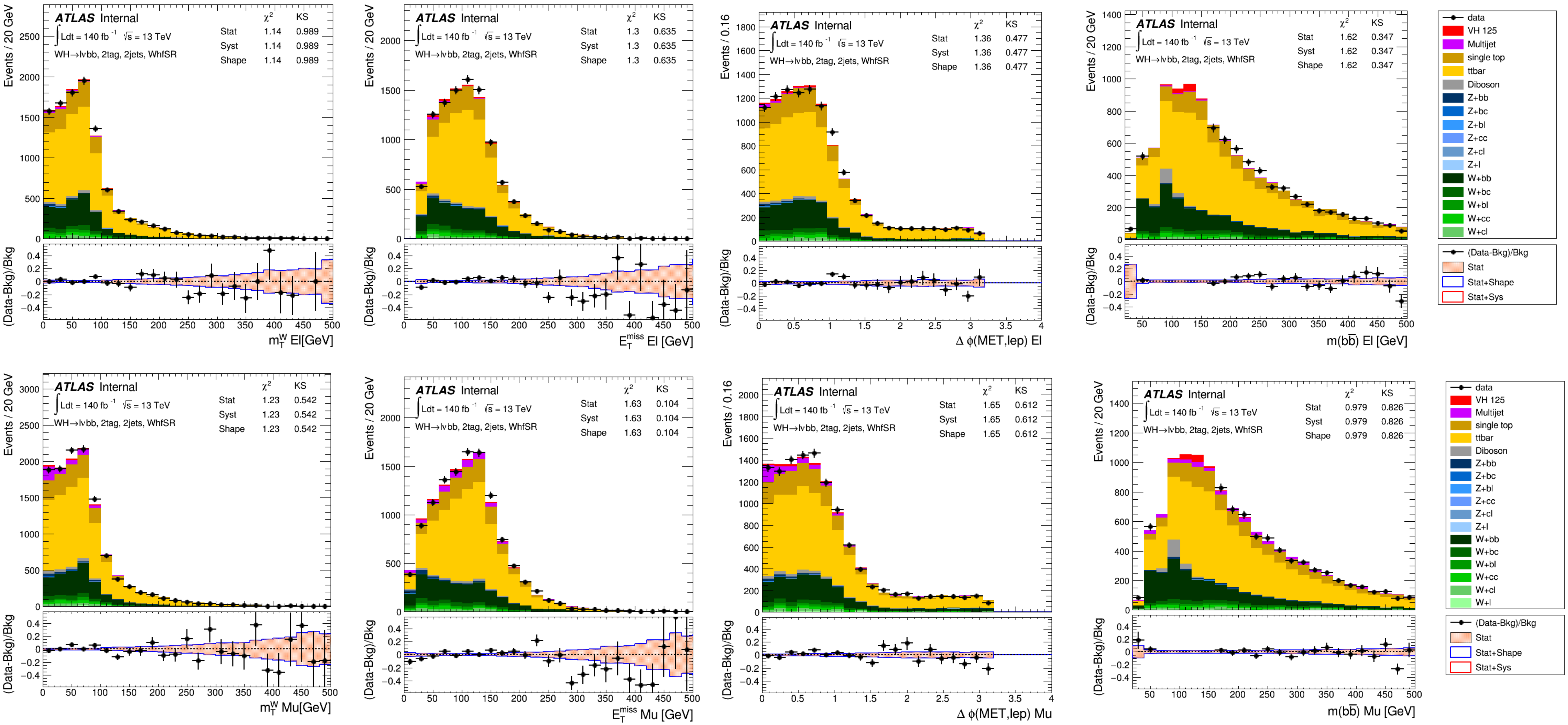

- Less MJ in the electron channel and more in the muon channel with the new fit: MJ fraction in El is 0.7% and 3.8% in Mu
- data/MC agreement is good with the new fit

Multi-jet template Fit: 3jet, $p_T^V > 150$GeV

- MJ is negligible in the 3jet category
- The fit seems to work well in this region
- Fit results plots are here

```
  Constant Parameter    Value
--------------------  ------------
   Others_SR_Nevents    6.5510e+02
        Others_scale    1.0000e+00
      Top_SR_Nevents    5.3735e+04
        W_SR_Nevents    4.9100e+03
multijetEl_SR_Nevents    1.4586e+04

  Floating Parameter  InitialValue    FinalValue (+HiError,-LoError)
--------------------  ------------  ----------------------------------
           Top_scale    1.0000e+00    9.0425e-01 (+6.01e-03,-6.01e-03)
             W_scale    1.0000e+00    1.2186e+00 (+5.08e-02,-5.02e-02)
    multijetEl_scale    1.0000e+00    1.0001e-05 (+1.04e-02,--0.00e+00)
```

```
  Constant Parameter    Value
--------------------  ------------
   Others_SR_Nevents    8.7778e+02
        Others_scale    1.0000e+00
      Top_SR_Nevents    6.0938e+04
        W_SR_Nevents    6.2486e+03
multijetMu_SR_Nevents    3.4273e+03

  Floating Parameter  InitialValue    FinalValue (+HiError,-LoError)
--------------------  ------------  ----------------------------------
           Top_scale    1.0000e+00    8.9900e-01 (+5.53e-03,-5.59e-03)
             W_scale    1.0000e+00    1.1273e+00 (+4.19e-02,-4.10e-02)
    multijetMu_scale    1.0000e+00    1.0662e-05 (+2.02e-02,--0.00e+00)
```

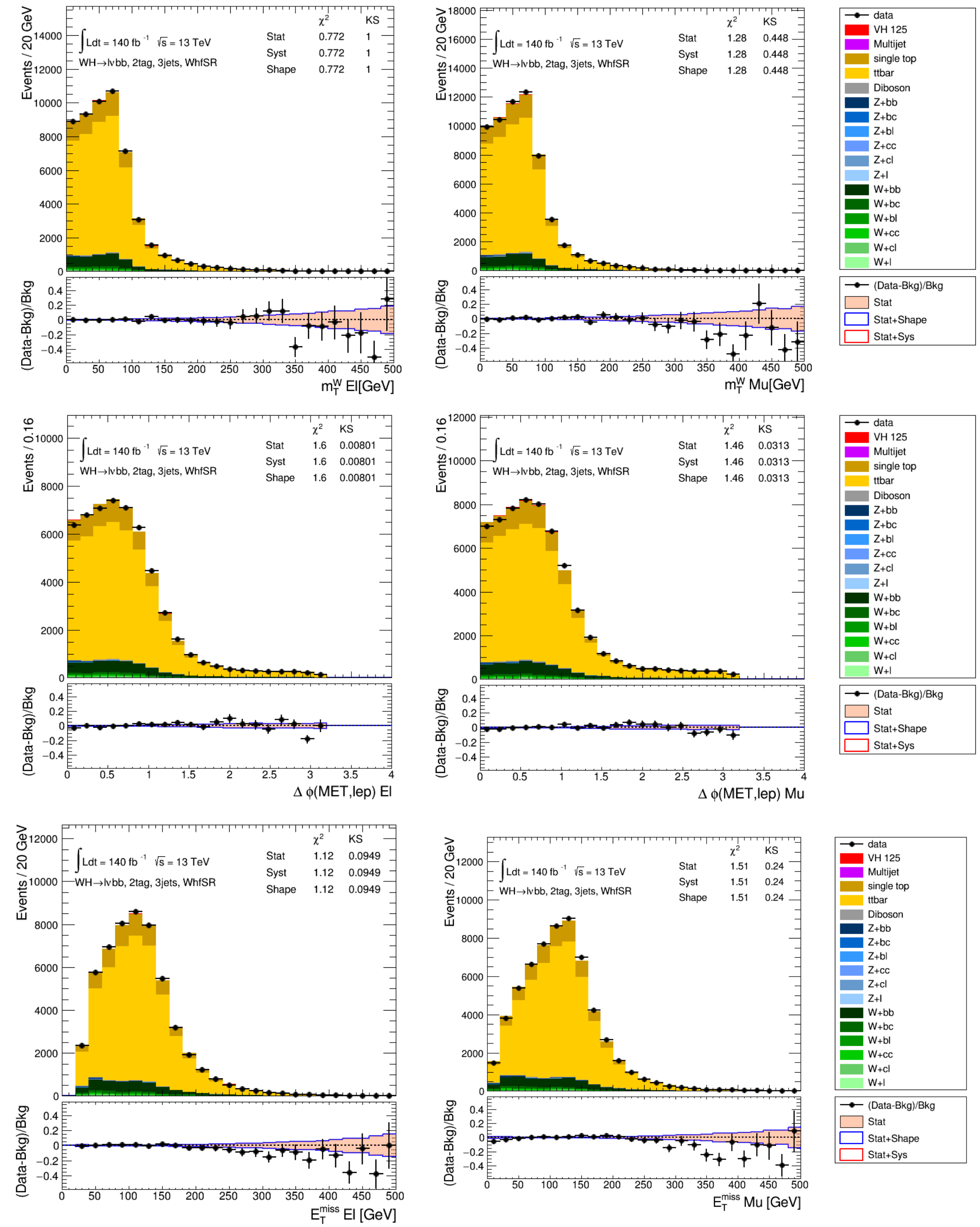

Multi-jet template Fit: 2jet, 75< p_T^V<150GeV

- The fit seems to work well in this region
- MJ fraction is 4.7% in El and 1.8% in Mu
- Fit results plots are here

```
  Constant Parameter    Value
--------------------  ------------
   Others_SR_Nevents    1.0150e+03
        Others_scale    1.0000e+00
      Top_SR_Nevents    5.2443e+04
        W_SR_Nevents    8.1228e+03
multijetEl_SR_Nevents     2.5307e+04

  Floating Parameter  InitialValue    FinalValue (+HiError,-LoError)
--------------------  ------------  ----------------------------------
           Top_scale    1.0000e+00    9.3022e-01 (+9.01e-03,-9.18e-03)
             W_scale    1.0000e+00    1.4373e+00 (+5.48e-02,-5.36e-02)
       multijetEl_scale    1.0000e+00    1.2216e-01 (+7.45e-03,-7.36e-03)
```

```
  Constant Parameter    Value
--------------------  ------------
   Others_SR_Nevents    1.6849e+03
        Others_scale    1.0000e+00
      Top_SR_Nevents    5.2902e+04
        W_SR_Nevents    9.2049e+03
multijetMu_SR_Nevents     3.5559e+04

  Floating Parameter  InitialValue    FinalValue (+HiError,-LoError)
--------------------  ------------  ----------------------------------
           Top_scale    1.0000e+00    9.8654e-01 (+8.89e-03,-8.79e-03)
             W_scale    1.0000e+00    1.3174e+00 (+4.93e-02,-4.97e-02)
       multijetMu_scale    1.0000e+00    3.3726e-02 (+5.44e-03,-5.39e-03)
```

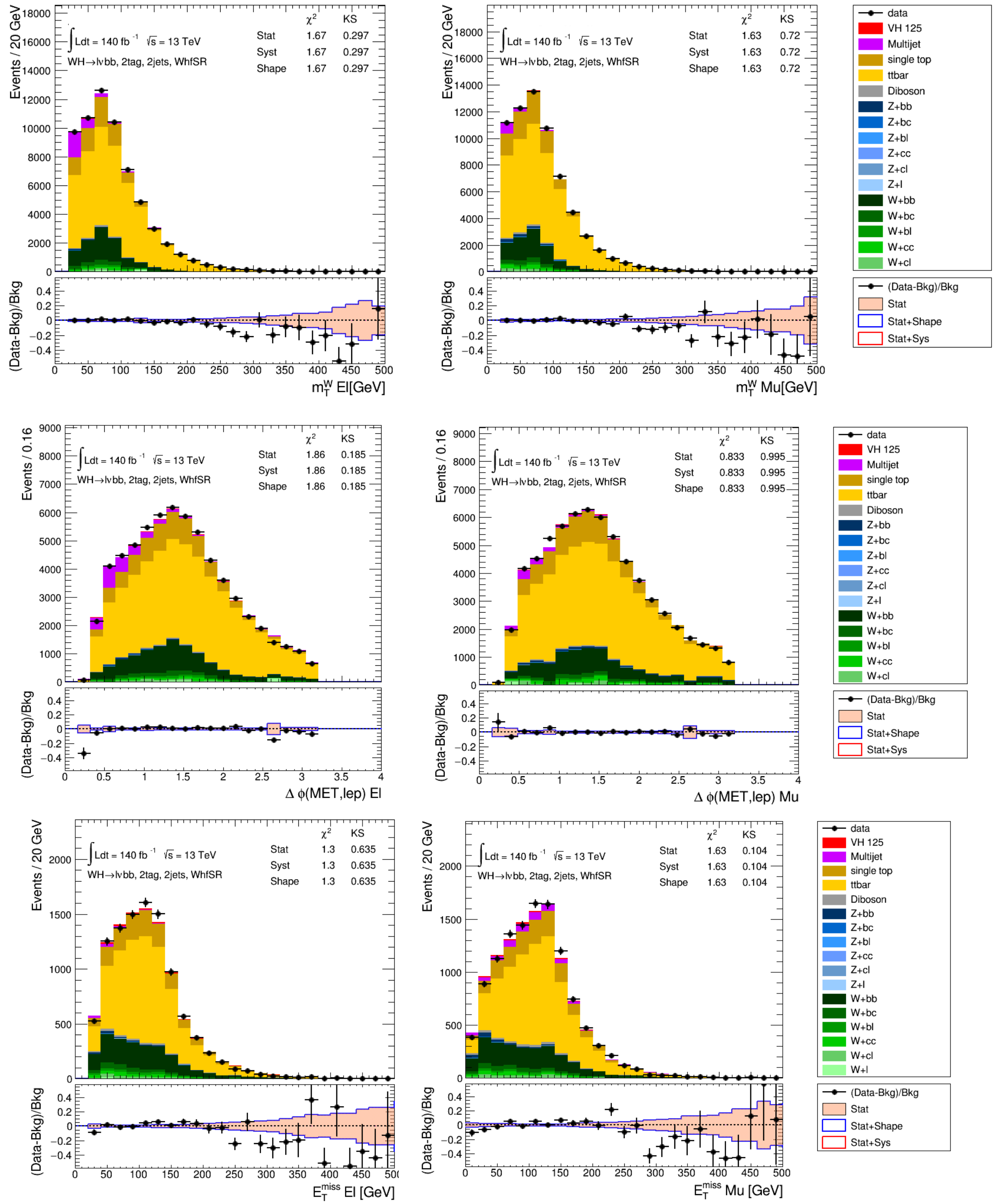

Multi-jet template Fit: 3jet, 75< p_T^V<150GeV

- Very small fraction of MJ in this region
- The fit seems to work well in this region
- MJ fraction is 1.8% in El and 1.6% in Mu
- Fit results plots are here

```
 Constant Parameter    Value
--------------------  ------------
   Others_SR_Nevents    1.8009e+03
        Others_scale    1.0000e+00
      Top_SR_Nevents    1.6925e+05
        W_SR_Nevents    1.1398e+04
multijetEl_SR_Nevents    2.6438e+04

 Floating Parameter  InitialValue    FinalValue (+HiError,-LoError)
--------------------  ------------  --------------------------------
           Top_scale    1.0000e+00    9.9094e-01 (+3.90e-03,-3.94e-03)
             W_scale    1.0000e+00    1.0975e+00 (+4.83e-02,-4.80e-02)
     multijetEl_scale    1.0000e+00    1.3320e-01 (+1.47e-02,-1.43e-02)
```

```
 Constant Parameter    Value
--------------------  ------------
   Others_SR_Nevents    2.0986e+03
        Others_scale    1.0000e+00
      Top_SR_Nevents    1.7513e+05
        W_SR_Nevents    1.3428e+04
multijetMu_SR_Nevents    3.5757e+04

 Floating Parameter  InitialValue    FinalValue (+HiError,-LoError)
--------------------  ------------  --------------------------------
           Top_scale    1.0000e+00    9.7656e-01 (+4.05e-03,-4.11e-03)
             W_scale    1.0000e+00    1.0978e+00 (+4.18e-02,-4.17e-02)
     multijetMu_scale    1.0000e+00    8.7266e-02 (+9.96e-03,-9.70e-03)
```

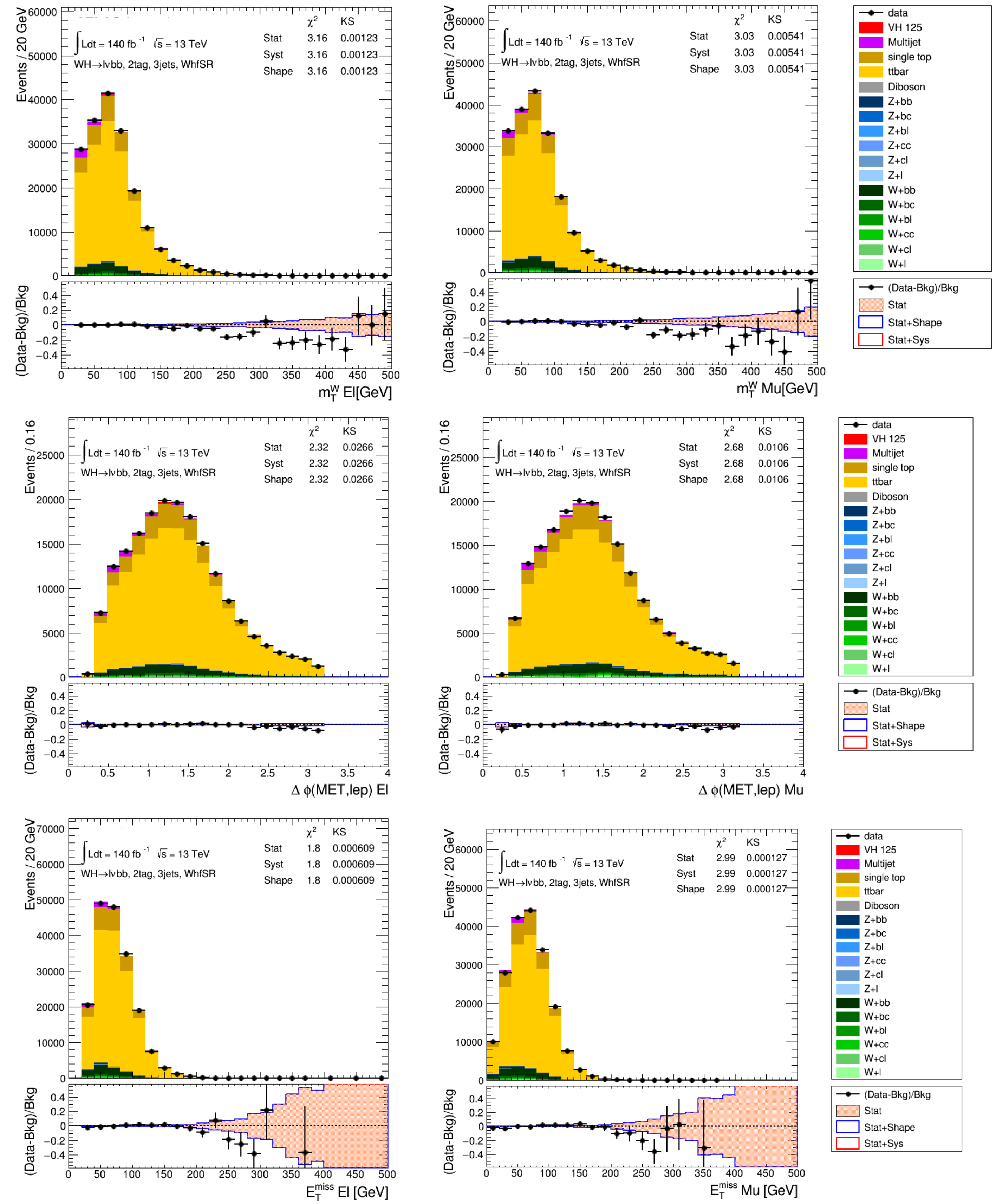

MJ shape uncertainties: dPhiLMET

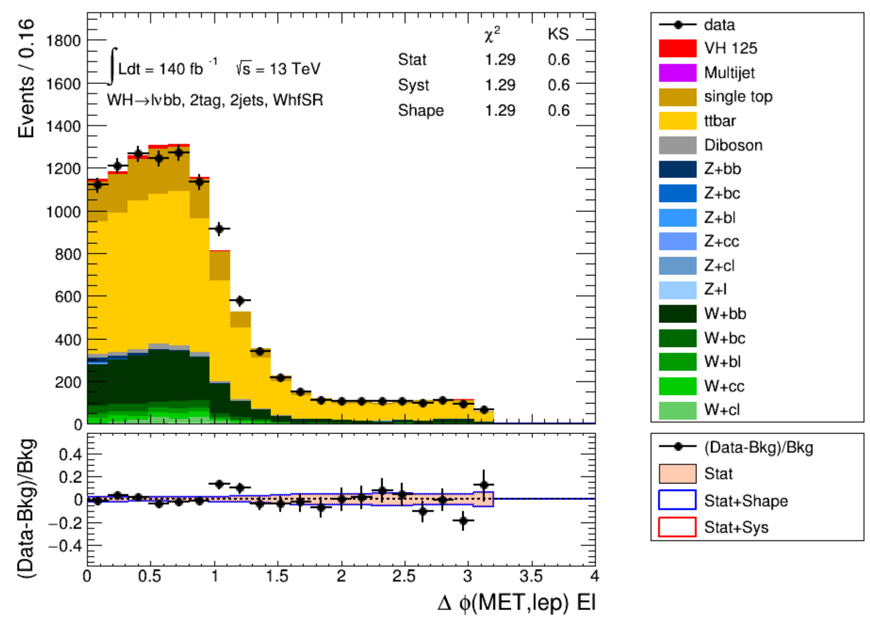

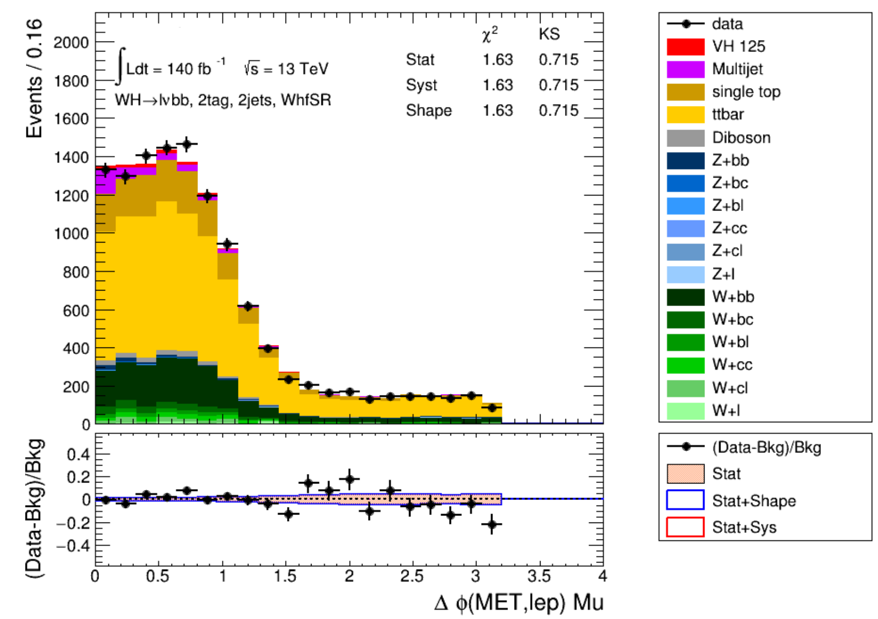

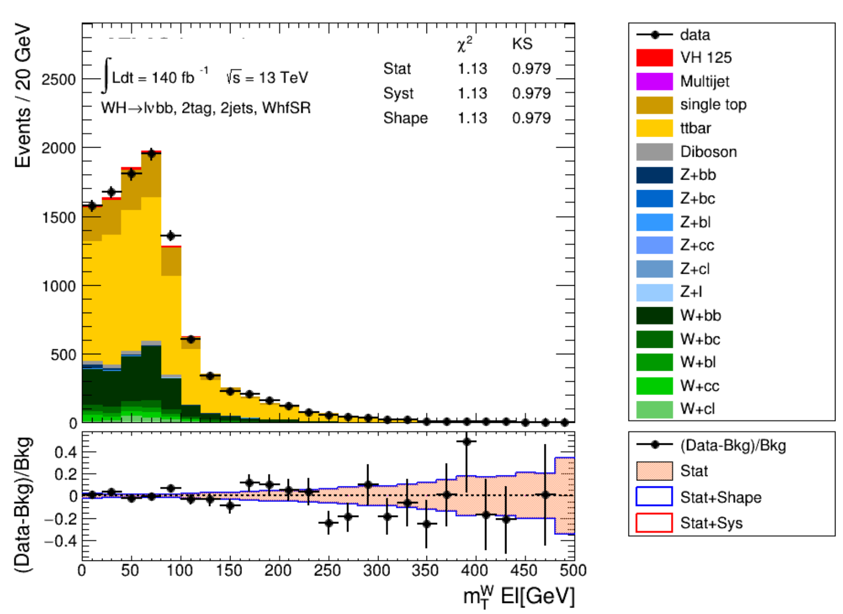

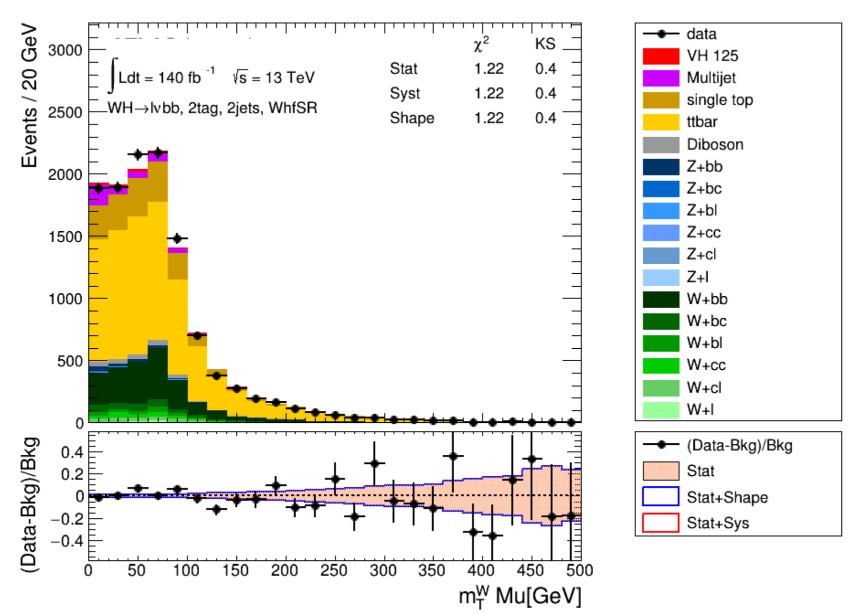

MJ shape uncertainties: Tighter isolation

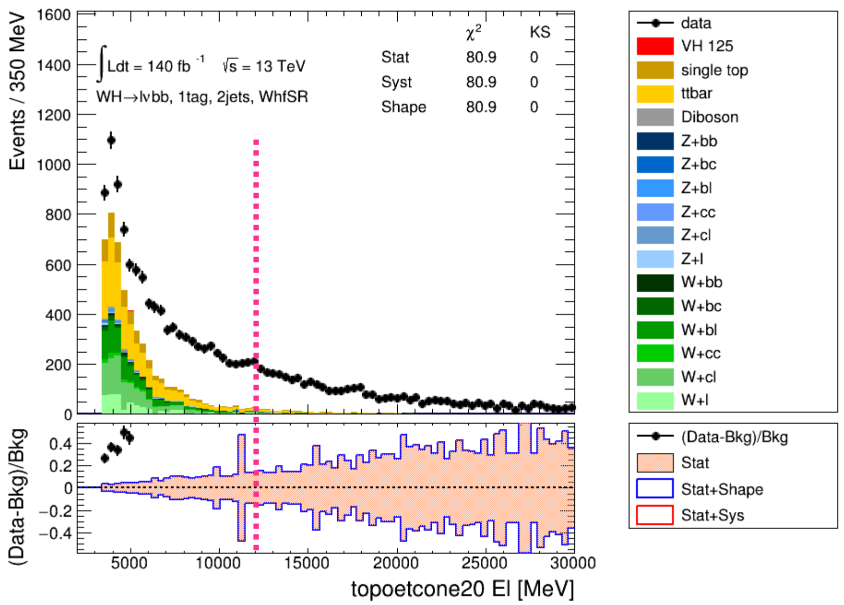

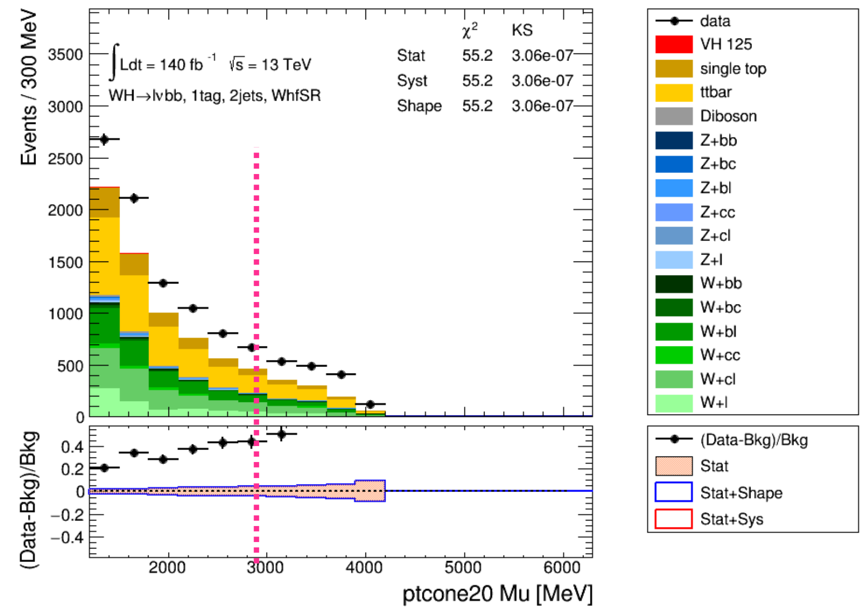

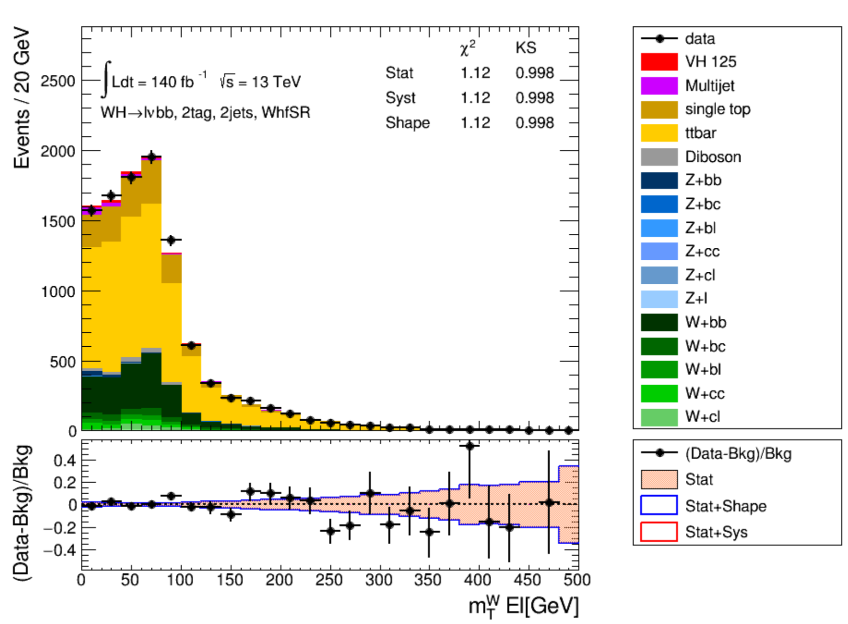

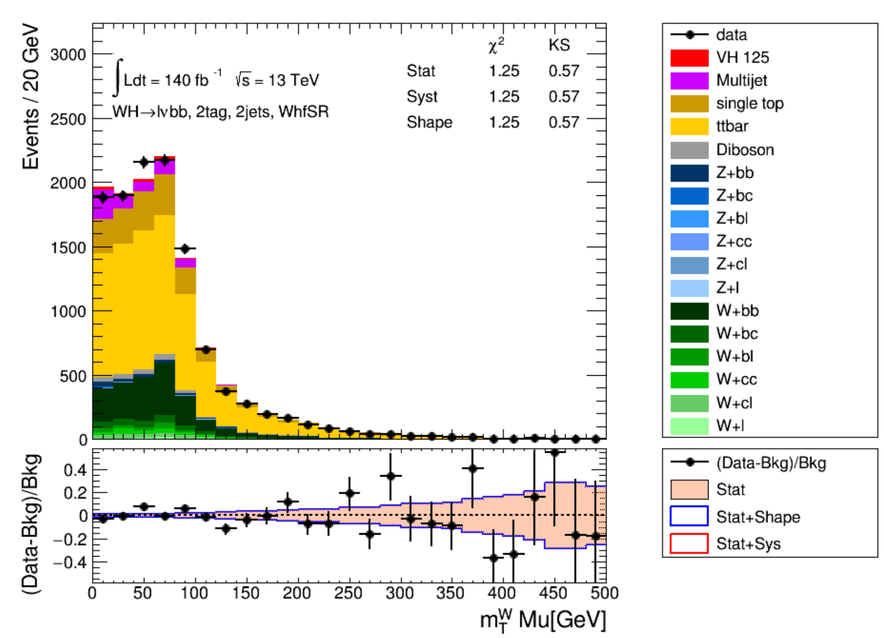

MJ shape uncertainties: EWK SFs

Floating Parameter	FinalValue
Top_scale	9.8654e-01
W_scale	1.3174e+00
multijetMu_scale	3.3726e-02

- Using the SFs results from the nominal MJ template fit

Floating Parameter	FinalValue
Top_scale	9.3022e-01
W_scale	1.4373e+00
multijetEl_scale	1.2216e-01

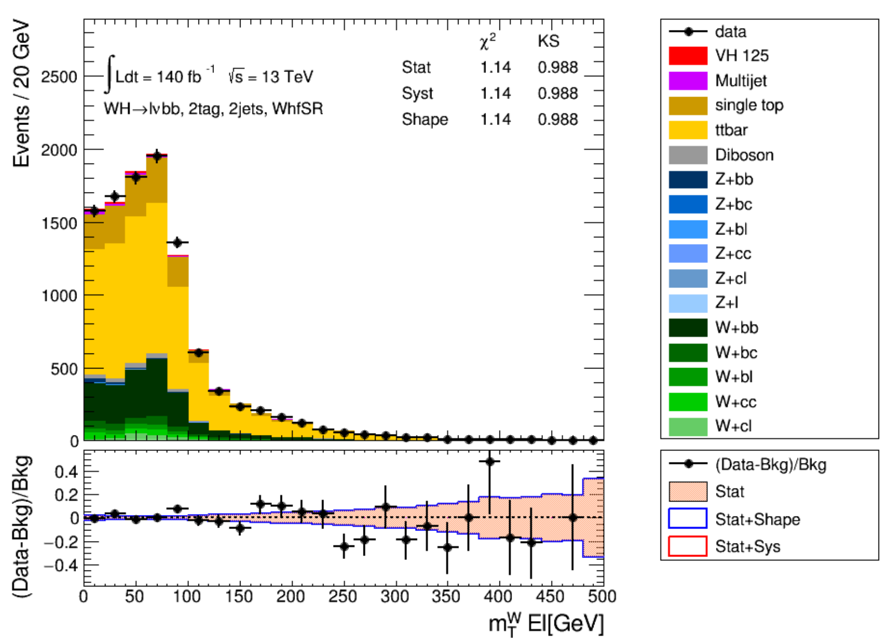

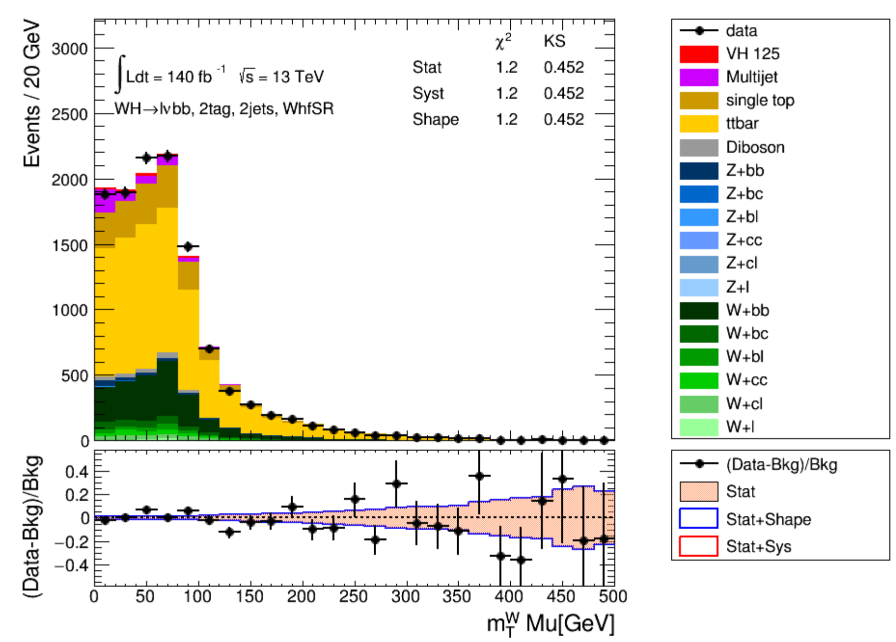

MJ shape uncertainties: MET cut

- Concerning only the electron sub-channel
- Include events with MET < 30GeV

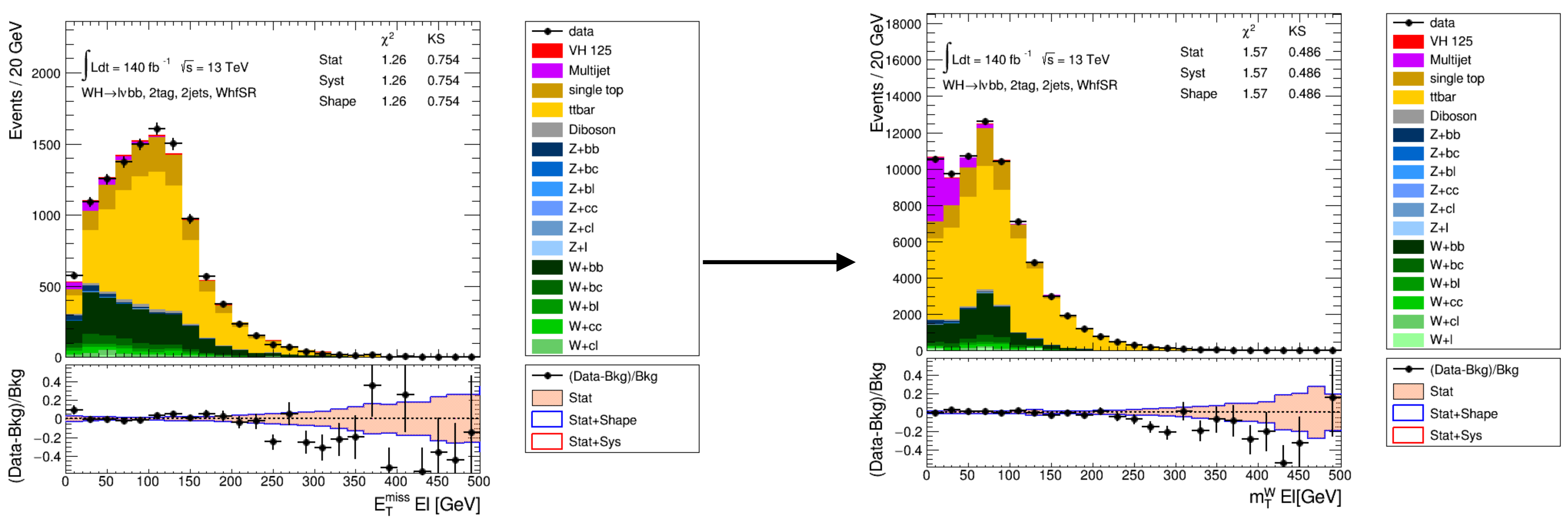

MJ uncertainties BDT distribution

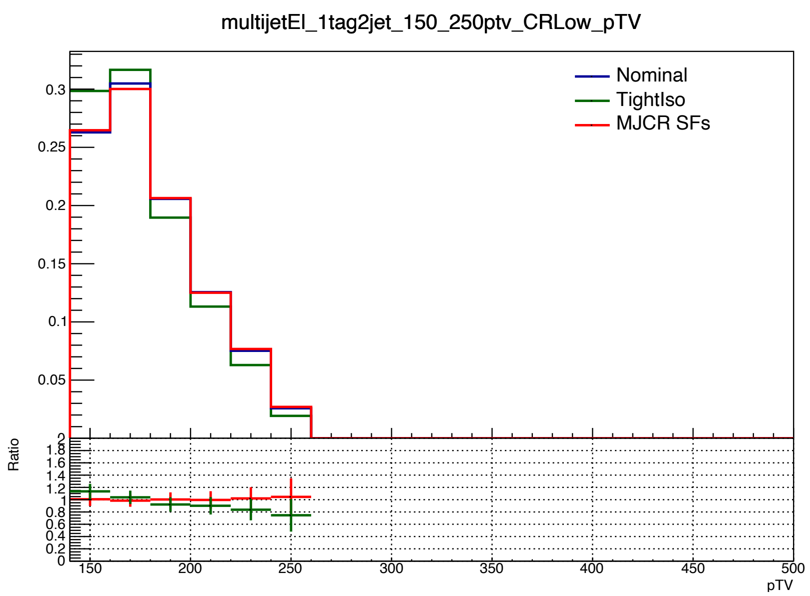

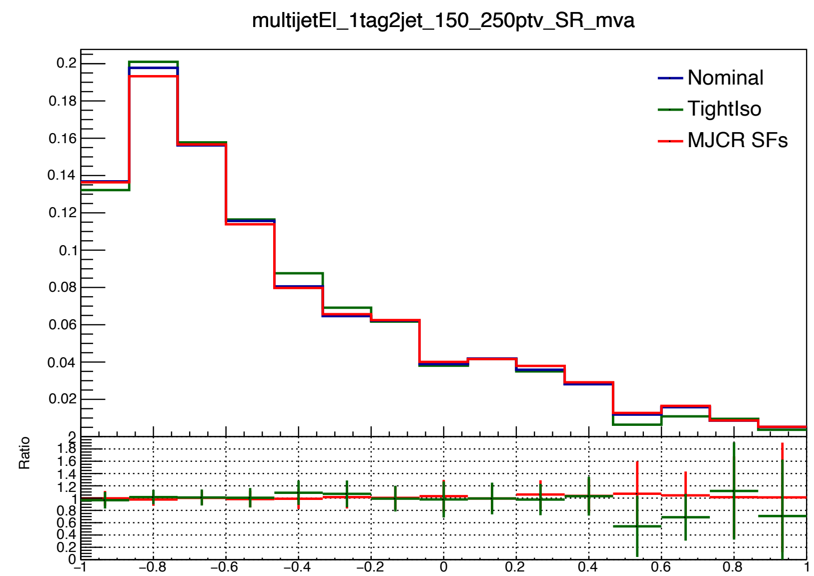

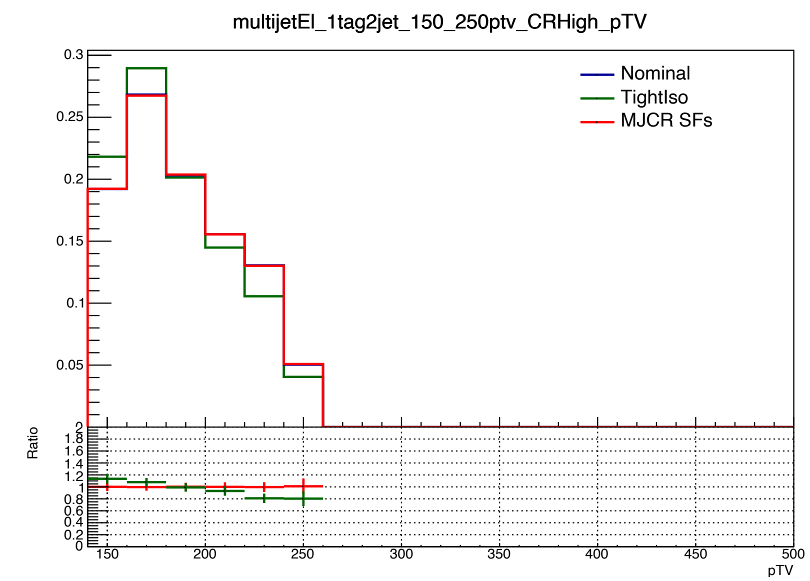

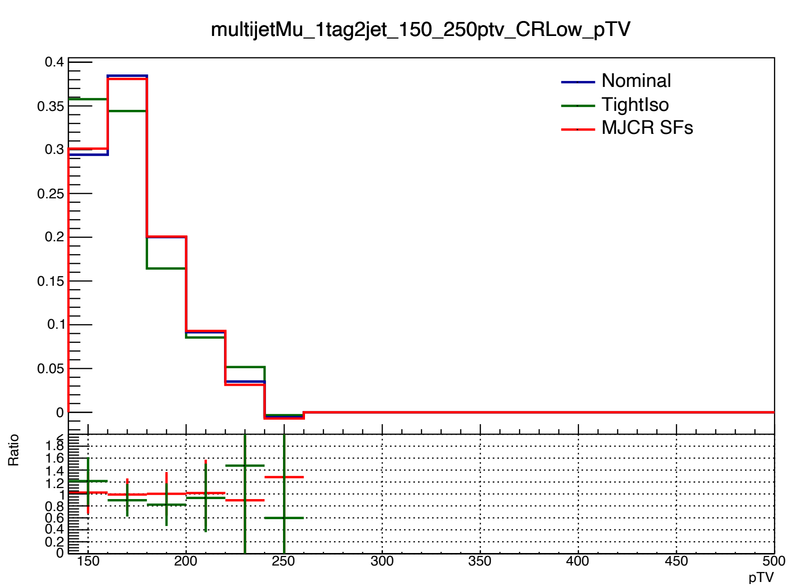

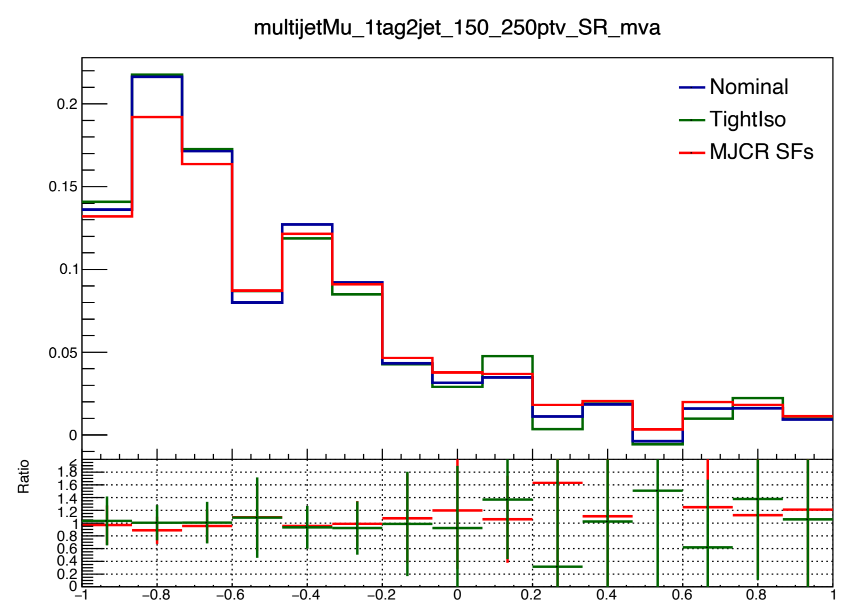

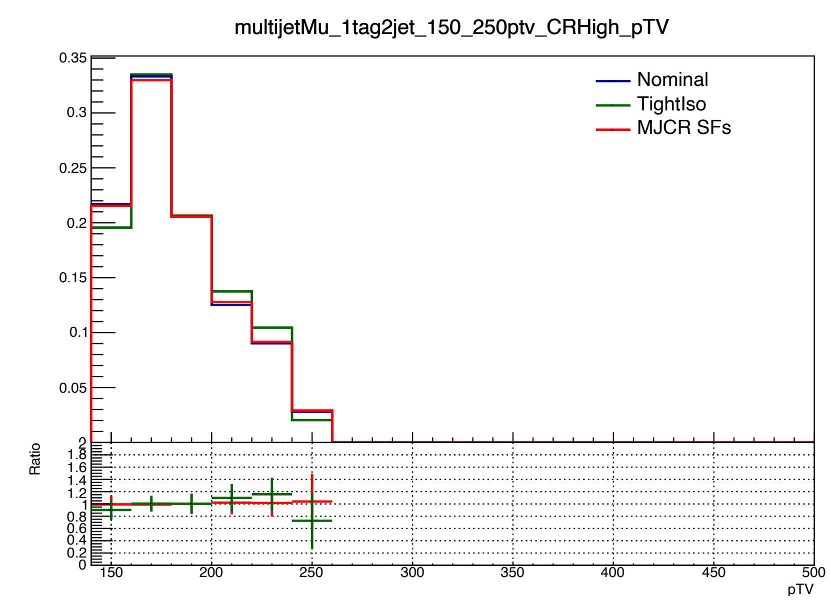

MJ uncertainties BDT distribution

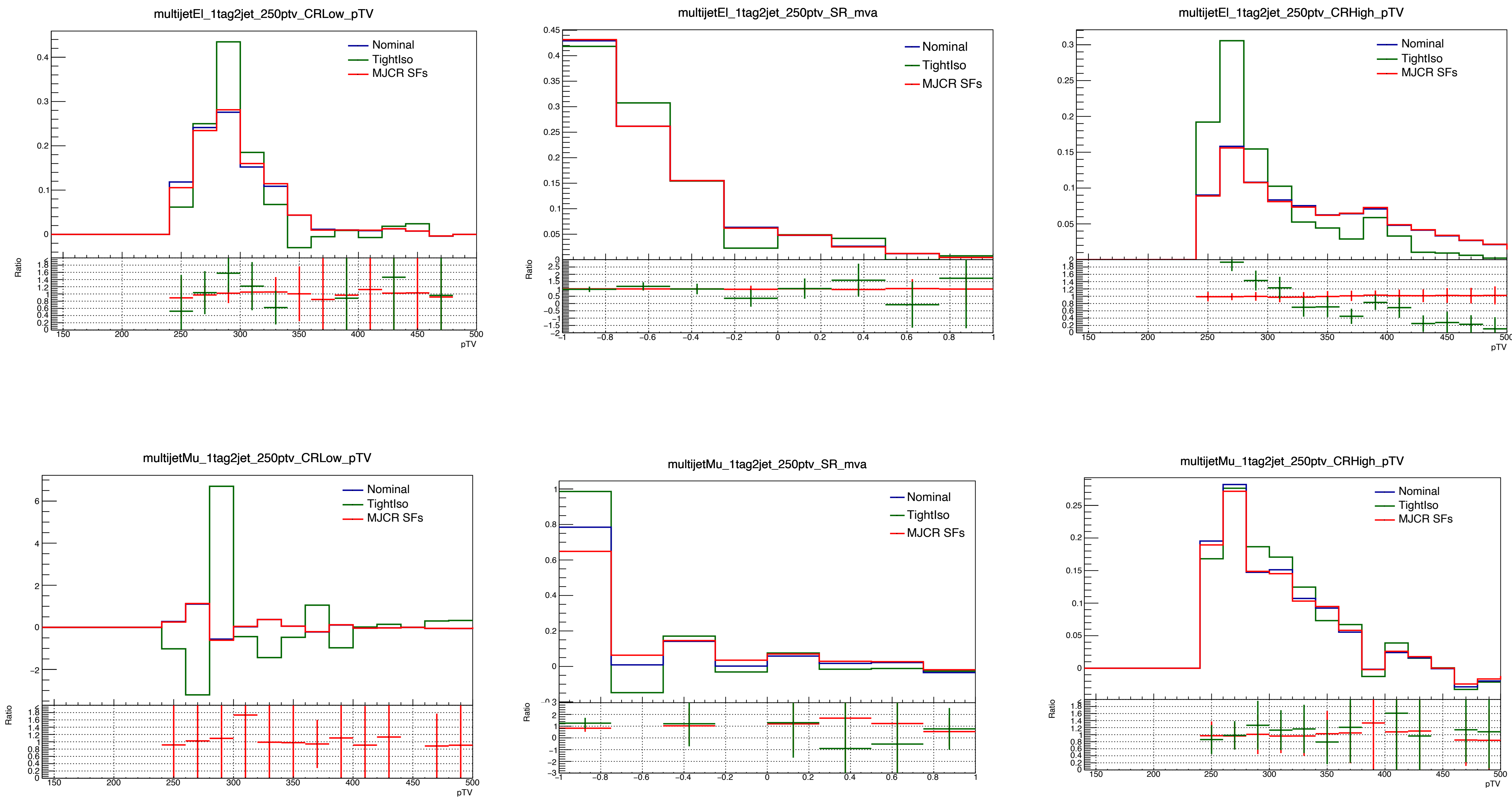

Multi-jet: Binned MV2C10 values in the 2tag region

- Illustration on how to evaluate the MVA for MJ events
    - Assigning values to MV2C10 based on the MJ estimation in the 2tag region (input variables for MVA training)
- The 2D distributions are normalised to unity in 2/3 jets and electron and muon channels

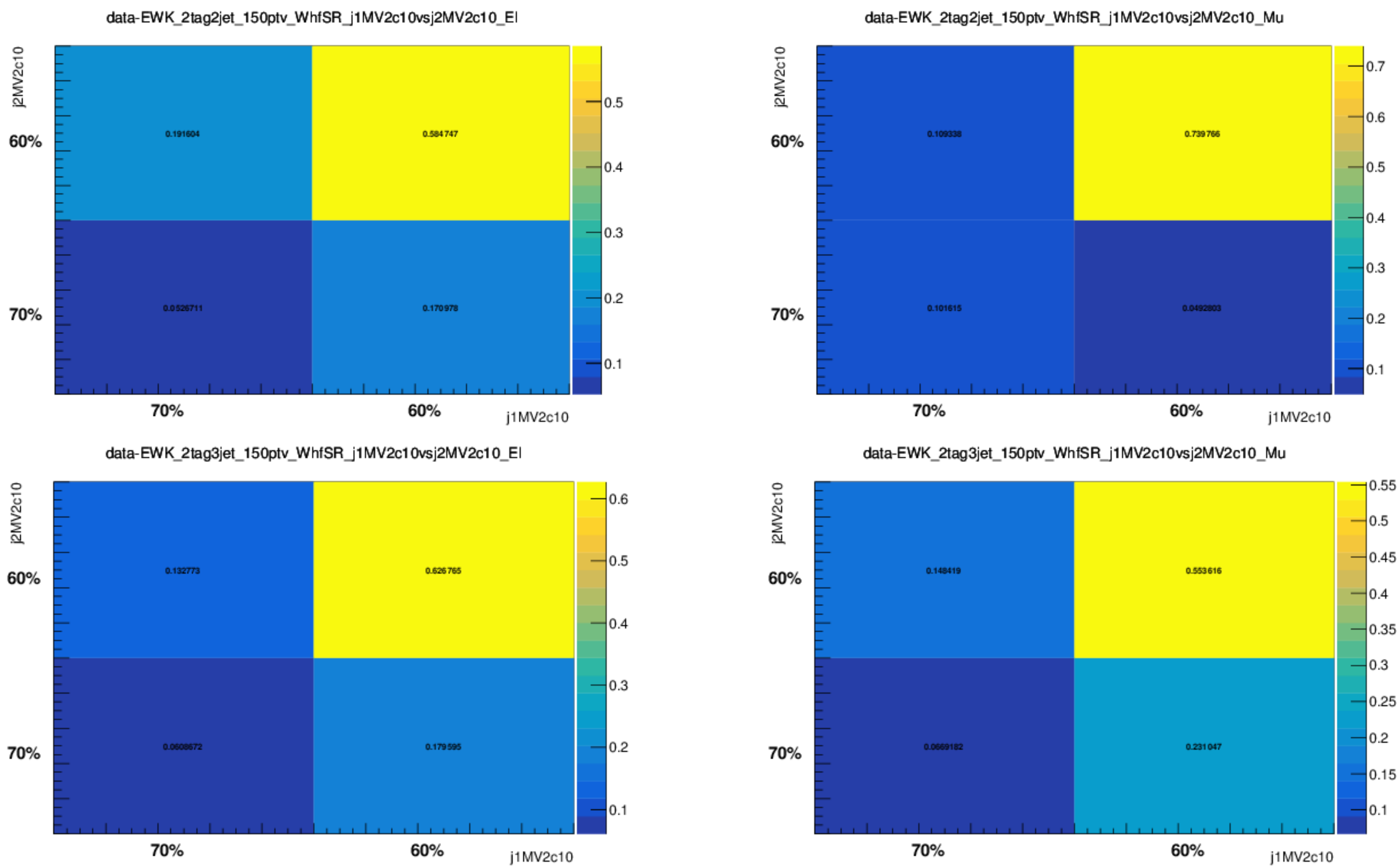

BDTr :0-lepton 2 vs 1 folds training

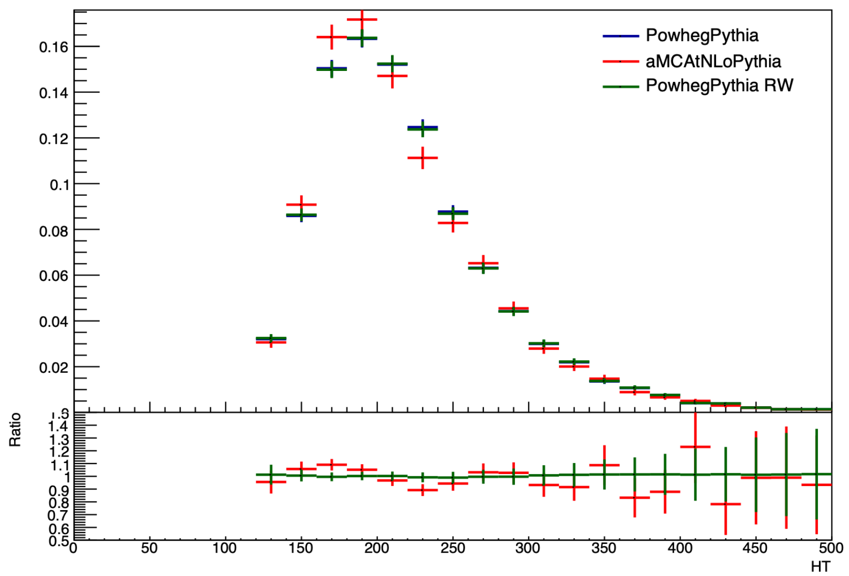

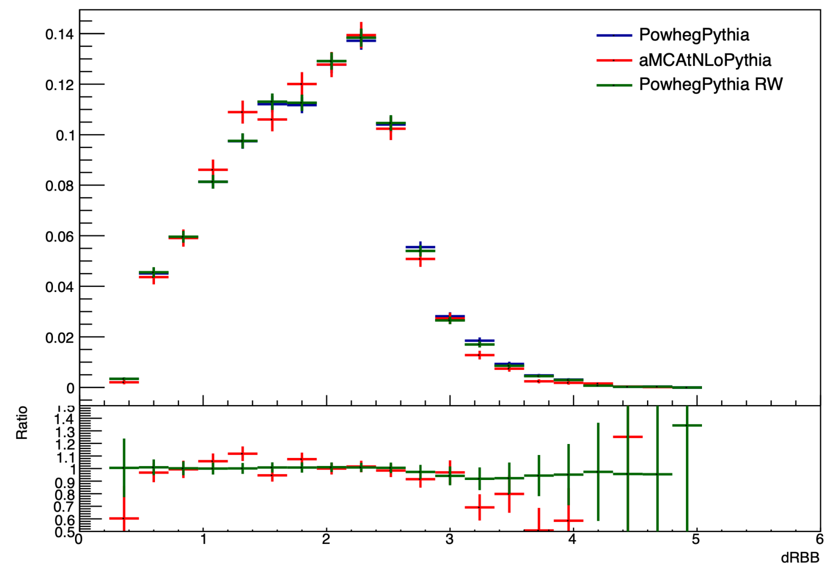

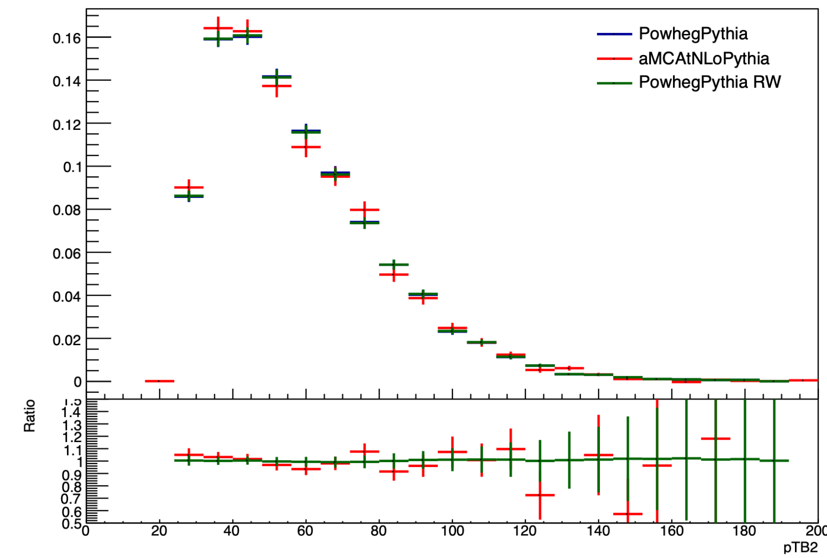

2-fold

1-fold

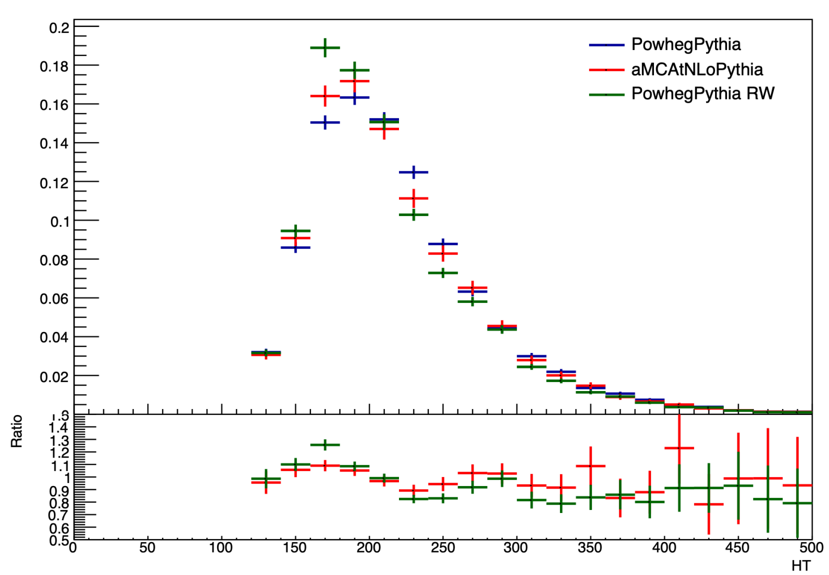

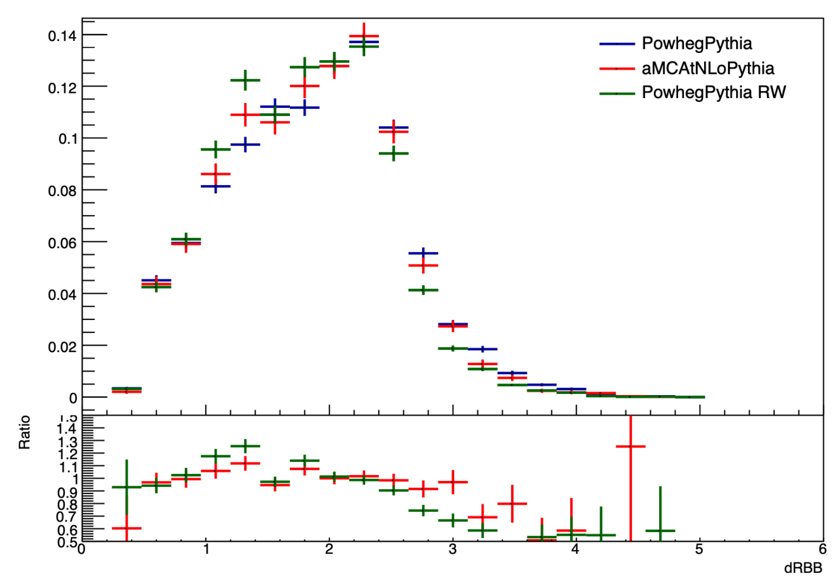

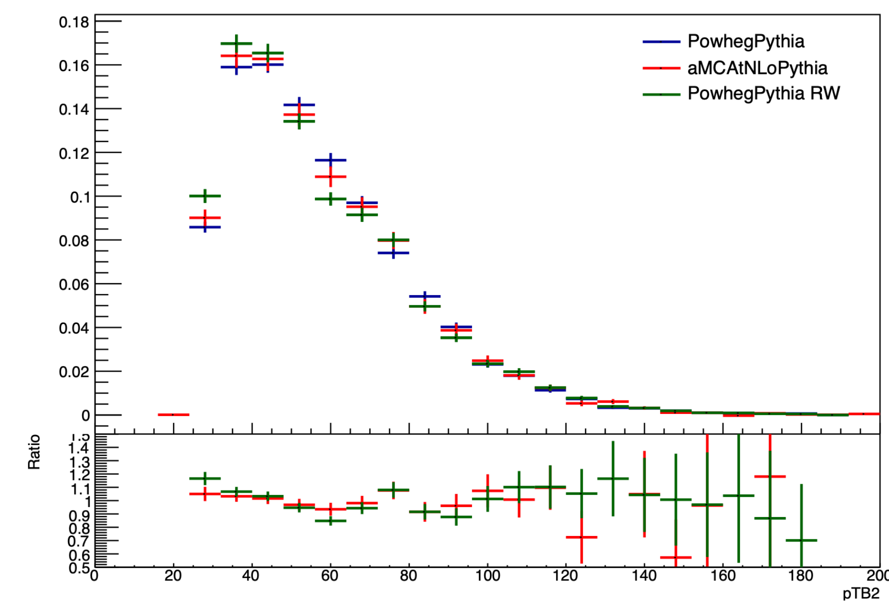

BDTr :1-lepton ME

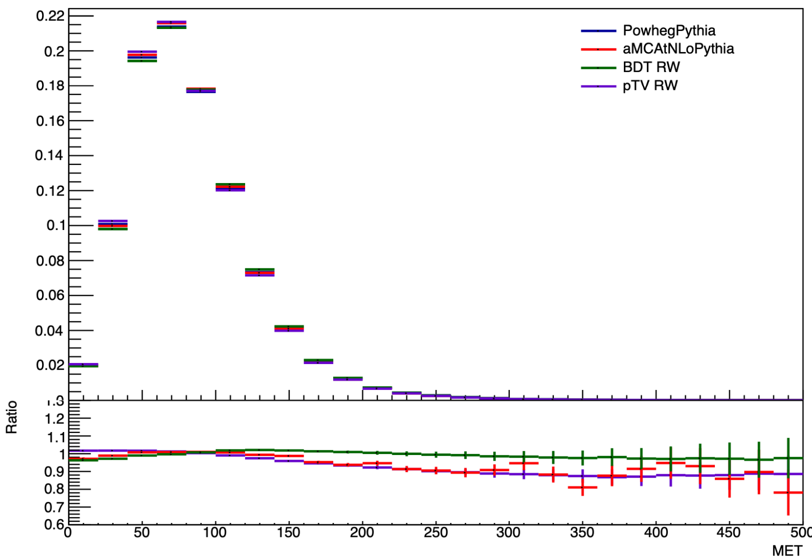

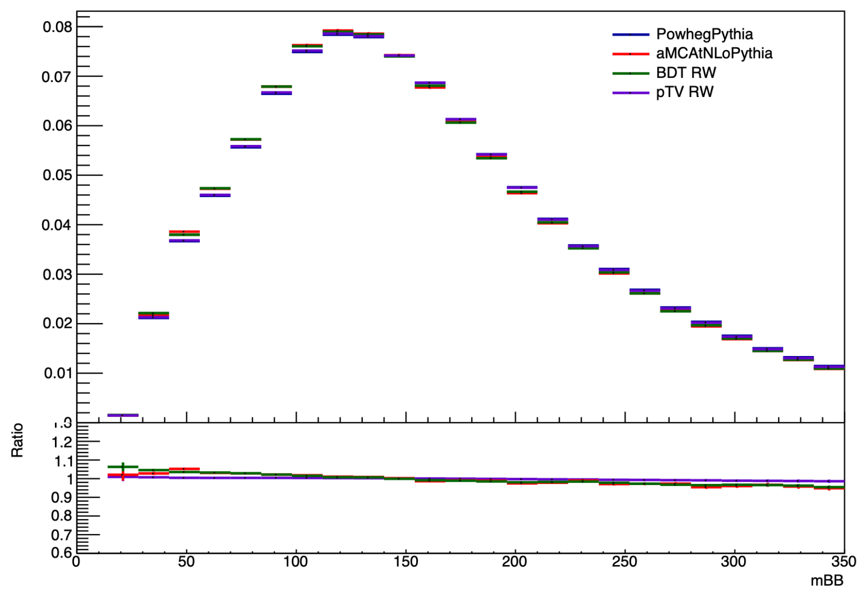

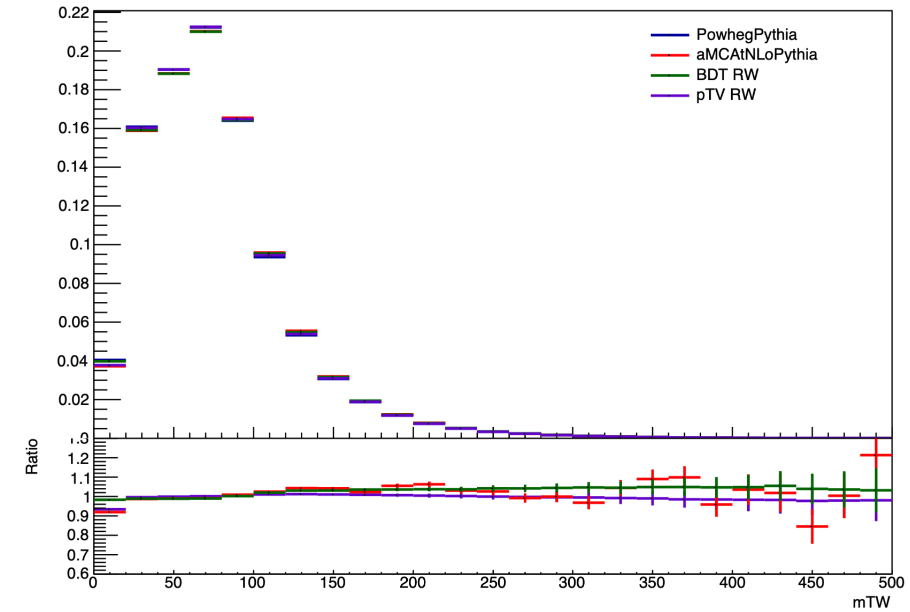

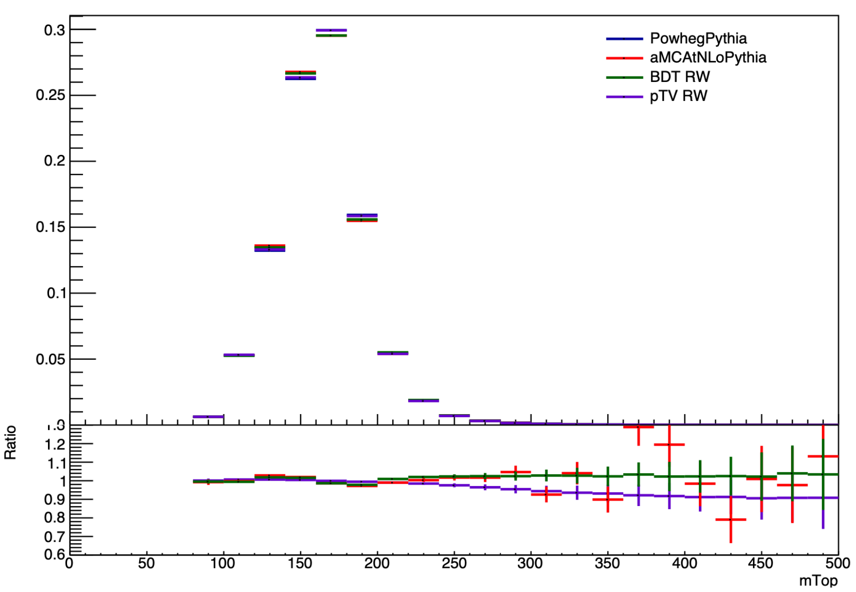

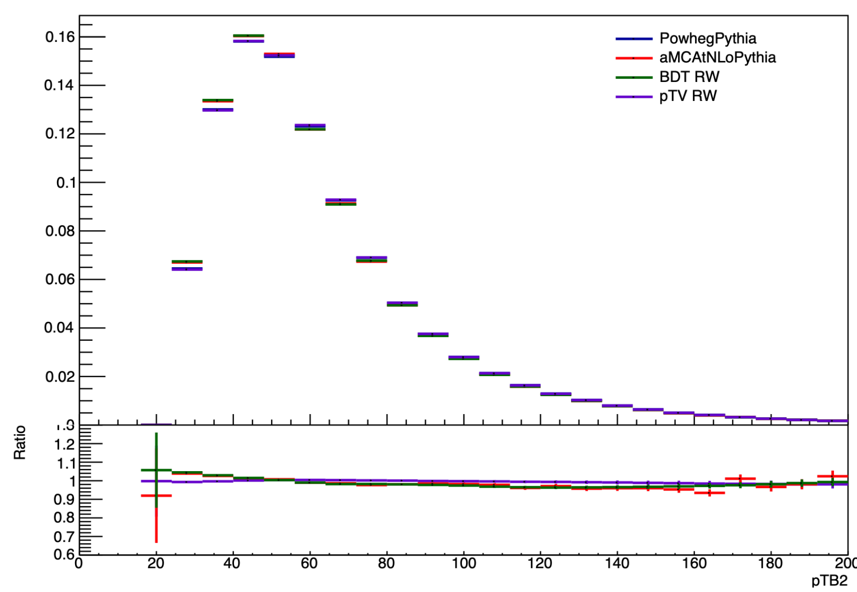

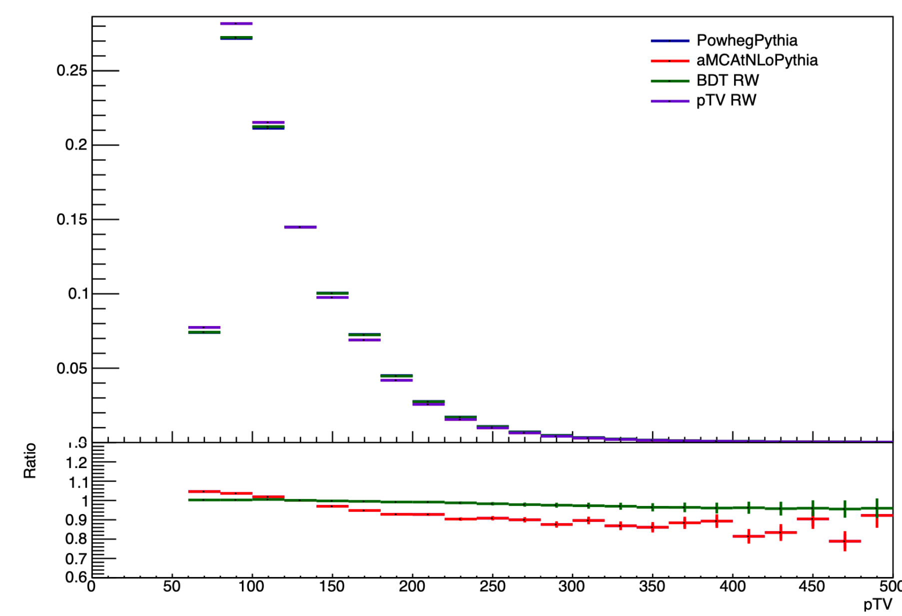

BDTr :1-lepton PS

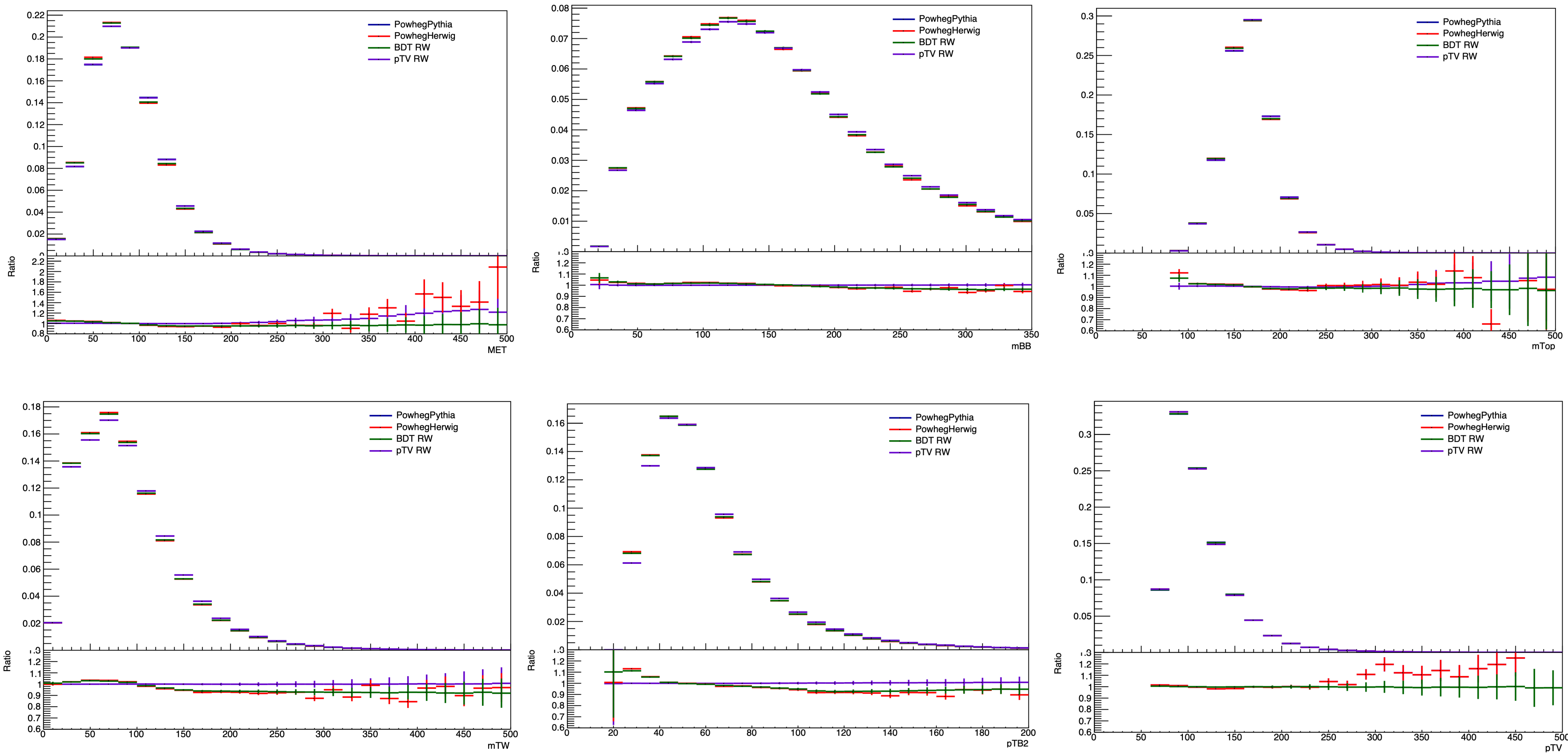

Diboson validation results

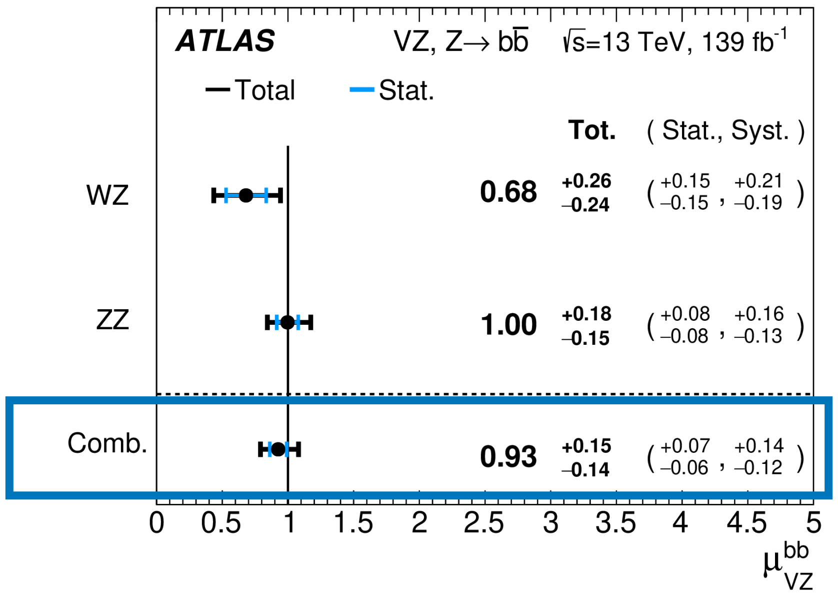

- The diboson analysis is a robust validation of the background model since the process is very similar to *VH*
  - It uses the same selection and strategy as the *VH* analysis
  - The BDT is retrained to consider the *VZ* as signal
- Results:
  - Good agreement between the channels
  - Validation of the method and **green** light to unblind at the *VH* analysis

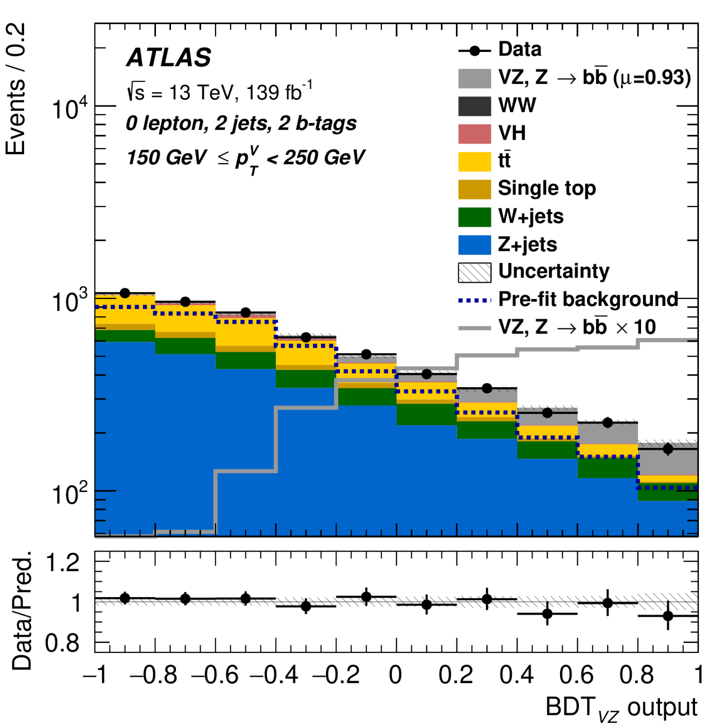

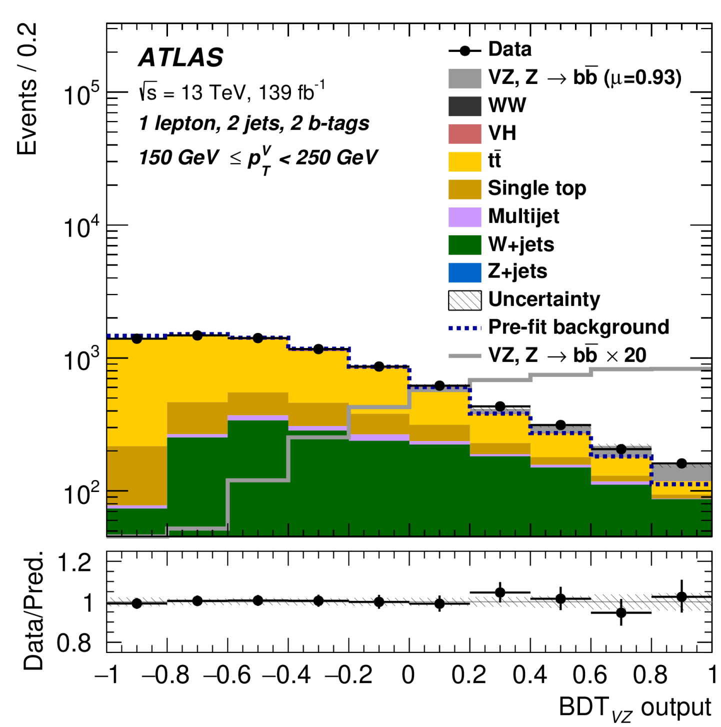

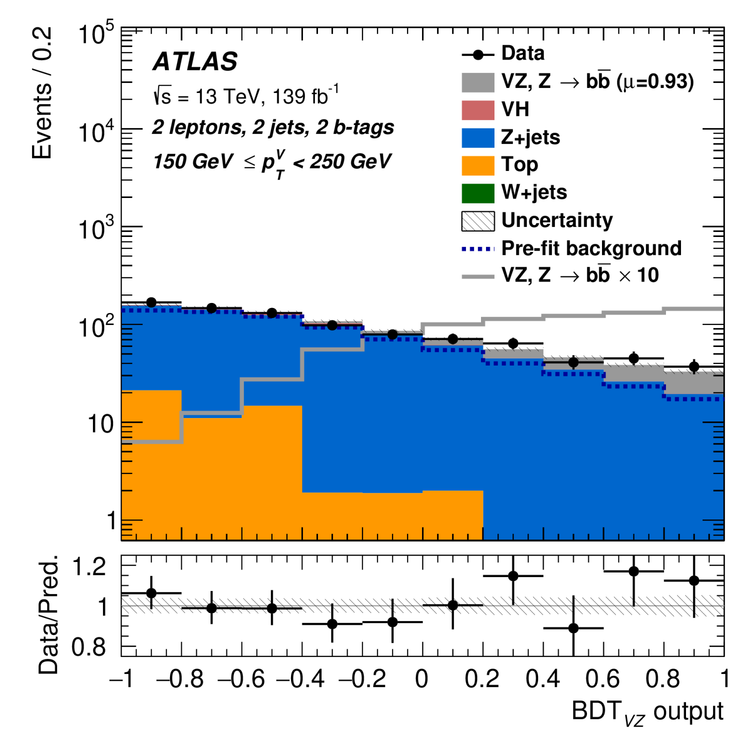

Differential cross-section measurements

- Differential cross-section (STXS) measurements were performed
- The analysis categories match the STXS bins definition
  - STXS measurement in 5 p_T^V bins
- Measured σ*BR in each of the bins in agreement with the SM within uncertainties

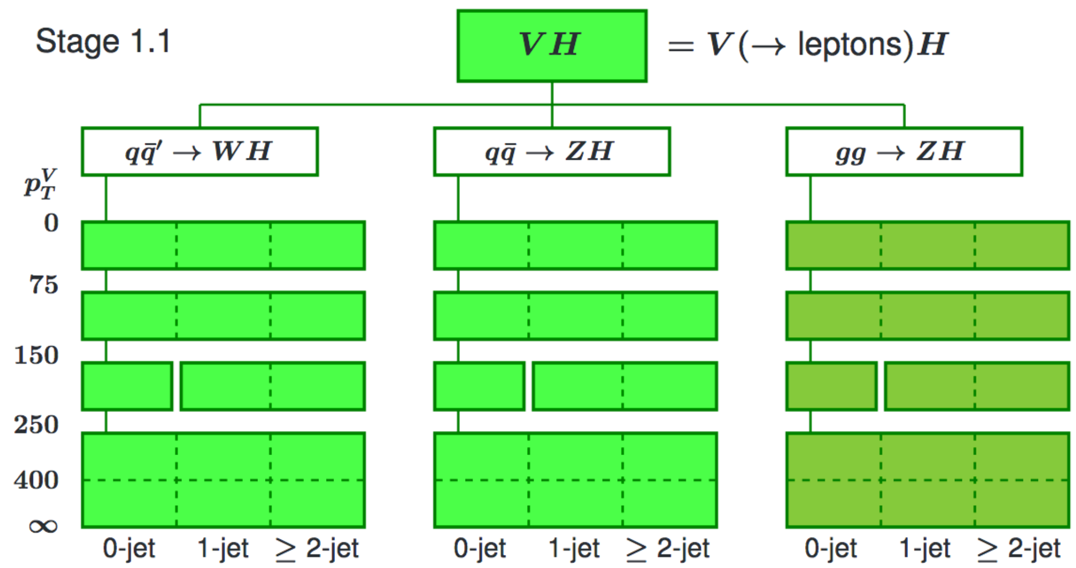

Measurement

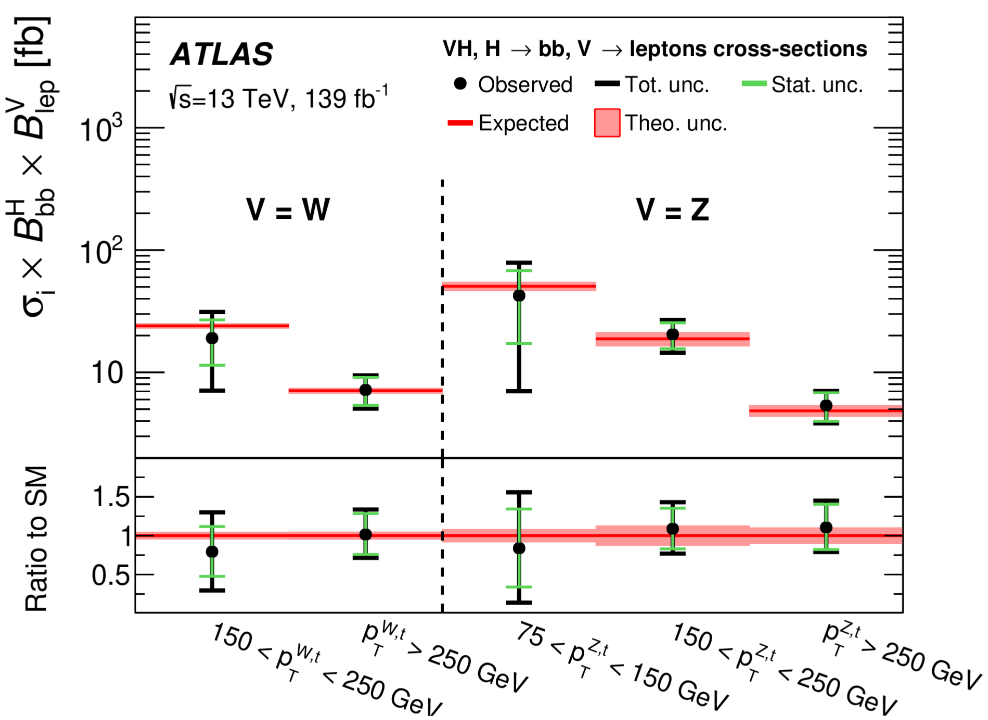

Interpretation